
Study of the phytotoxicity caused by cinnamon essential oil tree-injection in apple trees as a bio-insecticide

Auteur : Bouvry, Jean

Promoteur(s) : Fauconnier, Marie-Laure

Faculté : Gembloux Agro-Bio Tech (GxABT)

Diplôme : Master en bioingénieur : chimie et bioindustries, à finalité spécialisée

Année académique : 2020-2021

URI/URL : <http://hdl.handle.net/2268.2/12920>

Avertissement à l'attention des usagers :

Tous les documents placés en accès ouvert sur le site le site MatheO sont protégés par le droit d'auteur. Conformément aux principes énoncés par la "Budapest Open Access Initiative"(BOAI, 2002), l'utilisateur du site peut lire, télécharger, copier, transmettre, imprimer, chercher ou faire un lien vers le texte intégral de ces documents, les disséquer pour les indexer, s'en servir de données pour un logiciel, ou s'en servir à toute autre fin légale (ou prévue par la réglementation relative au droit d'auteur). Toute utilisation du document à des fins commerciales est strictement interdite.

Par ailleurs, l'utilisateur s'engage à respecter les droits moraux de l'auteur, principalement le droit à l'intégrité de l'oeuvre et le droit de paternité et ce dans toute utilisation que l'utilisateur entreprend. Ainsi, à titre d'exemple, lorsqu'il reproduira un document par extrait ou dans son intégralité, l'utilisateur citera de manière complète les sources telles que mentionnées ci-dessus. Toute utilisation non explicitement autorisée ci-avant (telle que par exemple, la modification du document ou son résumé) nécessite l'autorisation préalable et expresse des auteurs ou de leurs ayants droit.

STUDY OF THE PHYTOTOXICITY CAUSED BY CINNAMON ESSENTIAL OIL TREE-INJECTION IN APPLE TREES AS A BIO-INSECTICIDE

JEAN BOUVRY

**TRAVAIL DE FIN D'ÉTUDES PRÉSENTÉ EN VUE DE L'OBTENTION DU DIPLÔME DE
MASTER BIOINGÉNIEUR EN CHIMIE ET BIOINDUSTRIES**

ANNÉE ACADÉMIQUE 2020-2021

PROMOTER: Pr. MARIE-LAURE FAUCONNIER
CO-PROMOTER : Ir. PIERRE-YVES WERRIE

© Toute reproduction du présent document, par quelque procédé que ce soit, ne peut être réalisée qu'avec l'autorisation de l'auteur et de l'autorité académique de Gembloux Agro-Bio Tech.

Le présent document n'engage que son auteur.

STUDY OF THE PHYTOTOXICITY CAUSED BY CINNAMON ESSENTIAL OIL TREE-INJECTION IN APPLE TREES AS A BIO-INSECTICIDE

JEAN BOUVRY

**TRAVAIL DE FIN D'ÉTUDES PRÉSENTÉ EN VUE DE L'OBTENTION DU DIPLÔME DE
MASTER BIOINGÉNIEUR EN CHIMIE ET BIOINDUSTRIES**

ANNÉE ACADÉMIQUE 2020-2021

PROMOTER: Pr. MARIE-LAURE FAUCONNIER
CO-PROMOTER : Ir. PIERRE-YVES WERRIE

Acknowledgments

I would like to express my gratitude to my supervisor Pierre-Yves Werrie for his great availability, his patience and above all his judicious advice, which contributed to my reflection throughout my master thesis. I would like to thank him for all the time he devoted to providing me with methodological tools necessary to conduct this research in the best possible conditions.

I am also grateful to my promoter Marie-Laure Fauconnier for the monitoring of my progress in this work, her support and her valuable expertise.

I would like to say a huge thank you to all the members of the Laboratory of Natural Molecules' Chemistry for the technical support and advice, as well as for their kindness and the good atmosphere provided. I also greet my dear master thesis colleagues Alice, Soleiman and Thomas, for the mutual support and encouragement during the last months spent together in the lab. A special thanks to Tatiana, who was a great help to me in the manipulations carried out together but also alone in my absence, with results generated of great use in this work.

Thank you to Guillaume Le Goff, from the Biodiversity Research Center of the Catholic University of Louvain, for his valuable help in the aphid experiments and for providing us with environmental chambers to perform these experiments.

Thanks to Yves Brostaux for his help in my statistical analysis.

Finally, my deepest and most sincere gratitude goes to my family and friends for their moral support throughout these 5 years of study, and in particular to my grandmother, who lit a candle in every difficult moment in the name of my success.

Abstract

As a culturally and economically significant fruit tree worldwide, apple orchards protection has always been of great agronomic interest. Among its most detrimental insect pests, the rosy apple aphid (*Dysaphis plantaginea* Passerini) causes severe plant injuries and shows continuously increasing resistance to conventional pesticides. Commonly treated with sprayers in orchards, a trunk injection delivering system combined with an essential oil based biopesticide could be a solution to end the intensive use of conventional pesticides.

With this in mind, the research conducted for this master thesis focuses on the evaluation of possible phytotoxicity induced by a cinnamon essential oil 2% emulsion in apple tree *Malus domestica* Borkh (var. Jonagold). To do so, physiological, biochemical and transcriptomic parameters were looked into. This phytotoxicity study was carried out both in the short and long term, on young two-year-old micropropagated apples trees conserved in environmental chambers.

For the short term analysis, apple tree leaves were treated by foliar application of the essential oil emulsion, and sampled at different times in order to investigate molecular mechanisms usually quickly impacted after stress exposition. Concerning the hypothetical oxidative burst initiation and redox system unbalance, hydrogen peroxide (H₂O₂) production and glutathione (GSH) redox state were considered. Furthermore, lipid peroxidation, cellular membrane integrity and photosynthetic pigments degradation were the oxidative damages investigated, through the quantification of malondialdehyde (MDA), conjugated dienes (CD), electrolyte leakage (EL), chlorophyll a & b and finally carotenoids. Some of the previously cited metabolites are acknowledged as signal molecules and play a role for systematic acquired resistance induction. Therefore, a transcriptomic (RT-PCR) study was also carried out for 29 genes from major defence pathways to monitor potential eliciting properties of this treatment. For the long term study, apple trees were treated by trunk-injection and the plant physiological status was evaluated during one month by non-destructive measures, which are chlorophyll fluorescence and photosynthetic capacity. In parallel, insecticidal activity caused by the essential oil tree-injection on the survival of rosy apple aphid was monitored.

Results show that an oxidative burst has occurred in the few minutes after deposition of the essential oil emulsion on leaves. It seems that apple trees are able to cope with the resulting oxidative stress in the short term, with however an increase in MDA content and a decrease in chlorophyll a and b after 24h. From a long-term perspective, no evidence of phytotoxicity has been noticed on the ecophysiological parameters considered. The results are also conclusive in terms of efficiency of the treatment against rosy apple aphids, with a 60 % death rate after 5 days. Finally, cinnamon essential oil application lead to clear activation of PR defense genes. Extensive study may be considered to investigate the dose-effect relationship, to accurately determine the dose with sufficient insecticidal activity and low phytotoxicity.

Key words: trunk-injection, biopesticide, cinnamon essential oil, *Malus domestica*, phytotoxicity.

Résumé

En tant qu'arbre fruitier culturellement et économiquement important dans le monde entier, la protection des vergers de pommiers a toujours été d'un grand intérêt agronomique. Parmi les insectes ravageurs les plus nuisibles, le puceron cendré du pommier (*Dysaphis plantaginea* Passerini) cause de graves dommages aux plants et présente une résistance sans cesse croissante aux pesticides conventionnels. Couramment traité par des pulvérisateurs en vergers, un système de distribution par injection dans le tronc, combiné à un biopesticide à base d'huiles essentielles, pourrait être une solution pour mettre fin à l'utilisation intensive des pesticides conventionnels.

Dans cette optique, la recherche menée dans le cadre de ce mémoire se concentre sur l'évaluation de l'éventuelle phytotoxicité induite par une émulsion à 2% d'huile essentielle de cannelle sur le pommier *Malus domestica* Borkh (var. Jonagold). Pour ce faire, des paramètres physiologiques, biochimiques et transcriptomiques ont été étudiés. Cette étude de phytotoxicité a été réalisée à court et à long terme, sur de jeunes pommiers micropropagés de deux ans conservés dans des chambres environnementales.

Pour l'analyse à court terme, des feuilles de pommier ont été traitées par application foliaire d'émulsion d'huile essentielle, et échantillonnées à différents moments afin de surveiller les mécanismes moléculaires généralement affectés rapidement après exposition à un stress. Concernant l'initiation d'un hypothétique burst oxydatif et le déséquilibre du système redox, la production de peroxyde d'hydrogène (H_2O_2) et l'état redox du glutathion (GSH) ont été considérés. De plus, la peroxydation des lipides, l'intégrité de la membrane cellulaire et la dégradation des pigments photosynthétiques sont les dommages oxydatifs qui ont été étudiés, à travers la quantification du malondialdéhyde (MDA), des diènes conjugués (CD), de la perte en électrolytes (EL), de la chlorophylle a & b et enfin des caroténoïdes. Certains des métabolites cités précédemment sont reconnus comme des molécules de signalisation et jouent un rôle dans l'induction systématique de la résistance acquise. Par conséquent, une étude transcriptomique (RT-PCR) des principales voies de défense a également été réalisée pour 29 gènes afin de surveiller les propriétés d'élicitation potentielles de ce traitement.

Pour l'étude à long terme, les pommiers ont été traités par injection dans le tronc et l'état physiologique de la plante a été évalué pendant un mois par des mesures non destructives que sont la fluorescence chlorophyllienne et la capacité photosynthétique. En parallèle, l'activité insecticide, provoquée par l'injection d'huile essentielle dans l'arbre, sur la survie du puceron cendré du pommier a été examinée.

Les résultats montrent qu'un burst oxydatif se produit dans les quelques minutes suivant l'application d'émulsion d'huile essentielle sur les feuilles. Il semble que les pommiers soient capables de gérer le stress oxydatif qui en résulte sur le court terme, avec cependant une augmentation du contenu en MDA et une diminution de la chlorophylle a et b après 24h. Dans une perspective à long terme, aucune preuve de phytotoxicité n'a été remarquée sur les paramètres écophysologiques considérés. Les résultats sont également concluants en termes d'efficacité du traitement contre le puceron cendré, avec un taux de mortalité de 60 % après 5 jours.

Enfin, l'application d'huile essentielle de cannelle conduit à une nette activation des gènes de défense PR. Des études approfondies peuvent être envisagées pour étudier la relation dose-effet, afin de déterminer avec précision la dose ayant une activité insecticide suffisante et une faible phytotoxicité.

Mots-clés : injection dans le tronc, biopesticide, huile essentielle de cannelle, *Malus domestica*, phytotoxicité.

Table of content

Acknowledgments

Abstract

Résumé

Contents

List of figures

List of tables

Abbreviations

1. Introduction
 - 1.1. Tree-injection project
 - 1.2. Belgian apple production
 - 1.3. Apple orchards' insect pest: the Rosy Apple Aphid
 - 1.4. Essential oils as biopesticides
 - 1.4.1. Biological properties
 - 1.4.2. Use in pest management
 - 1.4.3. Cinnamon essential oil
 - 1.5. Trunk-injection application
 - 1.6. EO-induced phytotoxicity
 - 1.6.1. ROS generation & Oxidative stress
 - 1.6.1.1. Hydrogen peroxide
 - 1.6.1.2. Glutathione
 - 1.6.2. Cellular oxidative damages
 - 1.6.2.1. Lipid peroxidation
 - 1.6.2.2. Membrane integrity
 - 1.6.2.3. Photosynthetic pigments
 - 1.6.3. Plant physiological status
 - 1.7. Activation of plant defence genes
2. Objectives and strategy
3. Material and method
 - 3.1. EO emulsion formulation
 - 3.2. Trunk-injection settings
 - 3.3. Experimental design
 - 3.4. Phytotoxicity assessment
 - 3.4.1. Short term evaluation
 - 3.4.1.1. H₂O₂ content
 - 3.4.1.2. Glutathione content
 - 3.4.1.3. MDA & conjugated dienes content
 - 3.4.1.4. Electrolyte leakage
 - 3.4.1.5. Chlorophyll & carotenoids contents

3.4.1.6. Defence genes

3.4.2. Long term evaluation

3.4.2.1. Growth parameters

3.4.2.2. Chlorophyll fluorescence

3.4.2.3. Net photosynthetic rate

3.5. Statistical analysis

4. Results and discussion
5. General discussion
6. Conclusion
7. Perspectives
8. Bibliography
9. Appendices

List of figures

- Figure 1 : Leaf damages caused by the rosy apple aphid (Bessin, 2006).
- Figure 2 : Trans-cinnamaldehyde structure (Tripathi and Mishra, 2016).
- Figure 3 : Non-target drift from airblast sprayer foliar sprays versus trunk injection delivery (Wise *et al.*, 2014).
- Figure 4 : Generation of different ROS (Apel and Hirt, 2004).
- Figure 5 : ROS as an integrative part of cell signalling metabolism (Potters *et al.*, 2010).
- Figure 6 : H₂O₂ turnover in plant cells (Neill *et al.*, 2002).
- Figure 7 : H₂O₂ detoxification in the AsA-GSH cycle (Tausz *et al.*, 2004).
- Figure 8 : Glutathione structure (Noctor *et al.*, 2011).
- Figure 9 : MDA as a secondary product of lipid peroxidation (Morales and Munné-Bosch, 2019).
- Figure 10 : MDA different pH-dependent forms in aqueous solutions (Morales and Munné-Bosch, 2019).
- Figure 11 : (A) chlorophyll a and (B) chlorophyll b structures (PubChem).
- Figure 12 : β -carotene structure (PubChem).
- Figure 13 : Possible fate of light energy absorbed by photosystem II (Baker, 2008).
- Figure 14 : The Kautsky fluorescence curve (Hansatech Instruments).
- Figure 15 : Functioning of an open IRGA representation (Mulkey and Smith, 1988).
- Figure 16 : General scheme of stress plant response (Tausz *et al.*, 2004).
- Figure 17 : (A) Injected tree plants and (B) drilled hole focus.
- Figure 18 : Setup for long-term experiment in environmental chambers.
- Figure 19 : Schematic representation of the experimental protocol.
- Figure 20 : Reaction of monobromobimane with glutathione (Hogarth *et al.*, 2003).
- Figure 21 : Reaction between TBA and MDA (Weitner *et al.*, 2016)
- Figure 22 : LeafArea app interface.
- Figure 23 : Sequence of a typical fluorescence trace (Maxwell and Johnson, 2000).
- Figure 24 : Calculation of fluorescence parameters (Maxwell and Johnson, 2000).
- Figure 25 : Evolution of H₂O₂ production from elicitors-vacuum treated apple leaf discs.
- Figure 26 : Evolution of the GSH/[GSH+GSSG] ratio in apple leaves (n = 5).
- Figure 27 : Total glutathione content in apple leaves over time (n = 5).
- Figure 28 : (A) Chromatogram of 80 μ M standard (B) Superposition of calibration peaks (C) Shoulder peak in sample.
- Figure 29 : MDA content in apple leaves over time (n = 5).
- Figure 30 : (A) Superposition of calibration peaks (B) Chromatograms of T24h samples.
- Figure 31 : CD content in apple leaves over time (n = 5).
- Figure 32 : Percentage of electrolyte leakage in apple leaves over time (n = 5).
- Figure 33 : (A) Chl a and (B) Chl b content in apple leaves over time (n = 5).
- Figure 34 : Carotenoids content in apple leaves over time (n = 5).
- Figure 35 : Apple seedlings treated with (A) 0.5 % (B) 1% (C) 2% CEO emulsion.
- Figure 36 : Maximal quantum yield of PSII over time for the different treatments (n = 7).
- Figure 37 : (A) F₀ (B) Φ PSII (C) qP and (D) NPQ values over time for the different treatments (n = 7).
- Figure 38 : (A) A (B) C_i (C) E and (D) g_s values over time for the different treatments (n = 7).
- Figure 39 : Q leaf value over time for the different treatments (n = 7).
- Figure 40 : Variations of (A) stem height (B) trunk diameter and (C) leaf area between measures before and one month after treatment (n = 7).
- Figure 41 : Evolution of the number of living aphids on injected and non-injected trees.
- Figure 42 : Overview of the fit between the GLM model and the mean values of the dataset, with injected trees (blue coloured) and non-injected ones (red coloured).

List of tables

Table 1 : Dunnett's test results for GSH ratios comparison

Table 2 : Dunnett's test results for MDA contents comparison

Table 3 : p-values obtained for one-way ANOVA performed on Chl a (left) and Chl b (right), with Dunnett's test results

Table 4 : Gene expression heatmap for the 29 defence genes considered

Table 5 : p-values obtained for one-way ANOVA performed on chlorophyll fluorescence parameters over time

Table 6 : Dunnett's test performed on F0 at day 1 (left) and on Φ PSII at day 8 (right)

Table 7 : p-values obtained for one-way ANOVA performed on IRGA parameters over time

Table 8 : Dunnett's test performed on Ci at day 8 (left) and day 11 (right)

Table 9 : Dunnett's test performed on E at day 1

Table 10 : p-values obtained for one-way ANOVA performed on growth parameters

Table 11 : p-values obtained for one-way ANOVA performed on the number of living aphids over time

Abbreviations

AChE: Acetylcholinesterase
ANOVA: Analysis of variance
APX: Ascorbate peroxidase
AsA: Ascorbate
BHT: Butylated hydroxytoluene
CA: Cinnamaldehyde
Car: Carotenoids
CAT: Catalase
CD: Conjugated dienes
CEO: Cinnamon essential oil
CHES: 2-(Cyclohexylamino)ethanesulfonic acid
Chl: Chlorophyll
ChlF: Chlorophyll fluorescence
DAD: Diode array detector
DHA: Dehydroascorbate
DTT: Dithiothreitol
EDTA: Ethylenediaminetetraacetic acid
EL: Electrolyte leakage
EO: Essential oil
FLD: Fluorescence detector
FW: Fresh weight
GABA: γ -Aminobutyric acid
GLM: Generalized linear model
GPX: Glutathione peroxidase
GR: Glutathione reductase
GRAS: Generally regarded as safe
GSH: Glutathione
GSSG: Glutathione disulfide
HPLC: High performance liquid chromatography
HRP: Horseradish peroxidase
IPM: Integrated pest management
IRGA: Infrared gas analyzer
LISA: Low-input sustainable agriculture
LOD: Limit of detection
LOQ: Limit of quantification
MBB: Monobromobimane
MDA: Malondialdehyde
MEP: Methylerythritol phosphate
MPA: Metaphosphoric acid
MVA: Mevalonate
MWD: Multiple wavelength detector
PAR: Photosynthetically active radiation
PFPH: Pentafluorophenylhydrazine
PQ: Plastoquinone
PSII: Photosystem II
PUFA: Polyunsaturated fatty acid
RAA: Rosy apple aphid
RH: Relative humidity
ROS: Reactive oxygen species
SOD: Superoxide dismutase
TBARS: Thiobarbituric acid-reactive substance
TCA: Trichloroacetic acid
VOC: Volatile organic compound

1. Introduction

In the second half of the 20th century, the green revolution allowed an unprecedented increase in agricultural yields in developed countries. The foundations of this revolution were particularly based on the generalization of agricultural mechanization and the use of synthetic pesticides and fertilizers. Although the first consequence was a tremendous increase in crop yields, this policy for the transformation of agricultural methods resulted in an agricultural landscape simplification and produced numerous negative side effects on biodiversity, human health, and the quality of soil and water (Mossa, 2016 ; Albert *et al.*, 2017). This is why nowadays, a change in the current agricultural paradigm and the development of more environmentally friendly agricultural practices is strongly required. One of the recent trends in pest management is to reduce heavy reliance on synthetic pesticides and to move towards low-input sustainable agriculture (LISA) as a part of integrated pest management (IPM) (Singh *et al.*, 2002).

In this context, worldwide efforts have been made on integrating essential oils in insect-pest management (Tripathi and Mishra, 2016). Their recent use as plant protection agents includes their insecticide, pesticide and herbicide properties (Grana *et al.*, 2012). Among other advantages, essential oils are likely to break down quickly in the environment and should be acceptable for weed control by organic farmers. They are classified as “generally regarded as safe” (GRAS) (Twokorski, 2002). Despite these promising properties, problems related to their poor water solubility, high volatility, oxidation sensitivity and, more particularly in the frame of this study, the potential phytotoxicity to plants of interest have to be resolved before using essential oils in an alternative pest control system (Moretti *et al.*, 2002).

1.1. Tree-injection project

The "Tree-injection" project aims to create a new method of protecting trees against insect pests based on the injection of natural compounds produced by different plant species (essential oils, hydrodistillates) directly into the tree's vascular system. More specifically, this project focuses on apple orchards protection against the rosy apple aphid using cinnamon essential oil, injected into the xylem with a drilled hole injector (ENDOkIT Manual PRO ©). It runs in collaboration with the Laboratory of Natural Molecules Chemistry of Gembloux Agro-Bio Tech faculty (Liège University), the Biodiversity Research Center of the Catholic University of Louvain and the Walloon Agricultural Research Centre (CRA-W).

This study takes place during the third and last year of the project. Previously, the first objective was to screen among several essential oils the one presenting clear insecticidal properties against the rosy apple aphid, while also evaluating the essential oil translocation within apple tree plants. The next year, a field bioassay was conducted on adult apple trees (15 years old), as well as semi-controlled trial with young grafted apple plants. In parallel, a study of the possible essential oils' phytotoxicity on these trees was initiated. Finally, the present study aims to measure the oxidative stress generated by the essential oil treatment on two years old

micropropagated apple trees maintained in controlled chamber conditions, and its physiological, metabolic and transcriptomic impacts.

1.2. Belgian apple production

Malus domestica Borkh. (Rosales: Rosaceae) is an economically and culturally significant fruit plant grown worldwide, recommended for its useful nutrients (Shah *et al.*, 2020). The management of apple orchards is based on the intensive use of pesticides to control pests and pathogens. For example, protecting apple trees from insect pests can require as many as eight insecticide applications per season (Wise *et al.*, 2014). Currently, farmers are under strong pressure to develop environmentally friendly protection strategies to address the new challenges imposed by society, and environmental laws (Albert *et al.*, 2017).

In Belgium, apple is among the most important fruit production, with 5,810 hectares cultivated and production rising up to 259 840 tons of apples in 2019 (FAOSTAT, 2019). Among the ten or so varieties currently on the market, the Jonagold variety and its mutants account for over 60% of production (Apaq-W). This production can be severely impacted by abiotic and biotic factors. Yield losses due to frost, hail or even droughts can be significant. Apple trees may also suffer from severe attacks from fungal diseases like the apple scab, the powdery mildew and the Marssonina blotch, but also bacterial diseases like the fire blight (Kellerhals *et al.*, 2012) and finally insect pests such as aphids, psyllas, beetles and moths (Jenser *et al.*, 1999).

1.3. Apple orchards' insect pest: the Rosy Apple Aphid

Approximately 60 phytophagous arthropod species are considered to be apple pests (Albert *et al.*, 2017). The rosy apple aphid (RAA) *Dysaphis plantaginea* Passerini (Hemiptera: Aphididae) is among the most detrimental ones both in Europe and North America, causing significant economic losses by reducing yields through sap sucking from the phloem vessels, and exuding sticky honeydew which can promote the development of fungi like sooty mold (Blommers *et al.*, 2004 ; Bessin, 2006 ; Murray and Alston, 2020). Apple trees can be injured by deformation of growing shoots and leaf curling, due to the presence in the aphids' saliva of plant hormone-mimicking compounds (Figure 1) (Brown and Mathews, 2007). This aphid is a holocyclic, i.e., reproducing via asexual (parthenogenesis) and sexual reproduction, and host-alternating aphid species. Indeed, its life cycle is completed on two successive host plants: the apple tree *Malus domestica* Borkh. (Rosales: Rosaceae) as its primary host plant, from early autumn to late spring, and the plantain herb *Plantago* spp. mainly *P. lanceolata* L. (Lamiales: Plantaginaceae) as a secondary host plant, during summer (Dib *et al.*, 2010). Like other heteroecious aphids, the RAA overwinters as eggs on its primary host plant (Blommers *et al.*, 2004).



Figure 1. Leaf damages caused by the rosy apple aphid (Bessin, 2006).

The common strategy to control this aphid pest in conventional apple production is application in the spring of an aphicide, just before flowering and very often followed by a second application after flowering or in early summer. Normally, treatment is recommended if the pest is detected, which leads to routine treatment. In organic apple production, *D. plantaginea* can be controlled by sprays of neem extract (NeemAZal-TS, Trifolio-M GmbH), carefully timed against fundatrices in spring (Cross *et al.*, 2007). Due to its rapid life-cycle and several generations of offspring per season (as many as 40 generations annually under optimal conditions), its resistance to insecticides is ever increasing (Ikbal and Pavela, 2019).

Recent studies have been conducted on the biological control of rosy apple aphid in apple orchards using hymenopteran parasitoids (Bribosia *et al.*, 2005), predators (Brown and Mathews, 2007) but also entomopathogenic fungi (Bird *et al.*, 2004). Concerning predators, the most abundant natural enemies in the spring are the ladybirds *Adalia bipunctata* L. and *Harmonia axyridis* Pallas (Coleoptera: Coccinellidae), but also *Episyrphus balteatus* DeGeer (Diptera: Syrphidae) and *Aphidoletes aphidimyza* Rondani (Diptera: Cecidomyiidae). However, according to Dib *et al.* (2010), none of these predators provide an efficient control of RAA in orchards. *A. aphidimyza*, for example, occurs too late in the RAA lifecycle (Miñarro *et al.*, 2005). In contrast, *E. balteatus* and *A. bipunctata* are only effective in reducing RAA populations on apple seedlings under laboratory and field cage conditions.

1.4. Essential oils as biopesticides

1.4.1. Biological properties

Plants synthesize an array of chemical compounds that are involved in a variety of plant–plant, plant–microbe and plant–herbivore interactions. These exhibit a great structural and functional diversity, and are produced within plants as a result of secondary metabolism (Singh *et al.*, 2006). An essential oil (EO) is internationally defined as the product obtained from vegetable raw material, either by hydro-, steam- or dry distillation, or by a suitable mechanical process without heating (for the epicarp of Citrus fruits) (Rubiolo *et al.*, 2010 ; Turek and Stintzing, 2013). They can be synthesized by all plant organs : flowers, buds, seeds, leaves, twigs, bark, herbs, wood, fruits and root (Bakkali *et al.*, 2008). Composed of lipophilic and highly volatile secondary metabolites (generally named volatile organic compounds VOCs), essential oils are

characterized by a strong odor (Tripathi *et al.*, 2009). The quantity found is 1 to 2% in most plants, but rarely some can contain up to 10% (Grana *et al.*, 2012).

Plant terpenoids (oxygen containing hydrocarbons) are one of major chemical class of plant-derived secondary metabolites. Allowing a great variety of structures with diverse functions, monoterpenoids are notably the most representative molecules, constituting 90 % of the essential oils (Tripathi *et al.*, 2009). Monoterpenes contain a basic skeleton of 10-carbon atoms derived from fusion of two isoprene units (C₅H₈) and the plastids of plants are regarded to be the site of their synthesis (Ibrahim *et al.*, 2001).

Phenylpropanoids are other common constituents of essential oils. This family of aromatic compounds is characterised by a carbon skeleton formed by a benzoaromatic and a chain of three carbon atoms. Occurring less frequently than terpenoids, they are derived from phenylpropane e.g. aldehyde: cinnamaldehyde; alcohol: cinnamic alcohol; phenols: chavicol, eugenol, ... (Tripathi *et al.*, 2009). Biogenetically, terpenoids and phenylpropanoids have different primary metabolic precursors and are generated through different biosynthetic routes: the two main pathways involved in terpenoids are the mevalonate (MVA) pathway in the cytosol and the methylerythritol phosphate (MEP) pathway in the plastids, whereas phenylpropanoids originate through the shikimate pathway (Miguel, 2010 ; Pavella and Benelli, 2016).

1.4.2. Use in pest management

By definition, a biopesticide is “a generic term generally applied to a substance derived from nature, such as a microorganism or botanical or semiochemical, that may be formulated and applied in a manner similar to a conventional chemical pesticide and that is normally used for short-term pest control [adapted from ISPM Pub. No. 3, 1996 (IPPC, 2005)]” (FAO and WHO, 2017).

In addition to their widespread use as flavouring materials, essential oils represent a “green” alternative in the agricultural field due to reported antimicrobial, antiviral, nematicidal and antifungal properties (Turek and Stintzing., 2013). Their lipophilic characteristic may favour the expansion of cell membranes and its destruction through increasing fluidity or inhibiting membrane enzymes (Grana *et al.*, 2012). In addition, EOs have some properties that make them suitable for insect management. The main active constituents with insecticidal activity are monoterpenes, sesquiterpenes and related phenylpropenes (Mossa, 2016). Unfortunately, little is known about the physiological actions of essential oils on insects, but treatments with essential oils or their constituents have been reported to cause symptoms suggesting a neurotoxic mode of action (Coats *et al.*, 1991; Kostyukovsky *et al.*, 2002), notably through octopamine synapses, γ -aminobutyric acid (GABA) and acetylcholinesterase (AChE) inhibitions (Mossa, 2016; Pavella and Benelli, 2016). Octopamine acts as a neurotransmitter in insects, and interrupting its functioning results in total breakdown of nervous system. As this target site is not shared with mammals and fish, most essential oil chemicals are relatively non-

toxic to them in toxicological tests, and meet the criteria for “reduced risk” pesticides (Tripathi *et al.*, 2009). Another aspect is that while resistance development continues to be an issue for many synthetic insecticides, it is likely that resistance will emerge more slowly to essential-oil-based insecticides thanks to the complex mixtures of constituents characterizing these oils (Pavella and Benelli, 2016).

1.4.3. Cinnamon essential oil

Belonging to the Lauraceae family, the genus *Cinnamomum* includes about 250 species, with an inter- and intraspecific variability existing in volatile compound composition because of ecotypic and chemotypic variations between populations (Koul *et al.*, 2008 ; Wang *et al.*, 2009). Only the *Cinnamomum cassia* J.Presl essential oil (CEO, also named Chinese Cinnamon) will be considered in the present study.

Previous reports have pointed out that *C. cassia*-derived materials have insecticidal and antifeeding effects against insect pests (Huang and Ho, 1998; Lee *et al.*, 2008; Kim *et al.*, 2003). In their study, Park *et al.* (2000) demonstrated that the insecticidal constituent of the *Cinnamomum* bark was identified as trans-cinnamaldehyde (CA), a major compound of *Cinnamomum cassia* J.Presl (79.49% in CEO purchased from Pranarôm, batch number: CCB114, characterisation detailed in Appendix 1). CA (C₉H₈O) consists of a phenyl group attached to an unsaturated aldehyde (Figure 2).

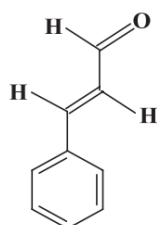


Figure 2. Trans-cinnamaldehyde structure (Tripathi and Mishra, 2016).

Previously, the Mycotech Corporation U.S. company has developed an aphicide/miticide/fungicide based on cinnamaldehyde (30% in the formulation) as the active ingredient (Koul *et al.*, 2008). Cinnamaldehyde is also synthesized chemically for use as an agricultural fungicide (e.g., VertigoTM, CinnacureTM) on a variety of crops. According to Dayan *et al.* (2009), its mode of action apparently consists in the inhibition of synthesis of the fungal cell wall component chitin. Concerning the antibacterial activity, cinnamaldehyde has been described as interacting with the monolayers of lipids mimicking bacterial membrane (Nowotarska *et al.*, 2014). More recently, it has been discovered that while the monoterpenes could disturb the lipid organization and/or domain formation, the phenylpropanoid cinnamaldehyde could rather interact with membrane receptors (Lins *et al.*, 2019). Finally, recent research demonstrated the herbicidal activity of CA against *Echinochloa crus-galli*, the world’s worst weed in rice (Saad *et al.*, 2019).

1.5. Trunk-injection application

The use of essential oils already looks promising for weed control in organic agriculture, but these natural pesticides are active for a relatively short time and they volatilize quickly, which limits their effectiveness (Dayan *et al.*, 2009). Another important issue is that with conventional airblast sprayers, only about 50 % of any pesticide comes into contact with the target pest, and as a consequence growers apply more pesticide than needed to account for the amount that does not reach the pest (Pimentel and Burgess, 2011). The third aspect is that while in developed countries mechanized sprayers are used by almost all farmers, smallholder farmers in developing countries often depend on even less efficient hand sprayers to deliver crop protection materials (Wise *et al.*, 2014).

In response to these issues, trunk injection has emerged as an alternative to conventional sprayers for treating and protecting fruit crops (VanWoerkom *et al.*, 2014) (Figure 3). For control of foliar pests, the results obtained by Wise *et al.* (2014) suggest that trunk injection is a promising plant delivering system, with numerous benefits. In addition to eliminating spray drifts, the pesticide load in agro-ecosystems is reduced, health and safety of farm workers is improved and small amounts of protection materials are required to be delivered per injection. Concerning the technical aspect, water soluble chemicals or emulsified preparations (in the case of non-water-soluble products) enter through an opening in the cambium of the tree and move into the tree mainly in the xylem sap. Because water evaporation (transpiration) pulls water up to the leaves through the vascular tissues, this method seems to be ideal for treating piercing-sucking insects like aphids (Kuhns, 2011).

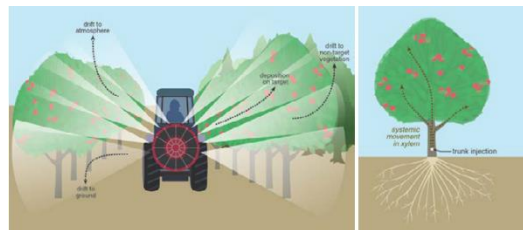


Figure 3. Non-target drift from airblast sprayer foliar sprays versus trunk injection delivery (Wise *et al.*, 2014).

1.6. EO-induced phytotoxicity

The concept of phytotoxicity is related to plant injuries caused by chemicals (Ibrahim *et al.*, 2001). Phytotoxicity of essential oils requires serious attention when formulating products for agricultural and landscape use (Tripathi *et al.*, 2009). It's also important to know if the phytotoxic activity of an essential oil could result either from a synergistic action of different oil components, or antagonistic (Koul *et al.*, 2008). Moreover, it is necessary to know specifically their potential influence on the plant species of interest because it's possible that one EO has a phytotoxic effect on one crop but not on another (Synowiec *et al.*, 2019).

The following sections will attempt to describe plant physiological and biochemical processes that could potentially be affected by a xenobiotic stress induced by cinnamon essential oil in apple trees, as well as chemical markers commonly studied to assess the plant stress status.

1.6.1. ROS generation & Oxidative stress

In plants, reactive oxygen species (ROS) are continuously produced in chloroplasts, mitochondria and peroxisomes (Ahuja *et al.*, 2015). The term ‘ROS’ includes singlet oxygen $^1\text{O}_2$, superoxide and hydroxyl radicals $\text{O}_2^{\cdot -}$ & OH^{\cdot} , and hydrogen peroxide H_2O_2 (Figure 4). These small molecules are highly reactive and toxic. They are implicated in most, if not all, stress responses: environmental stresses such as exposure to high light (photoinhibition, photooxidation), temperature, drought, heavy metals, air pollutants including ozone, mechanical and physical stresses, and finally pathogens invasion (Foyer *et al.*, 1997). As normal by-products of aerobic metabolism, ROS are partly formed through side reactions of electron transport chains. Under various stresses, the limitation of carbon fixation in the Calvin cycle leads to a decrease in utilization of NADPH and results in deviation of electrons from the electron transport chain to alternative acceptors, predominantly molecular oxygen (Tausz *et al.*, 2004 ; Gupta and Igamberdiev, 2010).

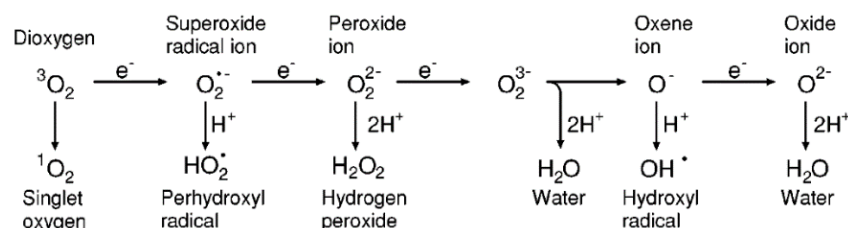


Figure 4. Generation of different ROS (Apel and Hirt, 2004).

The term oxidative stress still lacks a precise definition, but the key hallmarks are (1) enhanced ROS production (generally called oxidative burst), with production rates overwhelming the natural protective detoxifying rates; (2) oxidative damage to cellular components ; causing (3) the accumulation of damaged cellular components that somehow lead to loss of function and eventual cell death (Foyer and Noctor, 2011).

Within the plant cellular redox system, ROS possess a dual role as both toxic byproducts of aerobic metabolism and key regulators of growth, development and defense pathways (Mittler *et al.*, 2004). On the one hand, the excessive generation of ROS induces oxidative stress and damage membranes, DNA, proteins, photosynthetic pigments and lipids, ultimately leading to programmed cell death if not detoxified (Singh *et al.*, 2008 ; Uchendu *et al.*, 2010 ; Ahuja *et al.*, 2015). On the other hand, low levels of ROS could serve as signal molecules in the induction of defence genes against cadmium toxicity for example (Chen *et al.*, 2011). (Figure 5).

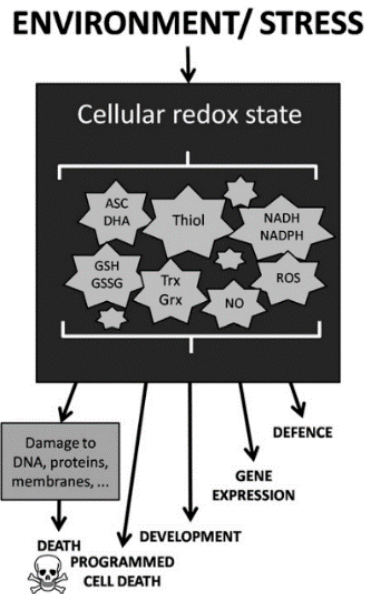


Figure 5. ROS as an integrative part of cell signalling metabolism (Potters *et al.*, 2010).

The antioxidative defense system is composed of hydrophilic (e.g., ascorbate, glutathione) and lipophilic antioxidants (α -tocopherol) as well as detoxifying enzymes. Antioxidative enzymes such as superoxide dismutases (SOD), catalases (CAT), ascorbate peroxidase (APX), glutathione peroxidase (GPX) and glutathione reductase (GR) are the major components in the ROS scavenging system. In the order of the reaction chain, SOD is a major scavenger of superoxide $O_2^{\bullet -}$ and its enzymatic action results in the formation of H_2O_2 , itself further detoxified into H_2O and O_2 by increased activity of CAT in peroxisomes, APX in chloroplasts and cytosol, and GPX in cell wall (Mutlu *et al.*, 2011 ; Hernandez *et al.*, 2015 ; Radhakrishnan *et al.*, 2018).

1.6.1.1. Hydrogen peroxide

As a strong oxidant, hydrogen peroxide can lead to disruption of metabolic functions and losses of cellular integrity at sites where it accumulates. H_2O_2 is the most stable of the ROS and is capable of rapid diffusion across cell membranes. During the oxidative burst, high quantities of H_2O_2 are produced by the action of the plasma membrane-associated superoxide synthase together with apoplastic SOD (Foyer *et al.*, 1997), but H_2O_2 is also produced by many other enzymatic and non-enzymic processes in plants (Figure 6). Whilst deleterious to some cellular components, H_2O_2 is essential to plants in various biosynthetic reactions and, as suggested by some studies, is possibly also involved in signal transduction pathways that could contribute to plant defence (Velikova *et al.*, 2000 ; Stone and Yang, 2006).

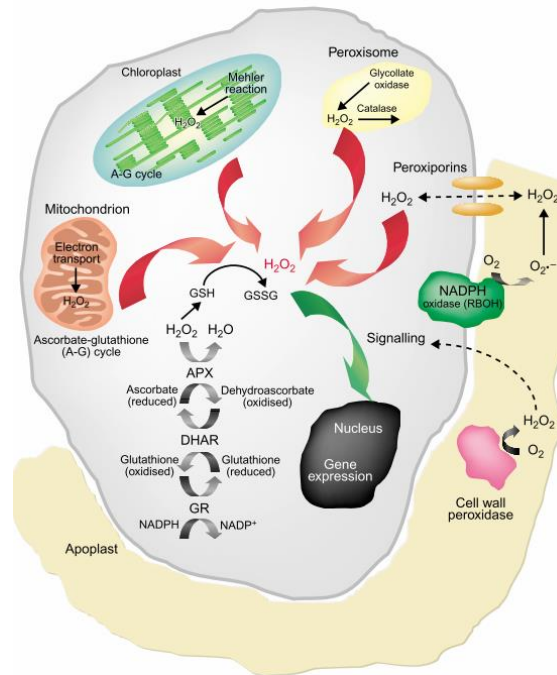


Figure 6. H_2O_2 turnover in plant cells (Neill *et al.*, 2002).

1.6.1.2. Glutathione

As mentioned above, plant cells are well equipped to efficiently scavenge ROS and its reaction products by the coordinated and concerted action of non-enzymatic and enzymatic antioxidant components. Among the non-enzymatic ones, glutathione is a major component of ascorbate-glutathione (AsA-GSH) pathway, playing a significant role in protecting cells against ROS-accrued potential anomalies (Gill *et al.*, 2013) (Figure 7). Most data suggest that enhanced ROS availability has less impact on the ascorbate-dehydroascorbate (DHA) ratio than on the redox status of the glutathione pool (Foyer and Noctor, 2011). Various stress conditions drive characteristic changes in the intracellular amount and redox state of glutathione. Thus, modifications in the whole glutathione status can be taken as a reliable marker of the degree of intracellular oxidative stress (Queval *et al.*, 2011; Hajdinák *et al.*, 2019). The main function of glutathione consists in redox-homeostatic buffering, serving as a ROS scavenger, but it also plays a role in stress perception, signalling and defence reactions (Davey *et al.*, 2003; Noctor *et al.*, 2012).

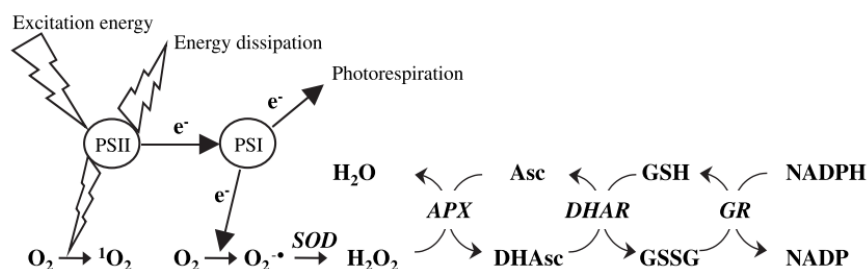


Figure 7. H_2O_2 detoxification in the AsA-GSH cycle (Tausz *et al.*, 2004).

The soluble tripeptide GSH (L- γ -glutamyl- L-cysteinyl-glycine) is the principal low-molecular-weight thiol compound in plants (Foyer *et al.*, 1997) (Figure 8). Glutathione typically accumulates in plant tissues in the range of 200-600 nmol /g FW (Noctor *et al.*, 2011). Under normal (unstressed) conditions, it is maintained mostly in its reduced form, resulting in a GSH/GSSG ratio of 10 to 1 (i.e. $GSH/(GSH+GSSG) = 91\%$) (Hogarth *et al.*, 2003). In contrast, under oxidative conditions, each sulfur atoms in two GSH molecules donate one electron and react together to form glutathione disulfide (GSSG) (Giustarini *et al.*, 2016). The thing is that, thanks to the specific enzyme glutathione reductase (GR), GSSG can be reduced back to GSH (Noctor *et al.*, 2011). In other words, GSH fluctuates in cells between two different forms: reduced GSH and oxidised GSSG, as a function of GR activity (with NADPH as an electron donor) (Ahuja *et al.*, 2015). Only in a strongly oxidizing environment, the proportion of GSSG increases substantially (Foyer and Noctor, 2011). Therefore, a decrease in GSH and GSH/(GSH+GSSG) ratio are interpreted as an evidence of redox unbalance (Giustarini *et al.*, 2016).

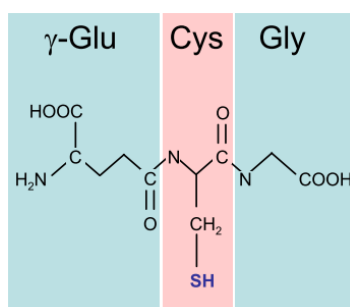


Figure 8. Glutathione structure (Noctor *et al.*, 2011).

1.6.2. Cellular oxidative damages

1.6.2.1. Lipid peroxidation

In biological systems, oxygen-derived free radicals have repeatedly been demonstrated to play a role in cellular injury through a chain reaction which leads to lipid peroxidation. Indeed, much of the injury caused by exposure to biotic and abiotic stresses is associated with oxidative damages at the cellular level, particularly losses in biomembranes integrity due to formation of lipid peroxides (Foyer *et al.*, 1997). Lipid peroxidation is the introduction of a functional group containing two catenated oxygen atoms O-O into unsaturated fatty acids in a free radical chain reaction (Wheatley, 2000). It should be noted that following a pathogen invasion or injury, this reaction may also originate from increased lipoxygenase activity (Morales and Munné-Bosch, 2019).

The initial reaction between ROS and polyunsaturated fatty acids (PUFAs), constituting the plasma membranes of plant cells, produces a lipid radical which then abstracts an allylic

hydrogen from neighbouring fatty acids to produce lipid hydroperoxide (LOOH) and a second lipid radical (Lykkesfeldt, 2001 ; Jambunathan, 2010). This dienyl radical is stabilised via double-bond rearrangements (electron delocalization), originating conjugated dienes and trienes (i.e. two or three double bonds separated by only one single bond) (Miguel, 2010). In brief, the process of lipid peroxidation causes the double bonds to move in fatty acid molecules, methylene-interrupted dienes becoming conjugated (Wheatley, 2000). With this in mind, conjugated dienes may be considered as an index of first damaged oxidized PUFAs (Sergent *et al.*, 1993).

Apart from that, as primary lipid hydroperoxides are highly instable and reactive, quantification of lipid peroxidation is usually estimated by focusing on secondary oxidation products derived from them (Davey *et al.*, 2005), such as malondialdehyde (MDA) (Figure 9). In studies related to oxidative stress, the measurement of MDA content has been demonstrated to be a reliable lipid peroxidation marker, thus representative of a rather late stage of oxidation (Miguel, 2010 ; Morales and Munné-Bosch, 2019).

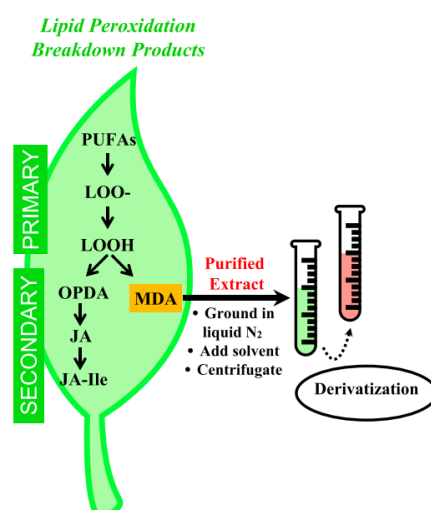


Figure 9. MDA as a secondary product of lipid peroxidation (Morales and Munné-Bosch, 2019).

Originating from polyunsaturated fatty acids, it's well known that in *Arabidopsis thaliana* leaves for example, mostly linoleic acid and other tri-unsaturated fatty acids are the source of up to 75% of MDA produced (Weber *et al.*, 2004). Chemically, this small and reactive organic molecule consists in a three carbon structure with two aldehyde groups. Present in all eukaryotes, MDA exists in different pH-dependent tautomeric forms in aqueous solutions. At an alkaline pH, the enolate anion is the dominate form, characterised by a low chemical reactivity. However, at lower pH than its pKa (4.46), the protonated enol aldehyde and dialdehyde forms are in equilibrium, which are both highly reactive (Seljeskog, 2006 ; Farmer and Mueller, 2013 ; Morales and Munné-Bosch, 2019) (Figure 10).

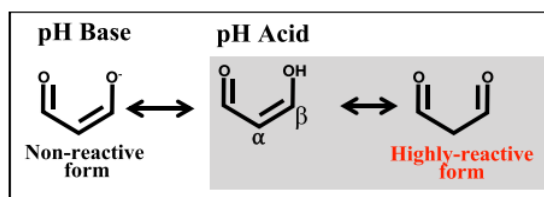


Figure 10. MDA different pH-dependent forms in aqueous solutions (Morales and Munné-Bosch, 2019).

1.6.2.2. Membrane integrity

In addition to enhanced lipid peroxidation, electrolyte leakage resulting in loss of membrane integrity is among the key factors that determine cellular injury (Singh *et al.*, 2006). Often via ROS-induced stress biomembranes peroxidation, breaches in the lipid bilayer lead to uncontrolled leakage of electrolytes and ultimately to cell death. (Dayan and Watson, 2011). Moreover, EOs components like monoterpenes being lipophilic, they could penetrate the cell membrane, change their fluidity and induce expansion resulting in the disruption of the membrane and hence ion leakage (Ahuja *et al.*, 2015).

1.6.2.3. Photosynthetic pigments

After treatments with EOs, a decrease in the photosynthetic pigments namely chlorophylls and carotenoids in a dose-dependent way have already been reported, resulting from a direct pigment degradation or from an impairment in pigment biosynthetic pathways (Chowhan *et al.*, 2011 ; Poonpaiboonpipat *et al.*, 2013).

As an easy to achieve measure, total leaf chlorophyll content is a popular trait to get an idea of the plant photosynthetic capacity. Chl a and Chl b are the two forms of pigments that predominate in higher plants. Differently involved in light assimilation, Chl a is linked to the photosystems energy-processing centres whereas Chl b is an accessory pigment for harvesting light energy and transmits it to Chl a (Bresson *et al.*, 2018) (Figure 11).

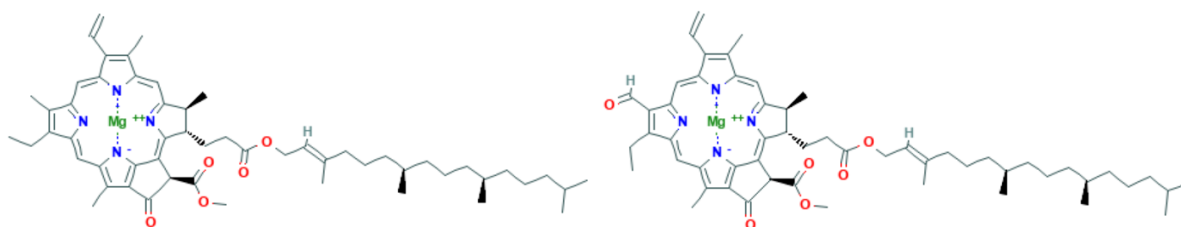


Figure 11. (A) chlorophyll a and (B) chlorophyll b structures (PubChem).

Concerning carotenoids (Car), they act first as collectors of light energy driving photosynthetic processes. Thanks to their long-unsaturated chain, the light-harvesting ability of carotenoids allows for utilization of blue-green light that is poorly or not absorbed by the Chls (Figure 12). As antioxidants, their second role is the photosynthetic system protection against detrimental

effects of light and O₂ (photooxidation), by scavenging ROS and the quenching of Chl excited states (Gitelson and Merzlyak, 2004 ; Radhakrishnan *et al.*, 2018).

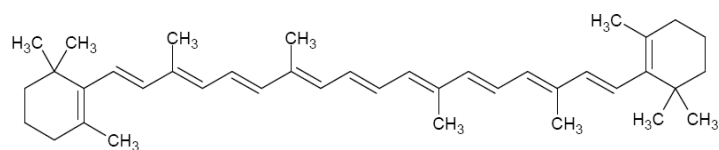


Figure 12. β -carotene structure (PubChem).

1.6.3. Plant physiological status

Physiological stress responses in plants are also the key to understand ongoing biological scenarios. Vegetative growth parameters showing a significantly inhibited development in plants exposed to cinnamon oil would be a clear indicator of plant stress. Previously, it has been reported that interactions between membranes and terpenoid content of oils could lead to changes in their structure and function, which, in turn, may impair growth and activity of the cells (Sikkema *et al.*, 1995). Moreover, damages to photosystems and pigments degradation might cause cell death and impairment of the histological characteristics of leaves and buds on plants, resulting in their poor growth and development (Shah *et al.*, 2020).

With this in mind, ecophysiological tools in chlorophyll fluorescence and gas exchange generally provide opportunities for the evaluation of the Calvin cycle capacity, photoprotective energy dissipation and photorespiration (Tausz *et al.*, 2004).

Photosynthetic efficiency can be assessed non-destructively by monitoring chlorophyll fluorescence (ChlF) with a fluorimeter in order to detect various plant stresses. The general principle behind this method is that, in a leaf, absorbed light energy can be managed in three different ways: it can be used to drive photosynthesis (photo-chemistry), dissipated as heat or it re-emitted as light-chlorophyll fluorescence for excess energy (Bourri , 2007) (Figure 13). These three processes occur in competition, in such a way that energy dissipation via chlorophyll fluorescence increases due to a decrease in photochemical pathways.

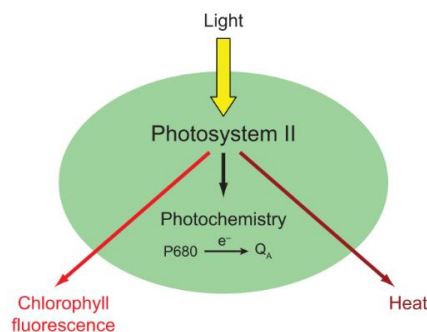


Figure 13. Possible fate of light energy absorbed by photosystem II (Baker, 2008).

ChlF provides an indication of the photosystem II (PSII) capacity to return to ground state after being exposed to a short burst of light (Dayan *et al.*, 2000). In fact, dark-adapted leaves re-emit light in red wavebands after receiving a saturating flash, which is quantified by the instrumental tool.

The “Kautsky effect” is observed when a leaf transferred from dark to light has its fluorescence that rapidly increases (within 1 s or so) and then slowly decreases to steady state (Figure 14). Basal fluorescence F_0 corresponds to the situation where energy is not transferred to the PSII reaction centres due to the dark adaptation step. On a physiological level, this operation removes the energy engine of photosynthesis (photons) and empties the electron transfer chain, making the reaction centres fully available (Bourri , 2007). Then, a brief saturating flash induces a maximum value of fluorescence (F_m). At this time, electron acceptors of PSII are saturated. The variable fluorescence F_v is calculated by difference between F_0 and F_m . Amongst the parameters defined to determine the PSII photochemistry status, the maximal quantum yield of PSII ($F_v/F_m = F_m - F_0/F_m$) is a widely used indicator of physiological status (Genty *et al.*, 1989).

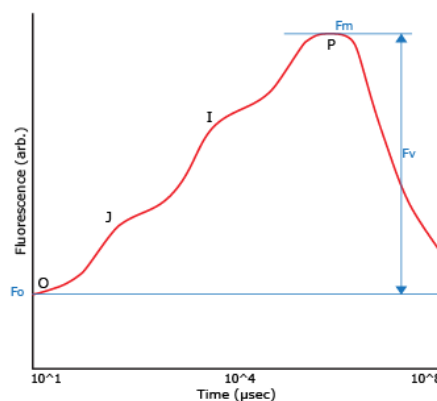


Figure 14. The Kautsky fluorescence curve (Hansatech Instruments).

Another noninvasive method of evaluating physiological effect of photosynthesis inhibitors on plants consists of monitoring carbon dioxide and water vapour exchange by using an infrared gas analyzer (IRGA) (Dayan *et al.*, 2000). The basic concept behind the system is that heteroatomic gases absorb infrared radiations (major absorption band at 4.25 μm for CO_2 with secondary peaks at 2.66, 2.77 and 14.99 μm , and H_2O molecules also absorbing in the 2.7 μm region), but gas molecules consisting of two identical atoms (e.g. O_2 , N_2) do not absorb this long-wave IR radiation (Long *et al.*, 1996). Thus, an IRGA measures the reduction in transmission of IR wavebands caused by the presence of a heteroatomic gas between the radiation source and a detector (Mulkey and Smith, 1988). In open systems (also called differential systems), estimations of leaf net assimilation and transpiration rates are based on differences of CO_2 and H_2O concentrations of two split fractions of air : one fraction passing through the leaf cuvette chamber to an IRGA, and the other one flowing freely from the entrance into a second IRGA as a reference (Gall  and Flexas, 2010 ; Douthe *et al.*, 2018) (Figure 15). It’s therefore possible to determine the leaf net assimilation and transpiration rates.

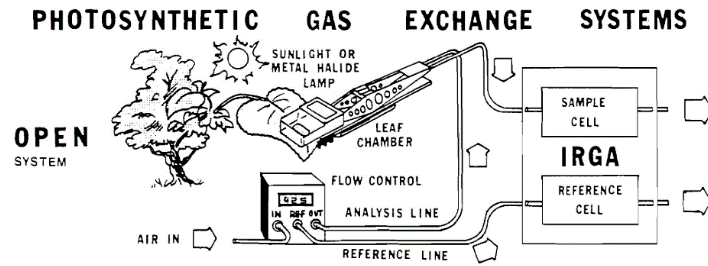


Figure 15. Functioning of an open IRGA representation (Mulkey and Smith, 1988).

Lastly, morpho-metrical characteristics including plant length, stem diameter, internodal lengths, leaf surface and color ratio can also provide information related to inhibition of the normal plant development.

1.7. Activation of plant defence genes

Pathogenesis-Related (PR) proteins have been defined as plant host proteins that are produced only in response to attack by pathogens or by a related event (van Loon *et al.*, 1994). Demonstrating the expression of PR genes has been widely accepted as a hallmark of plant defensive systemic acquired resistance (SAR) induction (Bonasera *et al.*, 2006 ; Oliveira *et al.*, 2016). The SAR, which is a form of induced resistance in plants with a specific defense signaling pathway, can also occur after spraying with a synthetic or natural compound, commonly known as an inducer (Dugé de Bernonville *et al.*, 2014). The most commonly screened PR genes expressed in apples and other plant-pathogen systems are PR-1 (antifungal activity), PR-2 (β -1,3-glucanase), and PR-8 (class III chitinase) (Ebrahim *et al.*, 2011).

Apart from those coding for PR proteins, other genes can represent a widest diversity of known plant defence mechanisms. The types of metabolic pathways to which these genes are related include secondary metabolic pathways (phenylpropanoids and isoprenoids), antioxidant mechanisms, cell wall modifications and hormonal signalling pathways in apple tissues (salicylic acid, jasmonic acid and ethylene).

A molecular tool such as quantitative real-time PCR may be useful to detect changes in expression levels of such defence genes, with the aim to challenge the hypothesis that cinnamon essential oil could play the role of a defence inducer in apple trees.

2. Objectives and strategy

During the previous years of the project, efforts have been focused on the biopesticide formulation and trunk-injection method. The aim of this work is to prove the biopesticide safety for plants in this kind of application. To do so, the phytotoxicity induced by the injection of essential oil into the trunk of apple trees was evaluated by studying physiological, phenotypic and biochemical parameters allowing the identification of the stress generated on plants.

As described by Larcher (2003), the ecophysiological response of plants to stressors in general can be described in a general kinetic concept, depending on acclimatisation to these factors or not (Figure 16). The capacity of plant metabolism to detoxify, compartmentalize, and transform natural compounds makes it especially important to monitor not only the primary, short-term effect, but also the secondary effects of natural products in the medium and long term, thus testing the persistence of the compound's phytotoxic action on the target plants (Graña *et al.*, 2013).

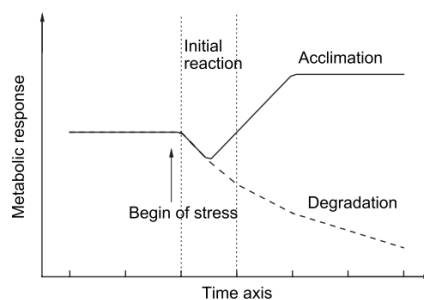


Figure 16. General scheme of stress plant response (Tausz *et al.*, 2004).

With this in mind, general objectives were separated into two main parts:

a) Short term toxicity

This part focuses on biochemical processes that are known to be impacted at a cellular scale relatively rapidly after stress exposition (from a few minutes to a few hours). In order to study the mode of action of the essential oil on plants, apple tree leaves were treated by foliar application with a hand sprayer (30 mL). The chemical markers therefore studied to assess the plant stress status and oxidative damages are as follows: hydrogen peroxide H₂O₂, glutathione GSH, malondialdehyde MDA, conjugated dienes CD, electrolyte leakage EL, chlorophyll a & b and carotenoids.

The aim of these experiments is to answer two sub-questions :

- * If it occurs, how long after CEO foliar application is an oxidative burst observed?
- * To what extent does this oxidative burst cause damages to the plant?

To do so, the impact of application time on the parameters described above was studied.

Apart from that, the study of the activation of several plant defence genes was also carried out on plants treated under the same conditions. The objective was to determine if sprays of CEO emulsions increase the expression of these genes specifically.

b) Long term toxicity

In this section, to be in the conditions of the application mode selected in the frame of the project, apple trees were treated by trunk-injection and physiological parameters such as chlorophyll fluorescence and photosynthetic capacity were assessed during one month to highlight possible stress signs in the medium and long term.

In parallel to this, the bioactivity caused by the essential oil tree-injection on the rosy apple aphid was measured by performing an aphid survival monitoring.

3. Material and method

3.1. EO emulsion formulation

In the previous years of the Tree Injection project, a suitable formulation for injecting cinnamon essential oil into the cambium of apple trees was developed. It's well known that due to their lipophilic nature, surfactants are often required to assist in the spreading of essential oils (Dayan *et al.*, 2009). In our case, to ensure optimal compound delivery, the physical properties of the solution delivered to the trees must be as close as those of xylem sap, which is an aqueous medium. So, the non-ionic surfactant Tween® 80 (CAS-No: 9005-65-6; Sigma–Aldrich Co.) was chosen as the emulsifier compound in order to facilitate absorption of the essential oil and to obtain a bio-compatible and stable EO emulsion in water. For trunk-injected solutions only, adding EDTA (Titriplex® III, Merck Millipore) to the formulation was considered to chelate Ca²⁺ ions that would otherwise participate in processes that seal the phloem like callose plug formation in sieve pores (Tetyuk *et al.*, 2013). The complete emulsion preparation protocol is available in Appendix 2.

3.2. Trunk-injection settings

Given the trunks' small diameter of the trees, a standardized and easily reproducible injection method was developed. A no-pressure system based on drip pockets (e.g. Baxter) and needles for medical practices is used, consisting for each tree of one drip with a conduct and a needle (Figure 17). Precautions were taken to avoid loss from the delivery system to weight the administrated quantity (by the difference in mass of the drip pocket between before and after injection). Details of the injection protocol can be found in Appendix 3.



Figure 17. (A) Injected tree plants and (B) drilled hole focus.

3.3. Experimental design

a) Short term experiment

The experiment was carried on two-year-old *Malus domestica* Borkh (var. Jonagold) micropropagated apples trees, free of flowers or fruits but having developed mature and fully expanded leaves (plant length = 53 ± 8 cm; stem diameter = 4.4 ± 0.6 mm). They were conserved in an environmental chamber operating under the following conditions: $21 \pm 0.5^\circ\text{C}$, 60 ± 10 % relative humidity RH, 16:8h light:dark periods and a PAR intensity equal to $50 \mu\text{mol} / \text{m}^2 \text{ s}$. Apple trees were watered every three days with 50 mL of water. It is noticeable that just before the experiment, trees were confronted to two main pests during their storage in the greenhouse : powdery mildew and mites. The phytosanitary products applied to fight these pests were Corbel (BASF) / Difcor (Globachem) and black soap 10% water solution respectively.

The factor defining this experiment is the time of foliar application. Thus, two different modalities were tested for the treatment applied:

- * Leaves treated with cinnamon EO emulsion at 2% (v/v) [CEO 2%]
- * Untreated leaves, considered as blanks [BI or T0]

Based on the literature and preliminary tests, application times were quite different depending on the metabolites measured:

H_2O_2 & GSH:	$t = 5 \text{ min} / 15 \text{ min} / 30 \text{ min} / 1\text{h} / 2\text{h}$
MDA:	$t = 1 / 2 / 4 / 6 / 24 / 48 / 72\text{h}$
CD, Chl a & b, Car and EL :	$t = 3 / 6 / 24 / 48 / 72\text{h}$

At each time step after foliar application of around 2 mL of CEO emulsion, five leaves for each modality were sampled at different heights from young apple trees, and directly immersed in liquid nitrogen (except for EL measurement, carried out on fresh leaf discs).

b) Long term experiment

The experiment was carried on two-year-old *Malus domestica* Borkh (var. Jonagold) micropropagated apples trees, conserved in the same conditions as for the short term experiment, in an environmental chamber at the UCLouvain from May to July 2021.

For this part, four modalities in the experimental design were considered:

- A) Non-injected trees, as Controls
- B) Non-injected trees with aphids deposited on leaves
- C) Trunk-injected trees during around 2 days (44h) with CEO 2% (v/v) emulsion
- D) Injected trees as C) with aphids



Figure 18. Setup for long-term experiment in environmental chambers.

Each treatment was tested on seven apple tree replicates ($n = 7$). For modalities B and D, 15 second instar larvae of *D. plantaginea* were deposited at the end of the injection, just after the drip pockets have been disconnected from the trees.

One leaf located at mid-height of the tree was selected for measurements of chlorophyll fluorescence and another one for photosynthetic capacity. All the measures were performed on the same leaves and at the same moment of the day between the sampling sessions, every two days during the first week, then every week during one month.

Concerning the aphid survival monitoring, the number of living individuals was recorded during 4 weeks (3 generations).

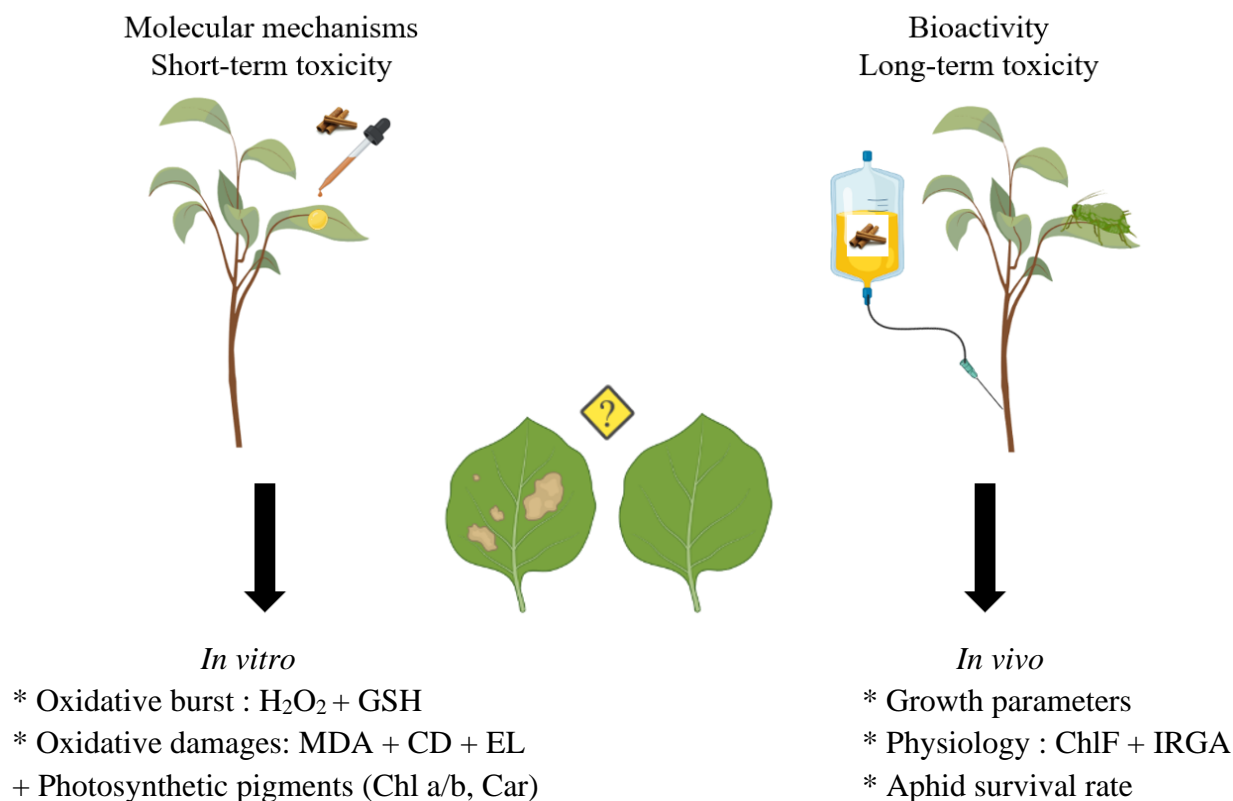


Figure 19. Schematic representation of the experimental protocol.

3.4. Phytotoxicity assessment

3.4.1. Short term evaluation

3.4.1.1. H₂O₂ content

Firstly, the Amplex® Red reagent (10-acetyl- 3,7-dihydrophenoxazine) reacts with H_2O_2 , with the enzymatic catalysis of horseradish peroxidase (HRP). The resulting product is the red-fluorescent compound resorufin, which can be detected fluorometrically or spectrophotometrically (Brumbarova *et al.*, 2016).

Protocol achieved

An Amplex® Red assay kit (Amplex Red, DMSO, HRP, phosphate buffer (5X)) was purchased from Sigma-Aldrich (Catalog No. MAK165). Based on Brumbarova *et al.* (2016) protocol, fluorescence measurements were carried out using a Tecan Spark® microplate reader, at λ_{EX} : 540 nm, λ_{EM} : 590 nm. Multiplexing was achieved using 96-well flat-bottom black plates. The method presented here is fully described in Appendix 4.

Secondly, in order to detect the oxidative burst as a kinetic measure, the luminol assay is based on the oxidation of luminol molecules in the presence of H₂O₂, catalyzed by the HRP (as for the Amplex Red assay). Excited luminol molecules thus release luminescence, and luminescence levels and duration are proportional to the H₂O₂ amount produced by elicited leaf discs. Unlike the Amplex Red protocol which quantifies intracellular ROS, the luminol protocol only measures extracellular ROS production.

Protocol achieved

In luminol assay, based on Bisceglia *et al.* (2015), luminescence intensities are measured over at least 5 minutes, with measures taken every minutes thanks to a Tecan Spark® spectrofluorometric reader. Multiplexing was achieved using 96-well luminometer plates, with apple tree leaf discs directly immersed in the wells. was performed using a microplate

In addition to the essential oil solutions applied to the discs, solutions with different concentrations of Fytosave (Syngenta, 12.5 g/L COS-OGA) served as reference elicitors to trigger extracellular ROS production. For further details, the entire protocol is described in Appendix 5.

3.4.1.2. Glutathione content

For measuring GSH *in vitro*, a range of useful sensitive techniques are available, with a distinction between HPLC and spectrophotometric enzymatic assays (Noctor *et al.*, 2011). Concerning the HPLC methods, GSH can be derivatized using monobromobimane (MBB), which can freely cross cell membranes. Bromobimane is a highly efficient labelling agent for cellular thiols and it forms a fluorescent adduct specifically with GSH (Hajdinák *et al.*, 2019) (Figure 20). The GSH–MBB adduct is then extracted, and detected by high-performance liquid chromatography (HPLC) with fluorescence detection (Hogarth *et al.*, 2003). Since MBB reacts only with the GSH form, the oxidized glutathione GSSG content of the samples has to be reduced by the addition of the reducing agent dithiothreitol (DTT) to know the total amount of glutathione (i.e. GSH + GSSG). So, it's possible to approximate glutathione redox state by comparing GSH-MBB peaks obtained from the same extract, pre-treated or not with DTT (Noctor *et al.*, 2011).

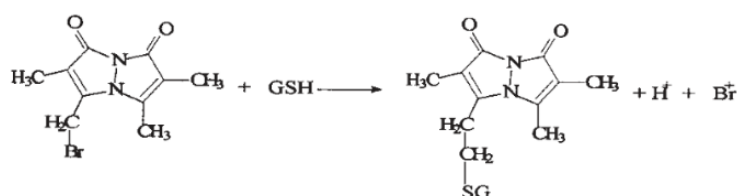


Figure 20. Reaction of monobromobimane with glutathione (Hogarth *et al.*, 2003).

Protocol achieved

The developed method is based on Queval and Noctor (2007), Queval *et al.* (2011) and Hajdinák *et al.* (2019). Briefly described, frozen ground leaf samples were extracted in 1M HCl, then neutralized with 1M NaOH in the presence of 1M NaH₂PO₄ (pH 5.6). The neutralized supernatant was separated into two aliquots derivatized with MBB in alkaline conditions with or without DTT, to measure total GSH and reduced GSH respectively. Concerning the HPLC apparatus, a Zorbax 300 SB column (C18; 150x4.6 mm, 3.5 μm) was used and the system was equipped with an FLD detector (λ_{EX}: 395 nm, λ_{EM}: 477 nm). Bimane derivatives were separated with a linear gradient of 0.25% acetic acid (v/v) (pH 3.5 by adding NaOH) as solvent A and with 100% methanol as solvent B. GSH content was estimated by referring to a standard GSH (Sigma-Aldrich) and expressed in nmol per g of FW. The fully described protocol can be found in Appendix 6.

3.4.1.3. MDA & conjugated dienes content

The thiobarbituric acid-reactive substances (TBARS) assay is an handy and relatively quick test for lipid peroxidation assessment, in which malondialdehyde is derivatized (Lykkesfeldt, 2001). The electrophilic character of MDA makes it bind to the nucleophilic site of thiobarbituric acid (TBA) at low pH and elevated temperature. The resulting MDA(TBA)₂ adduct of reddish color has an absorbance maximum at 532 nm (Esterbauer and Cheeseman, 1990) (Figure 21). Addition of an antioxidant like butylated hydroxytoluene (BHT) to the reaction mixture is essential to inhibit new artefactual lipid oxidation known to occur during the acid heating stage of the assay, without affecting the formation of the MDA(TBA)₂ chromogen (Suttner, 2001).

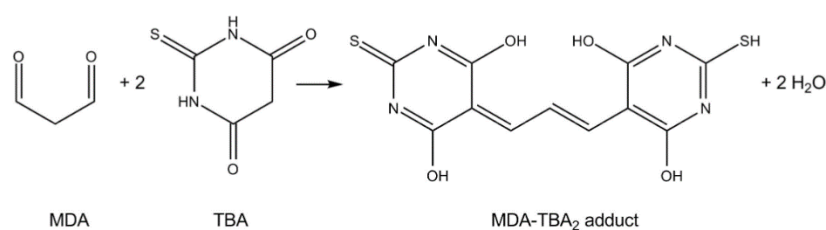


Figure 21. Reaction between TBA and MDA (Weitner *et al.*, 2016)

Protocol achieved

The TBARS content was determined according to the method of Davey *et al.* (2005) with modifications mainly based on Velikova *et al.* (2000) as well as Bresson *et al.* (2018). Briefly described, frozen ground leaf samples were extracted in 5% (w/v) HCl, then derivatized with TBA at 95°C in alkaline conditions in the presence of BHT. Sample compounds were eluted on a 75x4.6 mm, 2.7 μm Halo® C18 column, isocratically with 35% methanol in 50mM KPO₄ buffer (pH 6.8). Chromatograms were monitored at 532 nm thanks to a Multiple Wavelength Detector (MWD). TBARS content was estimated by referring to a standard MDA (Sigma-Aldrich) and expressed in nmol per g of FW. The fully described protocol can be found in Appendix 7.

Based on Singh *et al.* (2009) and Ahuja *et al.* (2015), CD content was determined by homogenizing 50 mg of cryo-frozen grinded apple tree leaf in 10 ml of 96% (v/v) ethanol. Put in the dark on ice for 15 min, the solution was then centrifuged at 4000 rpm during 10 min at 4°C. Then with an Ultrospec 7000 spectrophotometer, absorbance of the supernatant was measured at 234 nm at room temperature, with a 96% (v/v) ethanol blank. CD content was calculated using $\epsilon = 26.5 \text{ mM /cm}$ and expressed as $\mu\text{mol /g FW}$.

3.4.1.4. Electrolyte leakage

The method described hereafter is based on Jambunathan (2010), Rolny *et al.* (2011) and Shah *et al.* (2020), with several modifications. Fifteen leaf discs, rinsed with distilled water, were floated on 15 mL of deionized water with continuous shaking. The electrical conductivity of the bathing medium was measured immediately (C0) and after 2h (C2) of incubation at room temperature with a conductivity meter (TetraCon® 325). Then, total electrolyte content (TC) was determined in the same way after autoclaving the samples for another 20 min at 121°C, and after equilibration at 25°C. Results were expressed as percentage of electrolyte leakage: $\%EL = 100 \times (C2-C0)/TC$.

3.4.1.5. Chlorophyll & carotenoids contents

The sample preparation is the same as for the measurement of conjugated dienes. 50 mg of leaf sample was dried with liquid nitrogen and grinded into powder with mortar and pestle. After 15 min of extraction on ice, in the dark in 10 mL of 96% (v/v) ethanol, the extract was centrifuged at 4 000 rpm during 10 min at 4°C. The absorbance of the supernatant was measured at 470, 649 and 665 nm using an Ultrospec 7000 spectrophotometer.

The chlorophyll a and b concentrations were calculated as follows:

$$C_a (\mu\text{g/g FW}) = [(13.36 * A_{665}) - (5.19 * A_{649})] / \text{sample mass}$$

$$C_b (\mu\text{g/g FW}) = [(27.43 * A_{649}) - (8.12 * A_{665})] / \text{sample mass}$$

The concentration of carotenoids was calculated as follows:

$$C_{\text{carotenoids}} (\mu\text{g/g FW}) = [(1000 * A_{470} - 2.13 * C_a - 97.64 * C_b) / 209] / \text{sample mass}$$

3.4.1.6. Defence genes

The methodology to evaluate the CEO emulsion's ability to trigger activation of defences without the use of any pathogen includes the foliar spraying of CEO 2, 1 and 0.5% (v/v) emulsion on apple tree leaves or the foliar spraying of Bion (trade name of benzothiadiazole, a salicylic acid analogue) to simulate a pathogen attack (positive control), and then the monitoring of transcription levels of 29 carefully selected defence genes. Performed by the INRA institute of Rennes, the expression levels of these genes were quantified by qRT-PCR. The detailed list of the 29 genes can be found in Appendix 8.

3.4.2. Long term evaluation

3.4.2.1. Growth parameters

These basic physiological measures were carried out twice: at the beginning of the experiment and one month later. Trunk height was measured from above soil level to the terminal bud, stem diameter was determined 5 cm above soil level with a caliper and the leaf surface has been evaluated on one of the youngest leaves of each plant thanks to the LeafArea app (<https://www.quantitative-plant.org/software/easy-leaf-area>) (Figure 22). Vegetative shoot growth, as well as the increase in trunk size and leaf area were calculated by difference in values within one month.



Figure 22. LeafArea app interface.

3.4.2.2. Chlorophyll fluorescence

Measurements were done using a fluorescence monitoring system (FMS2, Hansatech Instruments, Kings Lynn, UK).

Before measurements, leaves were dark adapted for 30 min with leafclips (shutters in closed position). The baseline fluorescence is then measured (F_0). Then, a flash of saturating light is sent (“SP” : 18 000 $\mu\text{mol}/\text{m}^2\text{s}$) and the maximum fluorescence is measured (F_m). A constant light is sent for 2 minutes (“Actinic light”: 660 $\mu\text{mol}/\text{m}^2\text{s}$), after which a new saturating flash is used to measure the maximum fluorescence of the photosystem adapted to darkness (F_m') as well as the basic fluorescence in the presence of constant light (F' or F_s) (Figure 23).

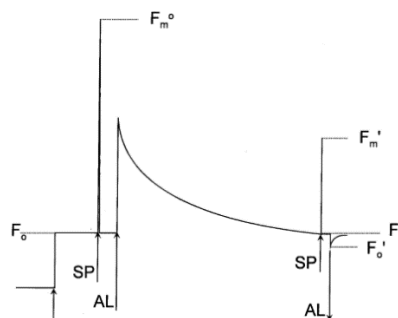


Figure 23. Sequence of a typical fluorescence trace (Maxwell and Johnson, 2000).

Other commonly used fluorescence parameters are directly calculated by the device, such as maximum quantum yield of PSII (F_v/F_m), quantum yield of PSII in light conditions (Φ_{PSII}), proportion of open PSII (qP), and non-photochemical quenching (NPQ) (Figure 24).

Photochemical quenching parameter:		
Φ_{PSII}	Quantum yield of PSII	$(F'_m - F_t)/F'_m$
qP	Proportion of open PSII	$(F'_m - F_t)/(F'_m - F'_o)$
F_v/F_m	Maximum quantum yield of PSII	$(F_m - F_o)/F_m$
Non-photochemical quenching parameters:		
NPQ	Non-photochemical quenching	$(F_m^o - F'_m)/F'_m$

Figure 24. Calculation of fluorescence parameters (Maxwell and Johnson, 2000).

3.4.2.3. Net photosynthetic rate

Water vapour and CO₂ exchange were measured with a portable infrared gas analyzer (ADC LCi-SD, ADC BioScientific Ltd., Hoddesdon, Herts., UK). The CO₂ assimilation rate (A , displayed in $\mu\text{mol}_{\text{CO}_2}/\text{m}^2 \text{ s}$), sub-stomatal CO₂ mole fraction (C_i , in $\mu\text{mol}/\text{mol}$), stomatal conductance (g_s , in $\text{mol}_{\text{H}_2\text{O}}/\text{m}^2 \text{ s}$) and transpiration rate (E , in $\text{mol}_{\text{H}_2\text{O}}/\text{m}^2 \text{ s}$) values were collected. The measurement conditions were as follows: leaf temperature, 21°C; leaf chamber area, 6.25 cm²; relative air humidity, 60 %.

3.5. Statistical analysis

All the data were gathered on Excel and processed using Minitab 19 and R studio softwares, with all results presented as means \pm standard deviations. The main statistical procedure performed was a simple one-way analysis of variance (ANOVA 1). In the case where the null hypothesis of ANOVA was rejected, a post-hoc Dunnett's test was performed to compare each modality with the control, and means not labelled with the letter A are significantly different from the control one. For short term analysis, the fixed factor was the treatment duration whereas for long-term analysis, the fixed factor is the type of treatment. In this case, ANOVA were performed for each parameter at each time independently.

For aphids counting, a Generalized Linear Model (GLM) with a Fisher test (family = quasipoisson (link= log)) was performed in addition to ANOVA 1. For all significance tests, $\alpha = 0.05$ was applied as probability cutoff.

4. Results and discussion

Short term toxicity

* H_2O_2

Results obtained by carrying out the two protocols related to hydrogen peroxide, namely Amplex Red and Luminol, will not be discussed in detail in the frame of this work. Indeed, they do not provide any real gain of information allowing a better understanding of the oxidative burst phenomenon.

Basically, the Amplex Red protocol allows to quantify H_2O_2 concentrations at a given time. So, the initial idea was to quantify the production of H_2O_2 after different treatment times of the leaves with 2% (v/v) essential oil. But the main information we were looking for in our case is : when oxidative stress occurs (if it occurs at all) ? This is why the Luminol protocol was considered in a second time, allowing hydrogen peroxide production to be monitored in the form of a kinetics. However, in this case, only extracellular ROS are quantified.

Three CEO emulsions as well as two Fytosave solutions (positive controls) were directly added on leaf discs in microplates. Figure 25 reflects the amount of peroxide produced by the discs within 5 minutes of adding elicitors.

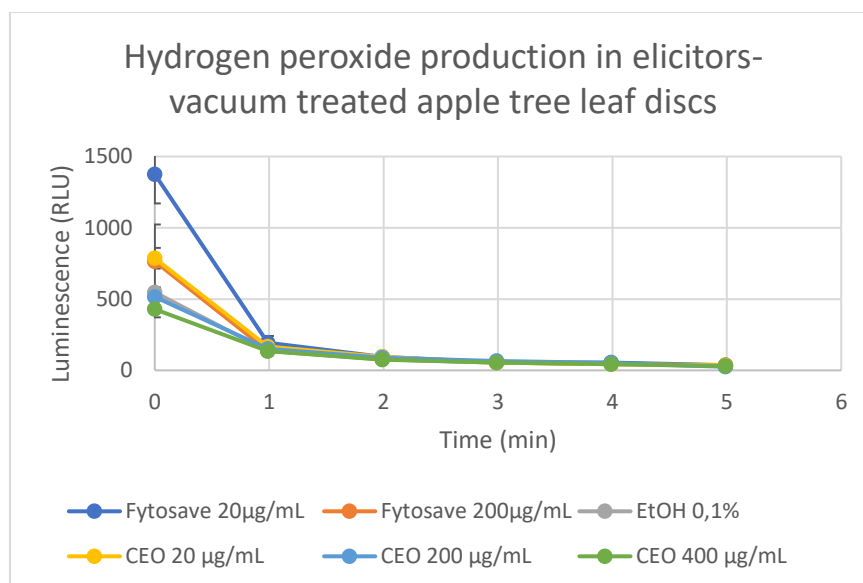


Figure 25. Evolution of H_2O_2 production from elicitors-vacuum treated apple leaf discs.

The amount of H_2O_2 already decreases after 1 minute of reading the luminescence, which could mean that the oxidative burst has already occurred! The same tendency has been obtained with and without vacuuming the leaf discs in the presence of elicitors.

At T0, it can be observed that H_2O_2 production decreases with the increase in concentration of both Fytosave (20 > 200 µg/mL) and CEO (20 > 200 > 400 µg/mL). Too high concentrations

of elicitor could therefore inhibit H₂O₂ production. On the other hand, the values obtained for CEO 200 and 400 µg/mL are identical to those of the 0.1% EtOH blank.

As for Amplex Red, the protocol is optimised for *A. thaliana* and not for *M. domestica* leaves, which are tougher and into which the solutions tested as elicitors would penetrate less.

* GSH

It has clearly been reported that, under oxidative stress conditions, GSH/(GSH+GSSG) ratio decreases because of the oxidation of GSH into GSSG, due to the presence of ROS (especially H₂O₂). Moreover, under normal (unstressed) plant growing conditions, the GSH/GSH Tot ratio is around 90% and global tissue content is in the range of 200-600 nmol /g FW (Noctor *et al.*, 2011).

In our case, we can notice in Figure 26 that at T0 (normal conditions), the ratio is equal to 92.25 % ± 9.88, which is consistent with the literature. It decreases until 30 min of CEO emulsion treatment to reach a value of 73.24 % ± 4.19, then increases after 1h and finally goes down again after 2h of CEO treatment. Standard deviations seem quite high for certain values: highest residual standard deviations ($RSD = \frac{\sigma}{\bar{x}} * 100$) were equal to 10.7, 9.6 and 14.4 % for T0, T60 and T120min respectively. But globally, the tendency for the ratio to decrease initially until 30 min can be interpreted as an evidence of unbalance in the redox detoxifying system following the generation of ROS, a sign that an oxidative burst may have occurred in the plant already in the first 5 minutes of treatment. The high variability of the last two points of the curve unfortunately does not allow to predict with certainty to what extent the plant seems to recover from this oxidative stress by reducing back GSSG to GSH.

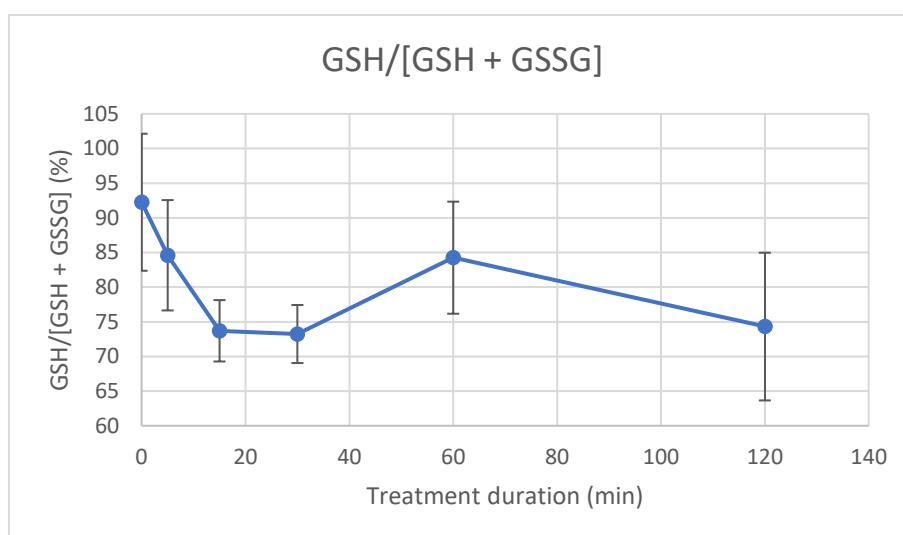


Figure 26. Evolution of the GSH/[GSH+GSSG] ratio in apple leaves (n=5).

ANOVA 1 with a fixed factor have therefore been performed to know the impact of the treatment duration. The means were separated with the least significant difference ($\alpha = 0.05$).

The null hypothesis is the equality of the means of the different treatments and if it is rejected, it means that there is at least one mean that is different from the others.

The first step was to verify the normality of the populations. As the number of observations per population (5) is lower than 10, normality is assumed for these populations. Then, the homogeneity of variances was verified through Levene's test. P-value obtained from the ANOVA tests is equal to 0.015. Thus the Dunnett's test was performed to compare each treatment with the control (T0) and confirmed that T30 and T120min display significantly lower values of the GSH/Tot GSH ratio compared to T0 (Table 1).

Table 1: Dunnett's test results for GSH ratios comparison

Treatment duration (min)	Mean (%)
0 (Control)	92.25 A
5	84.60 A
15	73.70 A
30	73.24
60	88.75 A
120	74.31

The total glutathione (GSH + GSSG) appears to be below 200 nmol/g FW, the lower limit of the range described above, with levels ranging from 59 to 144 nmol/g FW as shown in Figure 27. These lower levels may be explained by the fact that the study was conducted on young growing trees instead of mature trees. In comparison, the amount of Tot GSH determined in the leaves of adult apple trees in the orchard is equivalent to 186 ± 3 nmol/ g Fw (data not shown). Furthermore, a decrease in the amount of Tot GSH is observed over the different treatment times, with an initial quantity halved after 2 hours. As shown by Šircelj *et al.* (2007), this trend can be explained by the fact that glutathione pool is degraded in the leaf tissues due to oxidative stress, and the cell is unable to metabolise it again within that time. Statistically, only the value at T120min is significantly lower than the control (p-value = 0.000).

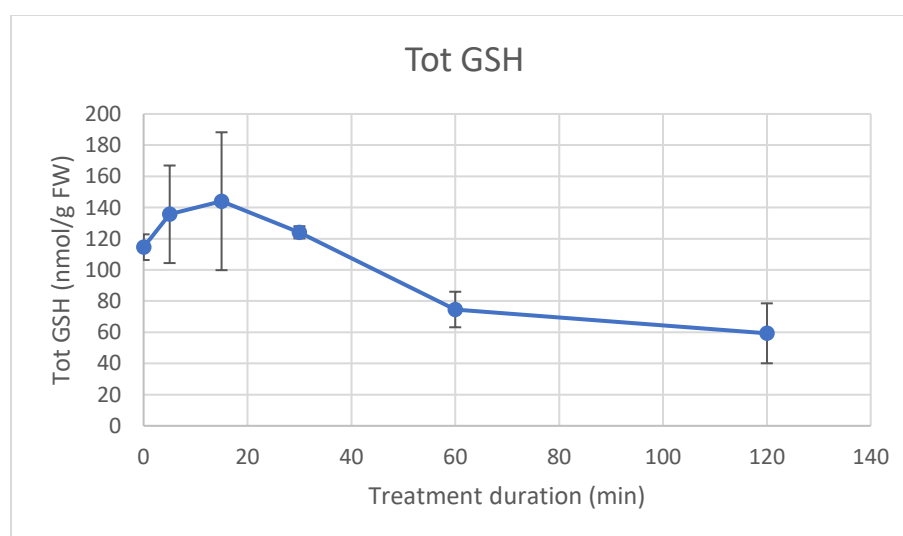


Figure 27. Total glutathione content in apple leaves over time (n = 5).

Concerning the chromatographic performances, the calibration curve linearity was assessed for concentrations between 0 and 80 μM , with a coefficient of determination R^2 equal to 0.9958 (see Appendix 9). Based on 0 μM peak heights and standard deviations, limits of detection (LOD) and quantification (LOQ) are equal to 0.53 μM and 2.27 μM , respectively. Negative controls for each sample analysed (without MBB addition) were prepared to confirm the absence of peak interference at a retention time close to that of the GSH-MBB peak. It's also important to mention that a major problem encountered with the peak integration is a shoulder of the peak of interest ($\text{RT} = 4,8 - 4,9$ min) with another of the quite same intensity at $\text{RT} \approx 5$ min, leading to a potential bias in the determination of peak areas (Figure 28 C).

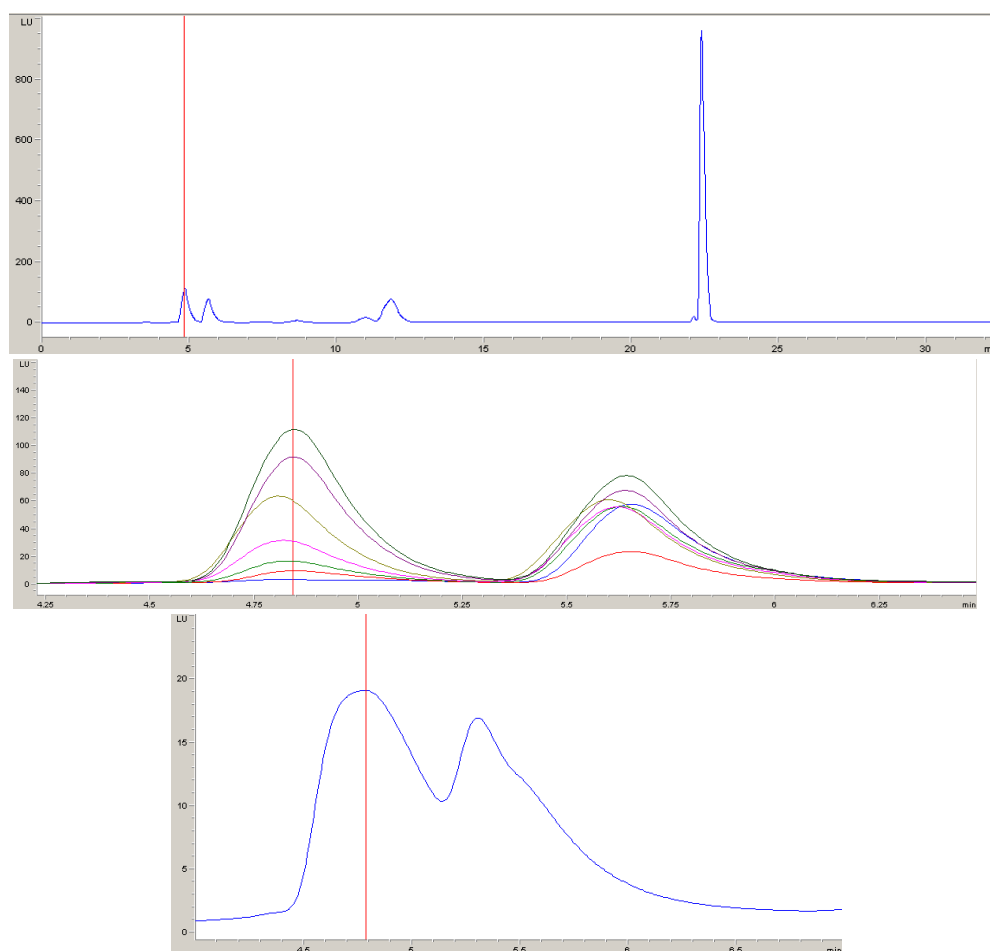


Figure 28. (A) Chromatogram of 80 μM standard (B) Superposition of calibration peaks (C) Shoulder peak in sample.

The bimane derivatives have the advantage of high fluorescence yield and are quite stable (up to several days in solutions kept in the dark). In addition, this HPLC technique permit to separate glutathione from other thiols present in the extract also reacting with MBB (Noctor *et al.*, 2011). But as seen in Figure 29, coelution can sometimes occur with monothiols peaks close to that of the GSH, like γ -glutamylcysteine (γ -EC) (Minocha *et al.*, 2008).

* MDA

Since the bulk of MDA originates from the lipid PUFAs peroxidation in response to oxidative stress, its leaf tissue content was monitored thanks to the TBARS assay, combined with a final HPLC-DAD separation step.

The main conclusion that can be drawn from Figure 29 is that, while the MDA concentration seems to fluctuate between 0 and 6h of treatment, it increases drastically after 24h to reach 12.6 ± 2.4 nmol/ g FW, then decreasing slightly while stabilising the following 2 days at ~ 10.5 nmol/ g FW. RSD is on average equal to 34 %, reflecting a fairly high variability between biological replicates. In view of this trend, we can affirm that the peroxidation of membrane lipids causing MDA production would occur between 6 and 24 hours of treatment with 2 % cinnamon essential oil. At this point, the initial concentration is almost tripled and is not reached again after 72h. Results of the ANOVA 1 test confirmed that T24, T48 and T72h display significantly higher values of MDA content compared to T0 (Table 2).

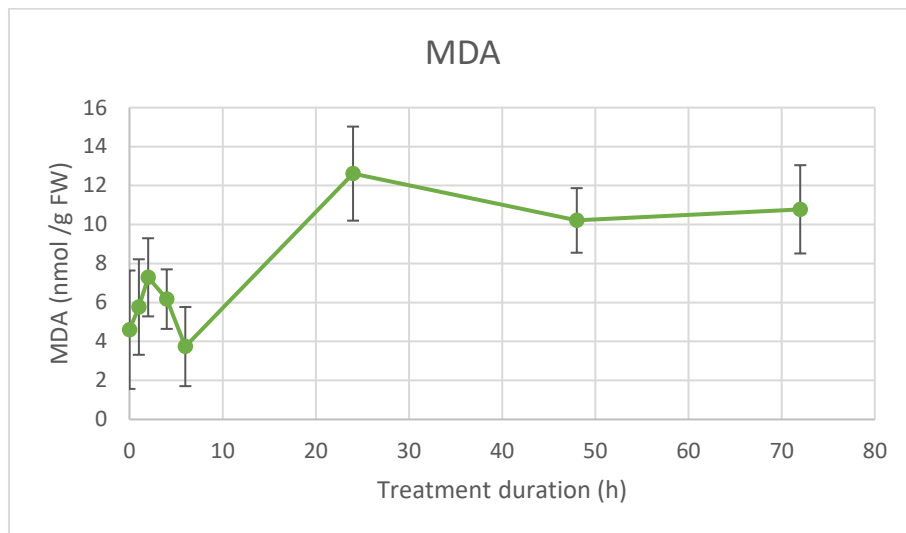


Figure 29. MDA content in apple leaves over time (n = 5).

Table 2: Dunnett's test results for MDA contents comparison

Treatment duration (h)	Mean (nmol /g FW)
0 (Control)	4.60 A
1	5.77 A
2	7.292 A
4	6.17 A
6	3.738 A
24	12.61
48	10.21
72	10.78

Among the protocols cited in the literature, HPLC methods generally yield lower concentration values than those based on spectrophotometrical measurements due to their higher specificity (Suttnar, 2001). That's why it is rather tricky to make comparisons. The closest values obtained by spectrophotometer quantification (at 412 nm) on *Malus domestica* Borkh. are those of Ma *et al.* (2008 ; 2011), with two-years-old grafted apple trees exposed to a 40°C heating stress during 8h, and 6 days of drought stress respectively. The control plants leaves have MDA levels in the range of 6-7.5 $\mu\text{mol /g FW}$, and stressed ones in the range of 9.5-11 $\mu\text{mol /g FW}$ (i.e. 1000 times more). In another extreme case, Davey *et al.* (2005) quantifies the MDA content in apple leaves at 23.5 pmol /g FW with a protocol similar to the one used in the frame of this study.

Concerning the chromatographic performances, the calibration curve linearity was assessed for concentrations between 0 and 8 μM , with a coefficient of determination R^2 equal to 0.9952 (see Appendix 10). Based on 0 μM peak heights and standard deviations, LOD and LOQ are equal to 0.19 μM and 0.79 μM , respectively. Negative controls for each sample analysed (without TBA addition) were prepared to confirm the absence of peak interference at a retention time close to that of the MDA(TBA)_2 peak (Figure 30).

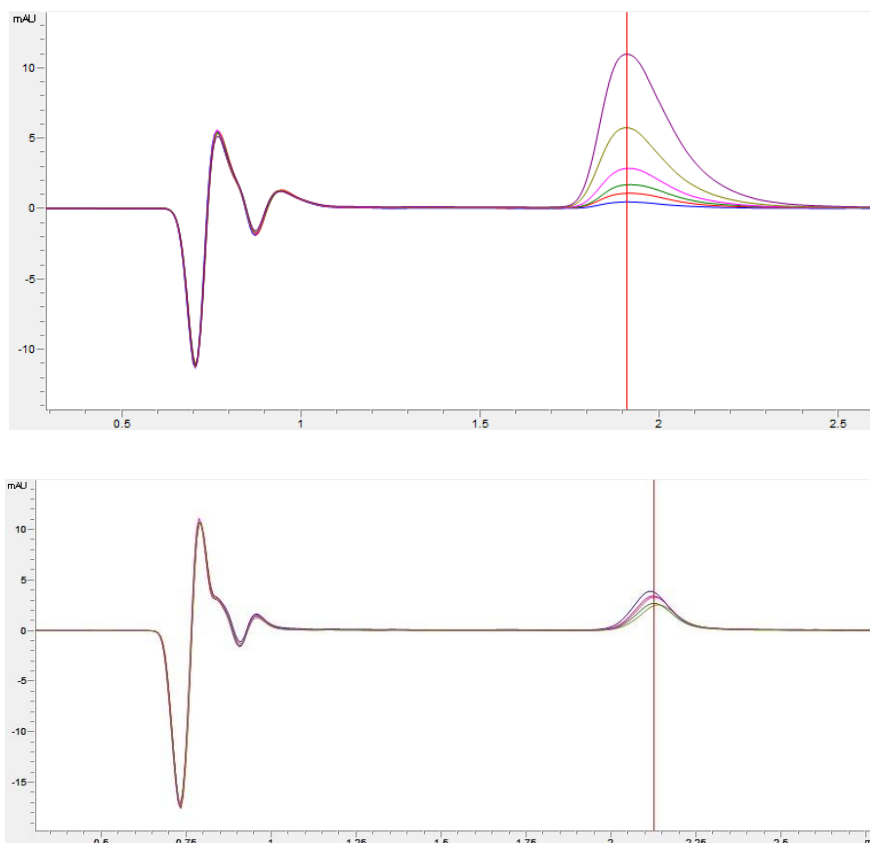


Figure 30. (A) Superposition of calibration peaks (B) Chromatograms of T24h samples.

* CD

As another index of lipid peroxidation (first damaged oxidized PUFAs), the evolution of conjugated dienes content was studied over 72h, with the results shown in Figure 31.

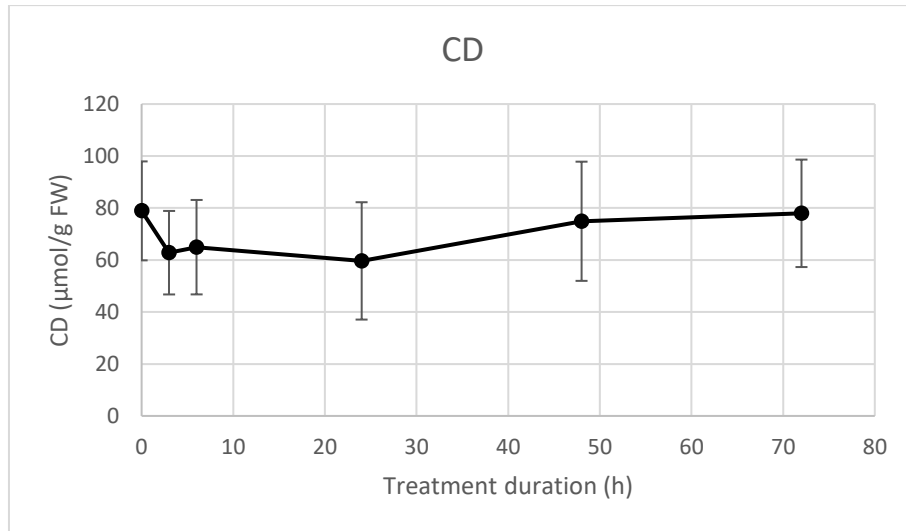


Figure 31. CD content in apple leaves over time (n = 5).

At first sight, the amount of CD does not vary a lot over time, with only a small decrease until 24h and then an increase to the initial value. Standard deviations are very similar between each time of foliar treatment (RSD between 24 and 38 %). The one-way ANOVA gives a p-value equal to 0.514, showing that there is no significant difference of CD content between all the durations of foliar treatment.

In contrast to MDA, this parameter does not seem to provide clear evidence of membrane degradation by lipid peroxidation.

* EL

As stated previously, the loss of lipid membrane integrity is measured with a conductivity meter and results are expressed in percentage of electrolyte leakage. Because of possible differences in background conductivity of the bathing medium between treatment solutions, results are expressed as a change in the conductivity between initial measurement and after boiling the leaf discs. Figure 32 shows an overall slightly decreasing trend over time. However, the expected values were all supposed to be greater than (or at least equal to) the control T0, meaning that possible breaches in the lipid bilayer membrane allow cellular ions to escape (or not) into the bathing medium. But statistically, no value is significantly different from any other (probably due to high standard deviations for T0 and T3h, with RSD = 89 and 95 % respectively), which suggests that the percentage of electrolyte does not change over the treatment time.

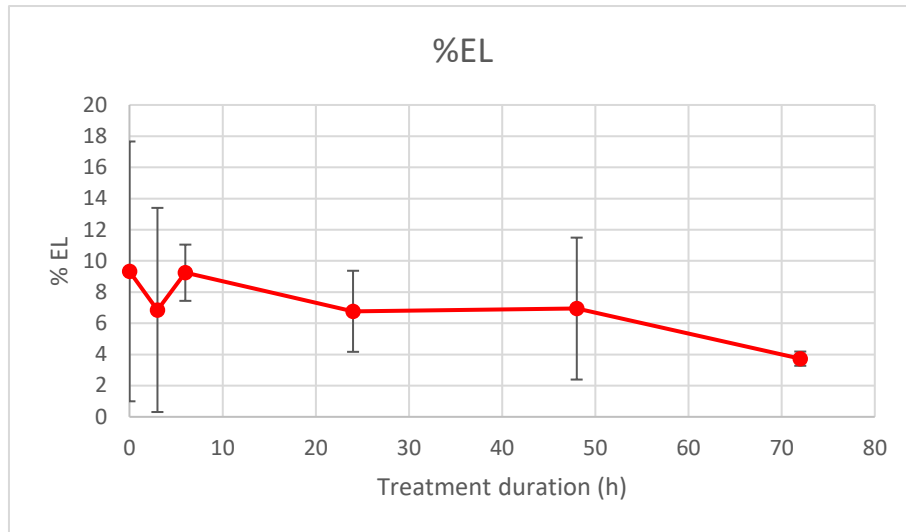


Figure 32. Percentage of electrolyte leakage in apple leaves over time (n = 5).

The electrolyte loss measured in this way does not seem to be reliable enough to point out possible plasma membrane ruptures. Indeed, in the potential absence of stress generated, the value of % EL would remain stable over time.

* Chlorophyll a & b + Carotenoids

We can see that Figure 33 of Chl a and b content shows a quite similar tendency, with values sharply decreasing after 24h of treatment and increasing again after 48 hours to finally reach initial values (T0). This could be a sign of a plant stress management achieved after 48h.

This hypothesis is confirmed by statistical analysis for both chlorophyll a and b, with the 24-hour treated plants significantly different from all others (Table 3). The variability appears to be twice as high for Chl b values compared to Chl a (RSD= 47 and 21 % on average). Chlorophyll a and b contents are in agreement with the literature, with on average twice the amount of chlorophyll a than b (Tamburini *et al.*, 2015).

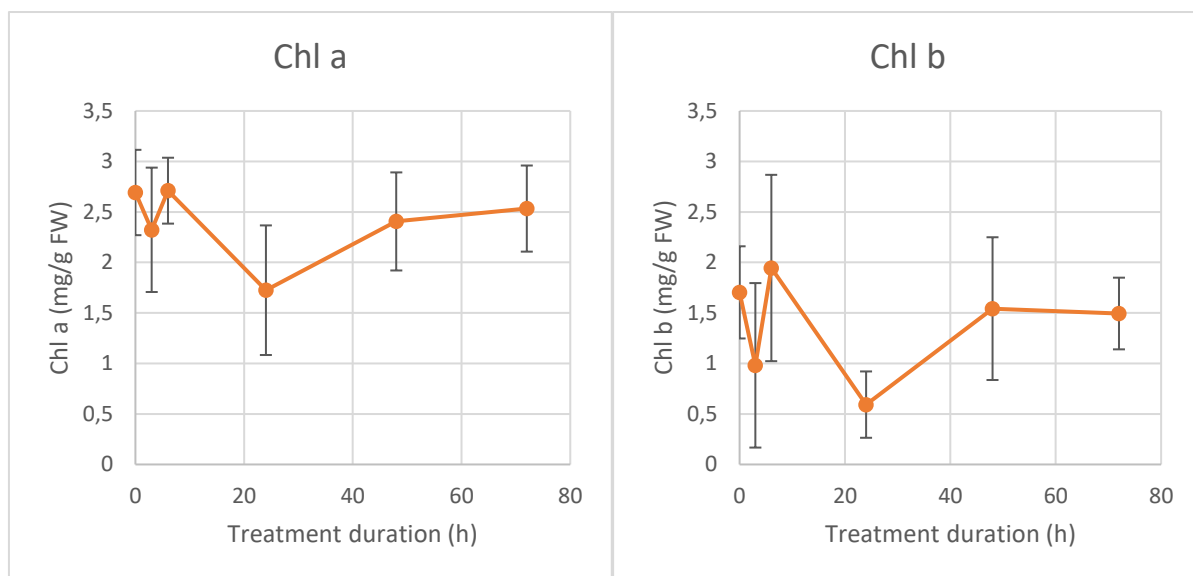


Figure 33. (A) Chl a and (B) Chl b content in apple leaves over time (n = 5).

Table 3: p-values obtained for one-way ANOVA performed on Chl a (left) and Chl b (right), with Dunnett's test results

	Chl a		Chl b
ANOVA p-value	0.048 *	ANOVA p-value	0.029 *
Treatment duration	Mean (mg /g FW)	Treatment duration	Mean (mg /g FW)
0h	2.693 A	0h	1,704 A
3h	2.323 A	3h	0,982 A
6h	2.711 A	6h	1,945 A
24h	1.725	24h	0,592
48h	2.406	48h	1,543 A
72h	2.534	72h	1,495 A

Concerning the carotenoids, the trend is quite different, with values remaining broadly stable from one time step to the next (Figure 34). This is confirmed by a p-value of the ANOVA test equal to 0.6, showing that there is no significant observable difference over time. With an RSD value= 52% on average, the variability is even higher because the calculation of the Car content depends on the values of Chl a and b.

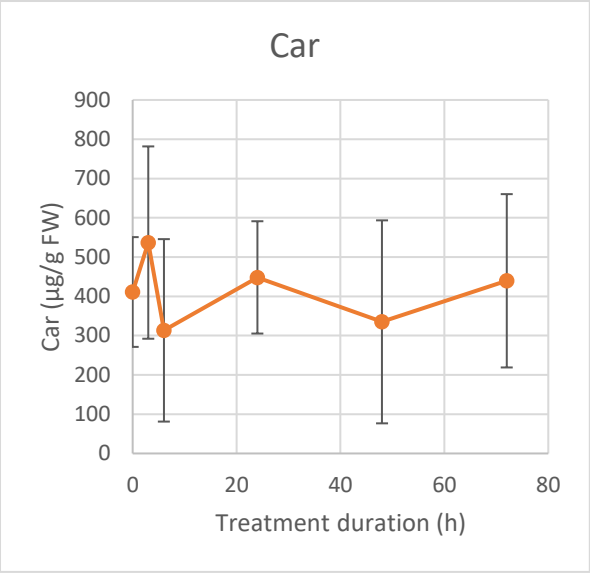


Figure 34. Carotenoids content in apple leaves over time (n = 5).

* Defence genes activation

Table 4: Gene expression heatmap for the 29 defence genes considered

	PR proteins							Phenylpropanoids pathway					Isoprenoids pathway			Cysteine
	PR1	PR2	PR4	PR5	PR8	PR14	PR10	PAL	CHS	DFR	BIS2	PPO	HMGR	FPPS	Far	CSL
Bion J1	3,8376	3,3305	0,9023	3,6548	1,8803	1,9404	0,5296	-0,3531	-0,3343	-0,6138	0,2819	1,8519	0,4258	-0,5463	2,3296	2,0434
Bion J2	1,8810	0,8469	-0,4231	3,1251	0,8248	2,2886	0,3365	-0,1963	0,3764	0,4264	1,0061	0,1134	0,9216	-0,0713	2,2103	1,0400
Bion J3	3,5216	5,3531	4,4100	4,9424	2,8108	3,3574	2,2224	-0,3210	0,1951	-0,0389	4,0543	-1,2135	0,7038	0,0450	1,9708	0,2491
Tween J1	3,6444	0,9157	1,7423	0,6116	2,1941	4,3566	2,1544	-0,6178	-0,3994	-0,4303	2,8931	2,5683	0,3894	-1,0262	1,2426	1,7380
Tween J2	0,0127	0,5351	-0,4776	-0,1026	0,6449	1,5330	0,7629	-0,7987	-0,0950	0,1745	1,9361	-0,3881	0,0856	-0,4402	0,5745	0,2356
Tween J3	0,9873	2,9764	1,9739	1,9711	1,4335	2,6386	1,6201	0,1889	0,5740	0,3849	0,8395	-1,0963	0,2524	-0,7370	0,5918	0,0254
Tw + CEO 0,5% J1	3,9638	2,4117	3,5989	1,9735	2,8930	4,0367	3,3826	1,2970	1,2191	0,9750	0,5967	0,9169	0,0520	0,9215	1,8880	2,4664
Tw + CEO 0,5% J2	-2,0464	0,1676	-1,3352	-0,7263	-0,3816	1,0768	0,4465	-0,4571	-0,3738	0,4948	-0,1097	0,4509	0,2254	-0,4728	-0,4269	0,1470
Tw + CEO 0,5% J3	0,5122	-1,3798	1,9290	0,0663	0,5761	0,5797	1,3295	0,6186	0,6284	0,4851	1,0243	-2,0024	0,0135	-0,4611	-0,8675	-0,5002
Tw + CEO 1% J1	5,8278	-0,0113	1,5776	1,0110	3,5217	6,4229	2,6082	1,3011	0,9416	0,8394	1,7703	2,6350	-0,0510	0,0001	1,1258	3,4929
Tw + CEO 1% J2	1,1620	1,0227	-0,4947	-0,3379	1,2710	3,4239	1,5588	0,2393	0,3693	1,0263	0,8997	0,9129	0,6199	0,0933	0,3579	0,8891
Tw + CEO 1% J3	3,1068	1,7823	1,9234	0,1938	1,6025	4,7915	1,6716	0,8204	0,9030	1,0353	2,1147	-0,9950	0,3206	-0,5628	-0,9540	0,4749
Tw + CEO 2% J1	5,6317	0,4929	2,7003	-0,5765	3,7126	7,1514	3,8726	1,6422	1,3396	1,8681	2,7558	0,7590	1,1831	0,3403	1,1361	2,7747
Tw + CEO 2% J2	0,7991	-2,1796	-0,5203	-1,3463	0,9775	7,3316	1,5756	-0,8436	-0,5443	0,7854	3,3435	2,0149	0,5026	0,5730	-1,9626	1,9618

	Oxidative stress			Cell wall modifications			Salicylic acid		Jasmonic acid		Ethylene		Agglutinin
	Apox	GST	POX	CalS	Pect	CAD	EDS1	WRKY	Lox2	JAR	ACCO	EIN3	AGG
Bion J1	0,0884	0,2548	0,6683	0,0228	-0,6853	-0,0497	2,5605	1,8244	-0,0479	0,1765	0,1057	0,1201	8,9002
Bion J2	-0,3188	-0,4628	0,8087	-0,2385	0,5755	-0,0801	2,6648	1,9089	0,1922	-0,4045	-0,6653	0,6849	7,5241
Bion J3	0,5108	0,4063	1,2847	0,0194	1,4947	0,4787	2,1839	2,9003	-0,1643	0,2336	0,2827	0,2192	7,3747
Tween J1	0,1098	0,7666	1,4149	-0,0941	0,2786	0,4042	0,7720	1,9779	0,0275	0,4011	0,7516	0,0223	7,0606
Tween J2	-0,6714	-0,2035	0,9687	-0,6665	-0,8930	0,0939	1,8290	1,6269	-0,1071	-0,5833	-0,3439	0,3515	3,7966
Tween J3	0,3234	-0,1317	1,9362	-0,0415	3,0184	0,1967	0,6830	2,2827	0,1981	0,3700	0,3062	0,2167	7,0190
Tw + CEO 0,5% J1	1,1594	1,3327	3,6909	1,0656	2,3723	0,5192	-0,1556	2,1492	0,0199	1,5208	1,5388	-0,2039	7,8454
Tw + CEO 0,5% J2	-0,6142	-0,3236	0,3616	-0,7200	-0,4145	0,1341	0,8133	0,8984	0,0139	-0,4838	-0,4940	0,5017	2,5240
Tw + CEO 0,5% J3	0,5958	0,4112	1,1940	0,0294	1,5683	0,3910	-0,8267	-0,0726	0,0910	0,3183	0,5562	-0,1180	2,4670
Tw + CEO 1% J1	-0,1326	1,6557	3,6052	0,6610	4,2622	0,9638	-0,1537	2,1887	0,0612	0,9449	1,5019	0,4224	5,5708
Tw + CEO 1% J2	-0,5998	0,4863	2,4601	-0,3264	1,5968	0,2110	1,5367	2,7810	0,1439	-0,2175	0,7389	1,0346	4,8907
Tw + CEO 1% J3	0,3145	0,8316	2,2882	-0,0079	5,2053	0,8868	-0,8189	-0,0663	0,0029	0,7776	0,9475	0,1019	2,7726
Tw + CEO 2% J1	-0,3625	2,0411	4,5814	0,3185	4,7105	0,9392	0,0546	2,4966	0,4565	0,3829	2,1319	1,2706	1,9199
Tw + CEO 2% J2	-2,0122	1,5298	1,5875	0,2943	2,0433	1,0072	0,2611	5,8984	0,3414	-0,0029	1,4549	1,5973	1,1132

Table 4 is a gene expression heatmap generated on the log base 2 of mRNA copy numbers for 29 defence genes considered, with all values normalised to a leaf water treatment as a blank modality. The different treatments consisted in foliar application on apple seedlings (4-6 leaves, from open-pollinated cv. Golden Delicious) of : Bion (salicylic acid analogue), Tween 80 aqueous solution (surfactant), and emulsions of CEO at three different concentrations (0.5, 1 and 2 % (v/v)). These solutions were applied and leaves were sampled after 1, 2 or 3 days (corresponding to J1, J2 and J3). Two biological replicates of the same modalities (5 apple seedlings each) were carried out at the same time and only their average is presented here. On a log base 2 scale, values below 2 can be considered as showing no clear sign of gene promoter activation.

Among the interesting information that can be derived from these transcriptomic values, the first is that, Tween 80 alone surprisingly produces effects, that are quite marked for PR proteins and agglutinin. However, Tween 80 has been assessed to be a nontoxic and biocompatible surfactant (Prieto and Calvo, 2013). Concerning CEO, the activation effects are visible especially after 24h of treatment, and there is a clear dose effect at this time between concentrations. This is consistent with the fact that such a dose effect is also seen in the burns that appear on young leaves for 2% emulsions (Figure 35 C). With a prolonged activation effect until day 3, the 1% CEO emulsion shows the most promising results. One last thing to mention is that the gene induction profiles are well differentiated between Bion and cinnamon for some genes, notably those related to oxidative stress.

Concerning the apple trees, it is important to note that they are from seedlings and not cloned as in all other experiments. They are therefore more heterogeneous, which leads to a certain variability between the replicates. Being also younger, it is understandable that in this case, signs of burning were observed on the young leaves.



Figure 35: Apple seedlings treated with (A) 0.5 % (B) 1% (C) 2% CEO emulsion.

Long term toxicity

* Amount of essential oil injected

As previously mentioned, the quantity of essential oil emulsion injected was measured by the difference in mass of the drip pocket between before and after injection. After 20 hours of injection, the quantity administered in the 14 trees is in the order of 21.24 mg, and is quite variable ($\sigma = 14.49$ mg). This amount appears to be very low compared to the results obtained during preliminary injection tests with the same device on trees of the same size : 50 mg after 24h (data not shown)! It was therefore decided to continue the injection for a further 24 hours. After this additional time, the average amount injected is equal to 29.52 ± 20.35 mg, which is much less than twice the value obtained after 20 hours, and with still a great variability of injection between plants.

The no-pressure injection system used here depends exclusively on the transpiration rate of the plant, which guides the ascension of the xylem in vascular tissues. So, plants with the highest quantities injected should therefore logically be those with the highest values for the E parameter measured with the IRGA (see below). However, this trend is not clearly observed, neither at the initial time nor after 1 day.

The injection device set up on such young apple plants would therefore need to be further optimised to ensure that a standardised amount of emulsion is injected, with less variability between plants.

* Chlorophyll fluorescence

The use of chlorophyll fluorescence measurements is now widespread to examine leaf photosynthetic performances and stress in plants. Among the different chlorophyll fluorescence parameters evaluated, Fv/Fm (i.e. maximal quantum yield of PSII) is a widely used parameter to evaluate the photochemical efficiency of PSII. It has been described that PSII can be inhibited by the action of terpenes which compete with the binding site of plastoquinone (PQ), hence blocking the electron transport chain (Achnine *et al.*, 1998). In a dark-adapted non-stressed leaf, Fv/Fm should range around 0.83 and values significantly below this threshold indicate an altered physiological state, with leaf tissues considered dead when showing values lower than 0.3 (Maxwell and Johnson, 2000 ; Woo *et al.*, 2008 ; Bresson *et al.*, 2018). Basically, the F0 (basal fluorescence) is higher in stressed plants than in healthy plants (Gamon and Pearcy, 1989), with also sometimes Fm values decreasing significantly (Ekmekci and Terzioglu, 2005). As $Fv = Fm - F0$, the global Fv/Fm ratio tends logically to be smaller.

Fv/Fm ratios, measured at several times (expressed in days after treatment) are displayed in Figure 36 . As a reminder, the four types of treatments applied on apple trees are as follows:

- A) Controls
- B) Controls with aphids
- C) CEO 2% emulsion
- D) CEO 2% emulsion with aphids.

The first important element to note is that all ratios are slightly higher than the 0,83 value reported in the literature for healthy fully green plants. Nevertheless, it is still possible to compare the results obtained for the different treatments with the control plants A) to point out stress signs.

Moreover, all values are located between 0.87 and 0.9 for every treatment at every given time, which indicates a global good health of both control and treated trees over time.

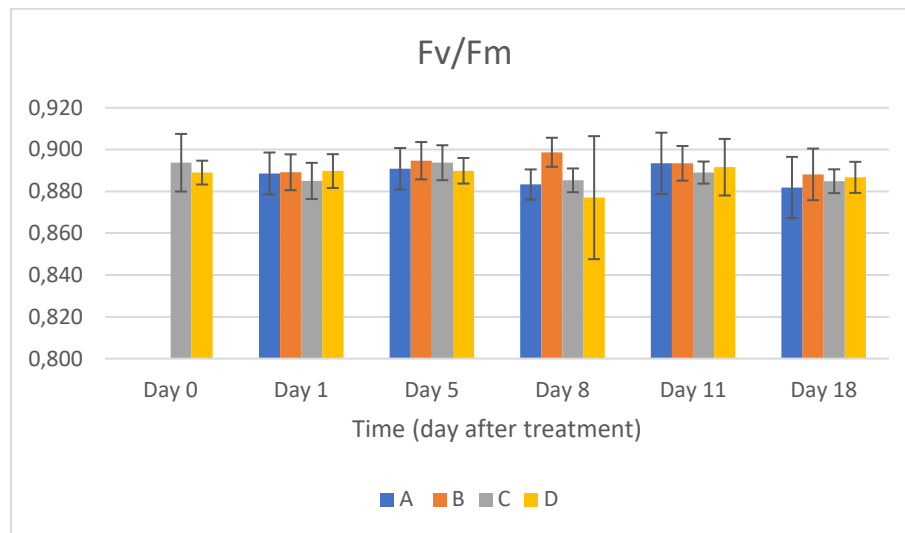


Figure 36. Maximal quantum yield of PSII over time for the different treatments (n = 7).

Although the Fv/Fm ratio is a relative value that makes it more comparable, F0 values could also be used alone for measuring the plant's stress level, as well as quantum yield of PSII (Φ_{PSII}), photochemical quenching (qP) and non-photochemical quenching (NPQ) (Figure 37). Briefly described, Φ_{PSII} represents the proportion of photon energy absorbed by PSII being used in photochemistry under light-adapted conditions (and no more dark-adapted by contrast with Fv/Fm). qP gives an indication of the proportion of PSII reaction centres that are open (with $\Phi_{PSII} = qP * Fv/Fm$). Then, NPQ corresponds to the excess of excitation energy that may be dissipated as thermal radiation (Maxwell and Johnson, 2000). The first two parameters have been reported to decline when stress factors are perceived by the plant, while the third one seems to peak before dropping drastically (Woo *et al.*, 2008).

As with the Fv/Fm ratio, the values obtained for these parameters look different from those of the literature but again, this is certainly due to different settings of the measuring device used (lower excitation light intensities) (Figure 37).

At first glance, F0 values seem to be higher for the injected trees C) and D) for several days, which may reflect a greater stress experienced compared to A) and B) plants. But apart from this parameter, any clear tendency appears in the results of the other ones without a statistical analysis, that should help in their interpretation.

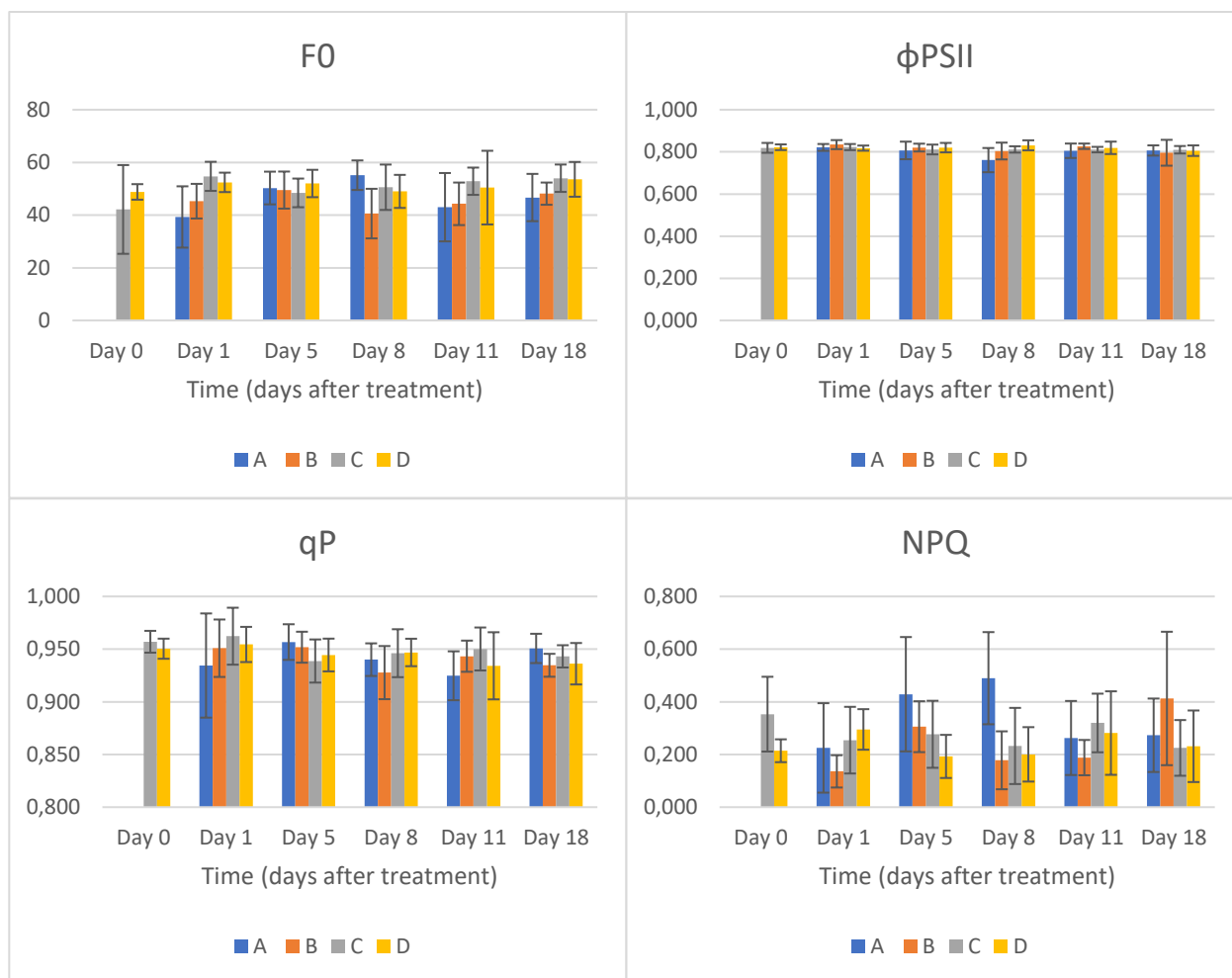


Figure 37. (A) F0 (B) Φ PSII (C) qP and (D) NPQ values over time for the different treatments (n = 7).

For each of these five fluorimeter parameters, ANOVA 1 with a fixed factor have therefore been performed to know the impact of the treatment, with each time tested independently and the qualitative factor being thus the treatment applied (30 ANOVA 1 in total: 5 parameters at 6 days of measurement). Again, as the number of observations per population (7) is lower than 10, normality of the populations is assumed. Then, the homogeneity of variances was verified through Levene's test (p-value > 0.05). P-values obtained from the various ANOVA tests are summarized in Table 5.

Table 5: p-values obtained for one-way ANOVA performed on chlorophyll fluorescence parameters over time

p-value	D0	D1	D5	D8	D11	D18
Fv/Fm	0.491	0.753	0.695	0.099	0.861	0.730
F0	0.409	0.003**	0.725	0.013*	0.271	0.107
ϕ PSII	0.813	0.281	0.769	0.014*	0.390	0.902
qP	0.287	0.447	0.244	0.297	0.214	0.216
NPQ	0.063	0.094	0.038*	0.002**	0.312	0.164

p-value<0.05: significant difference * / < 0.01: highly significant ** / < 0.001 : very highly significant ***
 Bold p-values mean that the homogeneity of variances is not respected for these tests.

The Dunnett's test was then performed on significant p-values to compare each treatment with the control (modality A).

The only tests which display a significant difference between injected (C & D) and non-injected apple trees (A & B) are on day 1 for F0 and on day 8 for Φ PSII (Table 6), with both higher values for injected trees.

Table 6: Dunnett's test performed on F0 at day 1 (left) and on Φ PSII at day 8 (right)

F0, D1		Φ PSII, D8	
Treatment	Mean	Treatment	Mean
A (Control)	39.29 A	A (Control)	0.7609 A
B	45.29 A	B	0.8040 A
C	54.71	C	0.81157
D	52.43	D	0.83100

A higher F0 value could support the assumption that these plants would be more stressed. However, the significant difference observed for F0 on day 1 is not visible in the Fv/Fm ratio, while it depends on F0. It's explained by the fact that Fm values follow exactly the same trend as F0, revealing a constant ratio in the end (see Appendix 11). Finally, it seems surprising that the injected plants also have a higher quantum yield of PSII.

To sum up, we can affirm that neither injection of CEO emulsion nor aphid deposition does seem to impact significantly the photosystem II and photosynthetic apparatus efficiency. It is consistent with the fact that visually, leaf tissues were and remain fully green, with no chlorophyll bleaching brown traces on apple leaves on which the fluorescence measurements were repeated.

* Photosynthetic rate

As the IRGA data were recorded at the same time and almost in the same manipulation as the chlorophyll fluorescence ones, they are processed in the same way. The different parameters recorded in this case are : CO₂ assimilation rate (A, displayed in $\mu\text{mol}_{\text{CO}_2}/\text{m}^2 \text{ s}$), sub-stomatal CO₂ mole fraction (C_i, in $\mu\text{mol}/\text{mol}$), transpiration rate (E, in $\text{mol}_{\text{H}_2\text{O}}/\text{m}^2 \text{ s}$) and finally stomatal conductance (g_s, in $\text{mol}_{\text{H}_2\text{O}}/\text{m}^2 \text{ s}$). It's important to mention that the leaf *in vivo* net CO₂ assimilation A measured is not a true photosynthesis rate, but rather the net balance between the rates of a carbon flux entering the leaf (the gross photosynthesis) and leaving the leaf simultaneously (the photorespiration and the mitochondrial respiration in the light) (Douthe *et al.*, 2018). In *Malus domestica*, net CO₂ assimilation reductions accompanied by decreases in intercellular CO₂ concentration and stomatal conductance were reported after fungicide application (Untiedt and Blanke, 2004). According to Dayan *et al.* (2000), plants that have been treated with compounds inhibiting photosynthetic electron transport exhibit a decreased CO₂ uptake, while compounds affecting mitochondrial electron transport result in lower CO₂ production in the dark. In opposition, the increase in dark respiration due to stress can be

explained by additional energy requirement, metabolic compounds breakdown, and/or activation of the alternative cyanide-insensitive respiration (Dias, 2012).

All results are shown in Figure 38. When looking at these graphs, several observations can be made. For the A parameter, values appear to be higher for non-injected plants A) and B) at the beginning but the trend seems to be reversed from day 5. While the parameter Ci appears constant over time and equal between the four modalities, the parameters E and gs related to leaf transpiration decrease until day 8 and 5 respectively, then increasing almost to the initial values. For these parameters, there is also no clear difference between the four treatments. The general tendency of these values to decrease and then increase again is therefore not explained by the impact of the treatment, but certainly by external environmental factors such as variations in the light intensity received by the leaves (see Qleaf below).

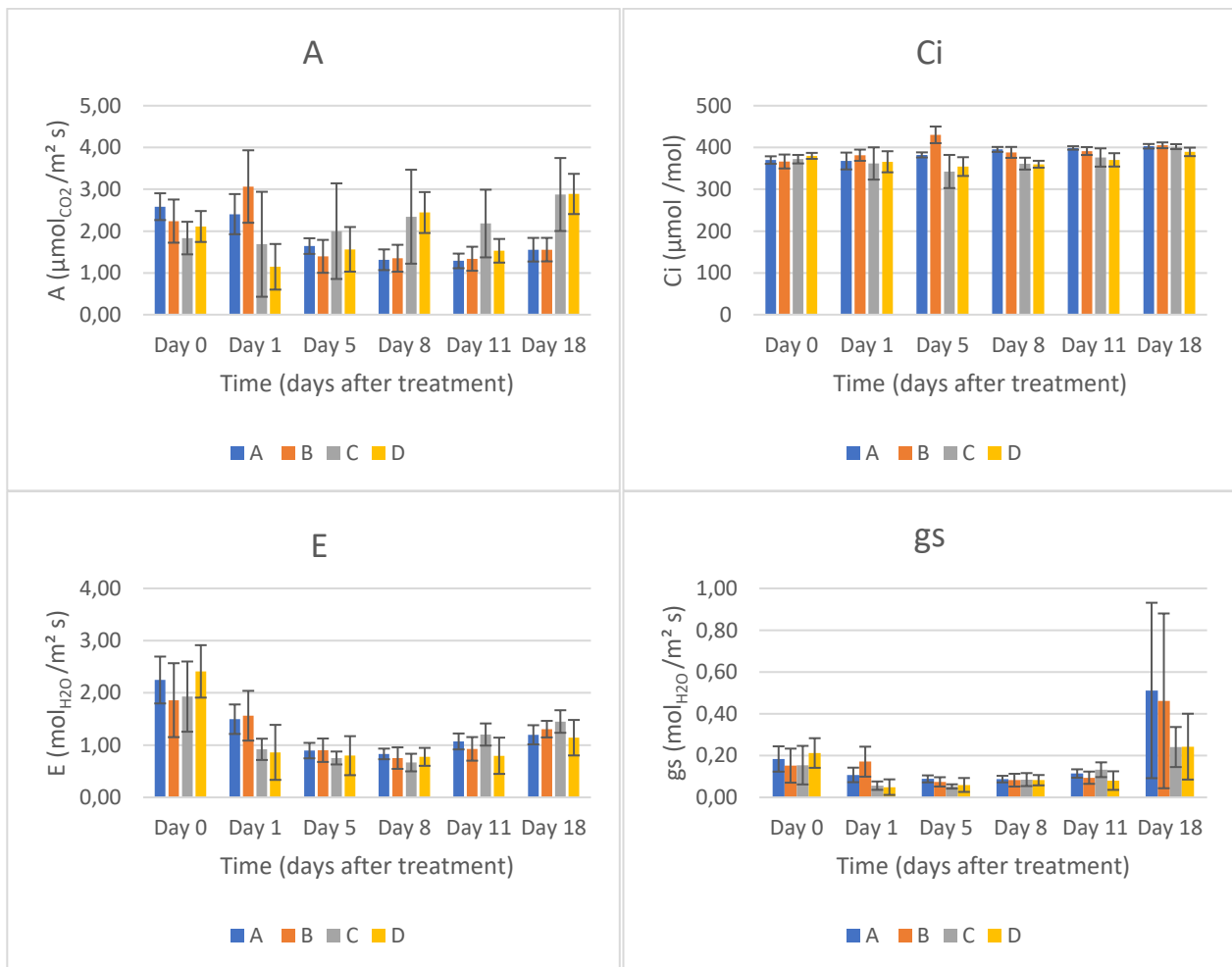


Figure 38. (A) A (B) Ci (C) E and (D) gs values over time for the different treatments (n = 7).

Concerning the statistical analysis, the CO₂ assimilation rates (A) at day 8 and 11 were the only set of values which did not fulfill the variance homogeneity condition (p-values equal to 0.012 and 0.001 respectively for the Levene's test). It was still decided to go on with the test for this set of data without any variable transformation. In total, 24 ANOVA 1 were performed (4

parameters at 6 days of measurement) and the corresponding p-values are summarized in Table 7.

Table 7: p-values obtained for one-way ANOVA performed on IRGA parameters over time

	D0	D1	D5	D8	D11	D18
A	0.017*	0.002**	0.011*	0.003**	0.005**	0.000***
Ci	0.182	0.529	0.000***	0.000***	0.004**	0.004**
E	0.280	0.003**	0.583	0.335	0.028*	0.132
gs	0.431	0.000***	0.027*	0.978	0.04*	0.290

p-value<0.05: significant difference * / < 0.01: highly significant ** / < 0.001 : very highly significant ***

A surprising thing to point out is that for the carbon assimilation rate A at day 0 (i.e. the beginning of the experiment, before any special treatment applied), there is a significant difference occurring, which continues to be observed thereafter until the end of the experiment (although care must be taken for days 8 and 11 results). It could imply that carbon assimilation rate is affected by events taking place in the previous days of the experiment, in addition to being affected by the treatment. But as previously reported, A is an integrative parameter that depends in particular on the PAR intensity. As this varies during the experiment and from one chamber to another (see Q leaf parameter below), the parameter A is inevitably affected (Yamori *et al.*, 2010). We can therefore conclude that in our case, this parameter does not seem to be very reliable to highlight the presence of stress due to the treatment.

Even if the results seem to be constant at first sight for the Ci parameter, it can be seen that injected trees have significantly lower values on day 8 and 11 (Table 8), meaning that as mentioned before, photosynthesis and CO₂ assimilation is probably slowed down and/or that mitochondrial respiration is impaired, thus reducing CO₂ cellular production.

Table 8: Dunnett's test performed on Ci at day 8 (left) and day 11 (right)

Ci, D8		Ci, D11	
Treatment	Mean (µmol /mol)	Treatment	Mean (µmol /mol)
A (Control)	395.43 A	A (Control)	398.95 A
B	388.29 A	B	391.52 A
C	361.43	C	376.10
D	359.95	D	370.43

Finally, for the E and gs parameters, the only distinction between injected and non-injected apple trees occurs on day 1 for transpiration rate E (Table 9). The lower E values for the injected plants are further evidence of a photosynthetic yield negatively impacted 24h after the beginning of the injection, accompanied by a closure of the leaf stomata.

Table 9: Dunnett's test performed on E at day 1

E, D1	
Treatment	Mean (mol _{H2O} /m ² s)
A (Control)	1.497 A
B	1.563 A
C	0.920
D	0.862

As another parameter measured by the device, Q_{leaf} is considered here separately since it provides information on the photosynthetic photon flux density (PPFD) reaching the leaf at the time of measurement, thus equivalent to the PAR value (in $\mu\text{mol}/\text{m}^2\text{ s}$).

As a reminder of the experiment, the plants were placed in two separate climate chambers, with plants A and B in one, and C and D in the other. The PAR intensity value was set at $50\ \mu\text{mol}/\text{m}^2\text{ s}$ on both sides (confirmed by a PAR meter at 50 cm from the light source). However, it is clear from Figure 39 that on day 0, the lights in the chambers were sending out three times too much light at the time the IRGA measurements were taken (around $150\ \mu\text{mol}/\text{m}^2\text{ s}$). However, even after adjustment, it can be seen that from day 5 until the end of the experiment, the apple trees do not receive the same light intensity from one chamber to another. The temporal fluctuations observed for the parameters A, E and g_s would therefore be due to these variations in light intensity reaching the apple trees.

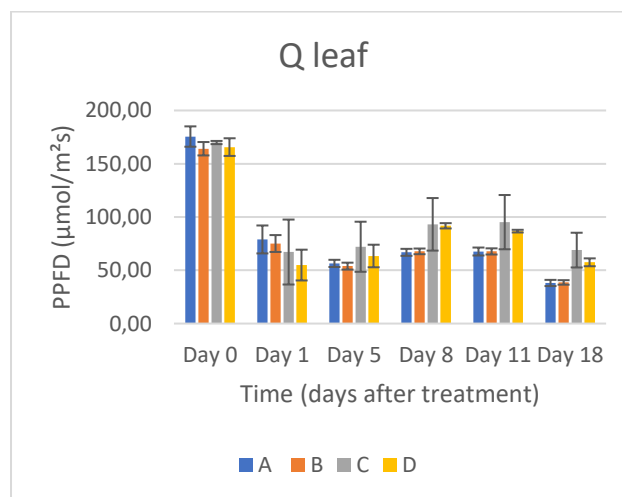


Figure 39. Q leaf value over time for the different treatments (n = 7).

The last thing that can be discussed in this part is the relatively small number of leaves analysed on each tree. Although the trees were small in size, if the biopesticide was not distributed uniformly through the tree, the analysis of a single mid-height located leaf could introduce a possible bias in the conclusions drawn. At least three to five leaf-clips placed at different heights could permit to better reflect the whole organism tissue health, but it would have cost a lot in handling time.

* Growth parameters

These fairly easy to take measures were carried out on each apple tree before any treatment was applied (20/05) as well as one month later (21/06). The values obtained at the beginning for these 3 parameters were already quite variable, with ranges from 34 and 67 cm for stem heights, from 3.18 to 5.42 mm for trunk diameter, and from 9 to 27 cm² for leaf surface (data not shown). Vegetative shoot growth, stem diameter increase and leaf surface increase are reported in Figure 40.

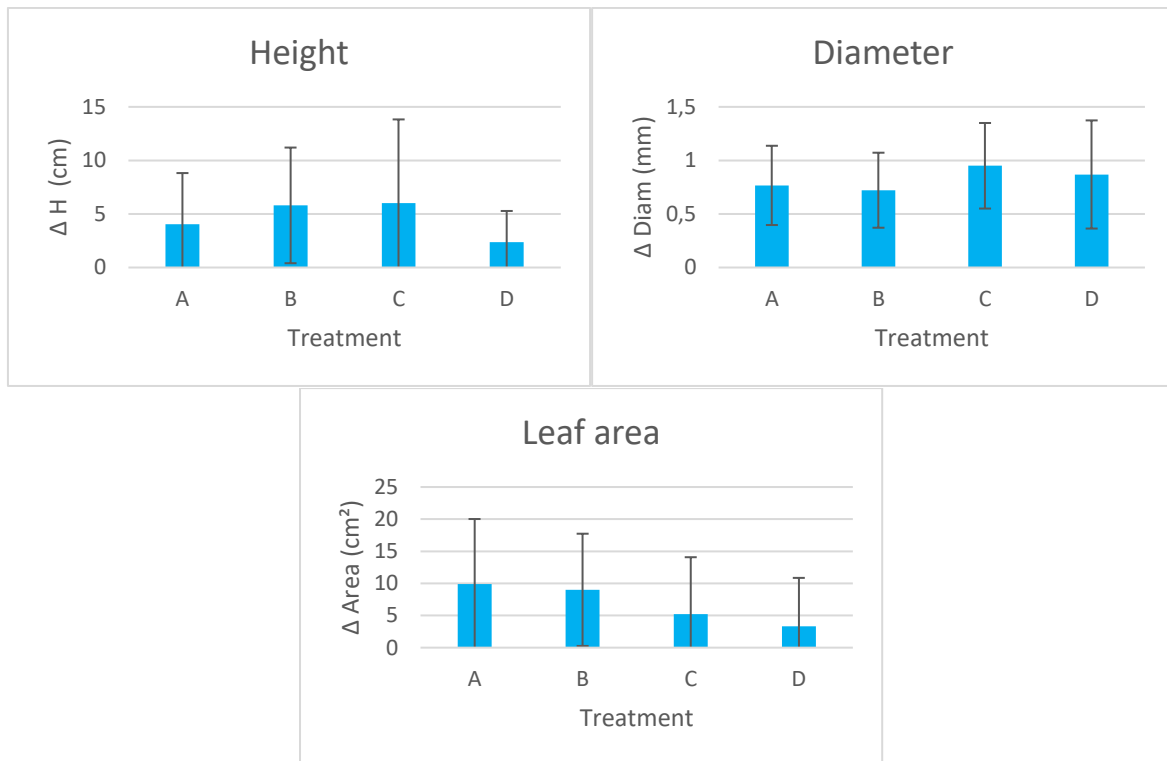


Figure 40. Variations of (A) stem height (B) trunk diameter and (C) leaf area between measures before and one month after treatment (n = 7).

Statistical analysis show no significant difference between the treatments for these parameters (Table 10), probably due to the great heterogeneity observed among the results.

Table 10: p-values obtained for one-way ANOVA performed on growth parameters

	Δ Length	Δ Diameter	Δ Leaf area
p-value	0.594	0.756	0.548

* Living aphids evolution

Fifteen aphids were deposited on C) and D) trees on the 22nd of May, around 2 days after injection (drip pockets removed after 44h) then the monitoring was performed until the 23rd of June (week 5). The number of living aphids counted in each colony evolved as shown in Figure 41. If we still consider the date of injection as day 0, aphids are therefore deposited on leaves on day 2.

From these graphs, an effect of the treatment on aphids' development seems pretty obvious. It can be observed that at Day 6, the number of survivors on treated plants dropped sharply by approximately 60 % compared to Day 2. Although standard deviations seem quite high, ANOVA 1 analysis reveals that there is well a significant difference of aphids mortality between treated and non-treated plants on days 6 and 11 (see Table x).

From Day 11 until the end, the number of aphids start to increase on both types of apple trees, but more rapidly on untreated ones. Five weeks after the beginning of the monitoring, the number of aphids on control plants is in average 4.6 times higher than on injected trees (172 compared to 37). The standard deviations are unfortunately so large that it is not possible to show significant differences between the two treatments after Day 11 (Table 11).

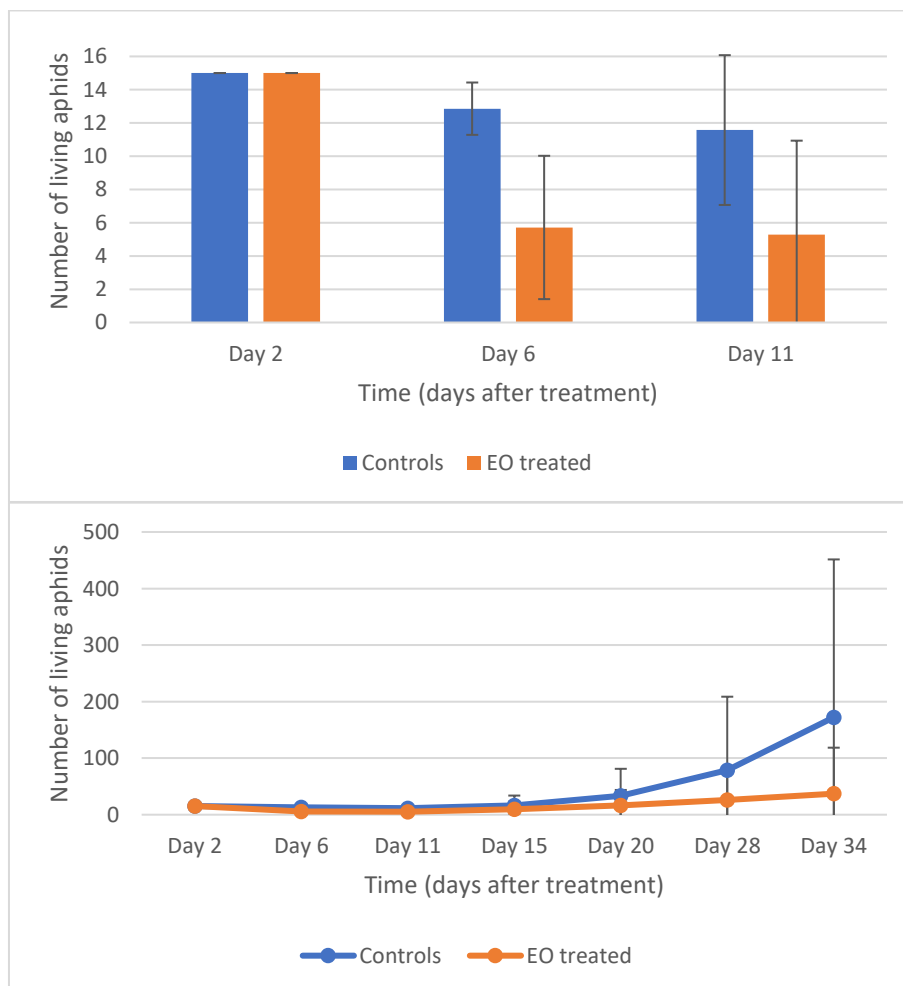


Figure 41. Evolution of the number of living aphids on injected and non-injected trees.

Table 11: p-values obtained for one-way ANOVA performed on the number of living aphids over time

p-value	D6	D11	D15	D20	D28	D34
#aphids	0.001**	0.04*	0.44	0.423	0.342	0.243

A GLM modelling would be more robust to highlight differences in population development, with both an expected effect of treatment and time on the number of living individuals, as suggested by Figure 42. The distribution family of the model is a quasipoisson (link= log) and a Fisher test is performed to know the effect of each factor separately.

As expected for this analysis, both effects of time and injection were found significant, with p-values equal to 2.919×10^{-6} and 0.001523 respectively, and no interaction between the two factors (p-val= 0.1737). Details of the statistical tests carried out can be found in Appendix 12.

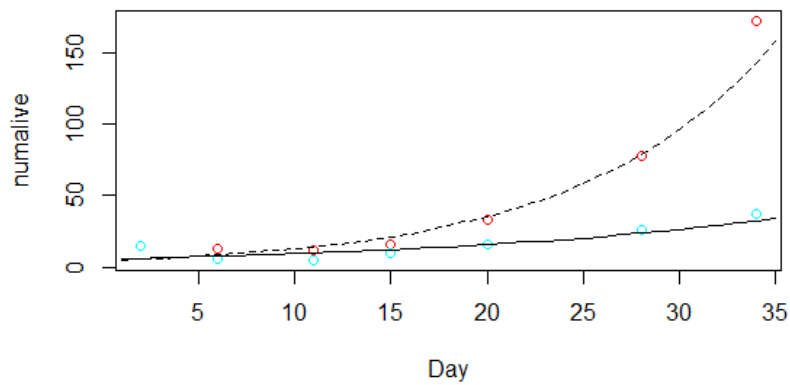


Figure 42. Overview of the fit between the GLM model and the mean values of the dataset, with injected trees (blue coloured) and non-injected ones (red coloured).

5. General discussion

In order to prove the biopesticide safety for plants, the aim of this project was to investigate the physiological, biochemical and transcriptomic apple trees' response to an essential oil based insecticide.

The primary research objective was to determine how long after CEO foliar application is an oxidative burst observed, if occurring. In a chronological order of reactions triggered within the plant cell, ROS production is known to be the most prevalent response to stress perception, but their quantification is rather delicate because of their great instability and reactivity. In our case, the only tangible conclusion that can be drawn concerning H₂O₂ is that the oxidative burst occurs within a few seconds (before 1 minute) for apple tree leaf discs in the presence of CEO emulsion. But as in this analysis only extracellular ROS are taken into account, it might not fully reflect the oxidative burst inside the cells. Then, the whole antioxidant system of plants is complex, and composed of plenty of (non)-enzymatic molecules working in interconnected pathways. The most relevant and integrative parameters have thus been considered. Among the apple tree redox system, glutathione plays a dual role of ROS detoxification and signalling. A decrease in the overall GSH/ Tot GSH ratio is already observed after 5 minutes of treatment (first time step considered) until 30 min. Moreover, over a period of 2 hours, the plant does not seem to produce additional glutathione to acclimatise to stress (Tot GSH remains constant).

The second objective was to detect the extent of cellular damage occurring as a result of oxidative stress. The only parameters showing that the antioxidant plant defence system cannot completely manage the oxidative stress in the first instance are malondialdehyde and chlorophylls a and b. Between 6 et 24h of treatment, the increase in MDA and decrease in Chl a & b contents indicate that there is indeed peroxidation of membrane lipids and degradation of photosynthetic pigments. But a return to the initial values linked to stress management is achieved after 48h. Besides that, other parameters studied do not change significantly over time of treatment : CD, EL and Car. It can be deduced that the amount of conjugated dienes assessed alone does not reveal lipid peroxidation. Then, Car content does not diminish to play the role of antioxidant as glutathione to protect photosystem II from photo-inhibition and ROS.

Concerning the long term study of the photosynthetic efficiency and damages to photosystems, it has been reported that a stressed plant tends either to modify its metabolic pathways, which reduces the PSII quantum efficiency, or metabolic constituents like ROS directly degrade the plant photosystem by interrupting the electron transport chain (Schöttler and Tóth, 2014). In our case, Fv/Fm ratio has been seen constant over time, with no significant differences between injected and non-injected trees. The same trend has been observed for the photosynthetic quenching qP for example, meaning that the xanthophyll cycle, which participates in protecting photosystem II by modulating the thylakoid membrane pH gradient, was not impacted (Sytykiewicz *et al.*, 2013). Apart from that, transpiration rate and sub-stomatal CO₂ mole fraction show several lower values for injected trees, showing a decreased photosynthetic yield

at such times. Finally, no impact on vegetative growth parameters (length, diameter, leaf area) has been reported.

While a clear insecticidal effect was observed by monitoring the aphid survival rate, it is questionable whether the small amounts of CEO 2% emulsion injected (30 mg on average, thus 600 µg of CEO) are sufficient to cause their death by ingestion of toxic compounds in the xylem. Indeed, it has been reported that *C. cassia* possesses a lethal dose 50 equivalent to 17.41 µg /cm² on aphid *Myzus persicae* (Ikbal and Pavela, 2019). In our case, it seems unlikely that this amount was translocated to the leaves after the injection.

But as previously mentioned, H₂O₂, GSH and MDA can play the role of systemic acquired resistance (SAR) inducers as they are involved in signal transduction pathways that could contribute to plant defence (Velikova *et al.*, 2000 ; Davey *et al.*, 2003 ; Stone and Yang, 2006 ; Noctor *et al.*, 2012). An important aspect of GSH redox regulation is the oligomer-monomer transition of the NPR1 protein, which is an essential plant regulator of SAR. Indeed, present as an oligomer in uninduced plants, NPR1 is reduced to a monomeric form upon SAR induction. Monomers thus accumulate in the nucleus and lead to increased disease resistance and elevated expression of PR genes (Gullner and Komives, 2006 ; Malnoy *et al.*, 2007). The fact is that Warneys *et al.* (2018) affirmed that SAR induction negatively impacts the rosy apple aphid fitness and survival. Monoterpenes have also been acknowledged to support SAR amongst different plants (Maffei, 2012 ; Riedlmeier *et al.*, 2017). Induction of defence enzymes such as peroxidase activity have been observed for different essential oil/constituents like *Cinnamomum zeylanicum* oil and trans-cinnamaldehyde (Perina *et al.*, 2018). As some EOs are characterized by a direct activity against pathogens and an indirect effect by priming the plant defences, it could also be the case for the cinnamon essential oil.

By RT-PCR analysis, it can be observed that for leaves in contact with the essential oil, those molecular stress signals have effectively been sent to activate the promoters of the defence genes, with PR genes expression particularly demonstrated. This analysis thus makes it possible to establish the link between short-term oxidative stress which, even if it can be managed by the plant, leads to an induction of the plant's defence system, with then medium- and long-term repercussions, notably impacting photosynthetic yield and leaf transpiration. Among activated genes, production of α-farnesene also seems to result from SAR activation by the CEO treatment, and this volatile compound is well known as an aphid repellent (Warneys *et al.*, 2018).

6. Conclusion

As part of the Tree-injection project, this study led to three major findings. The first is that neither the foliar application, nor the trunk-injection of CEO emulsion showed an evidence of serious damage to the apple tree's physiological state. The second is that oxidative stress is managed by the plant and enables it to trigger its defence systems (SAR induction). The third and last one conclusion is that trunk-injection has an insecticide effect against RAA, rather due to the triggering of SAR and defence mechanisms than ingestion of aphicide compounds (like cinnamaldehyde).

As mentioned before, phytotoxicity of essential oils requires serious attention in such biopesticides formulation. In addition to mitigating potential phytotoxic effects, a well-studied formulation should also offset the high volatility of EOs and ensure the prolonged release of the active substance. A compromise concerning the injected dose must also be found to ensure that it is not too high and that the product acts well as an inducer of systemic defences. Therefore, the mode of EO application, the formulation and the selection of the active substance must be adapted for specific purposes and carefully evaluated.

As a whole, the use of cinnamon essential oil as bioinsecticide combined to a tree-injection method seems a very promising alternative to conventional plant protection products to treat RAA and could be part of a larger Integrated Pest Management program for organic production.

7. Perspectives

Many aspects concerning phytotoxicity could still be investigated.

The first one should be the impact of the emulsion concentration. Working with 0.5 and 1% emulsions should be interesting to see if lower CEO concentrations would lead to the same results regarding oxidative stress, and to make links with the transcriptomic analysis performed. Additional sampling times could also been integrated to the experimental design, to consider shorter time steps before 1 min for H₂O₂ luminol assay , and between 0 and 5 min for GSH redox state evaluation for example.

Secondly, numerous other cellular markers of oxidative stress often reported in the literature could be quantified, like ascorbic acid (AsA) as the other major component of ascorbate-glutathione pathway (Gill *et al.*, 2013). Glutathione being a non-enzymatic antioxidant, ROS scavenging enzymes such as superoxide dismutase (SOD), catalase (CAT) and ascorbate peroxidase (APX) could also be considered (Ahuja *et al.*, 2015). Knowing that the proline amino acid content increases in plants under drought stress conditions, it can also be suggested as another evaluating stress parameter (Khare *et al.*, 2019). Another aspect is that high *in vitro* MDA contents may irreparably alter proteins and DNA, RNA (Esterbauer and Cheeseman, 1990). As they are also sensitive to ROS, damage to DNA and proteins would be an additional

area of study to consider (Desikan *et al.*, 2001). Finally, physical damages due to trunk-injection could also occur on the plant vessels and this could be evaluated by plant histological sections.

Given the few conclusions that could be drawn from the quantification of hydrogen peroxide, ROS could rather be detected by histochemical staining techniques, like superoxide anions with nitroblue tetrazolium (NBT) and hydrogen peroxide by Diaminobenzidine tetrahydrochloride (DAB) staining. Moreover, one of the most commonly used dyes for determining total ROS is 2',7'-dichlorofluorescein (H₂DCF) (Jambunathan, 2010). Instead of MDA and CD quantification to assess the membrane lipid peroxidation, other aldehydic products derived from polyunsaturated fatty acids could be quantified like n-hexanal, 4-hydroxynonanal and 4-hydroxyhexenal (Esterbauer and Cheeseman, 1990 ; Shulaev and Oliver, 2006).

Compared to a uniform foliar application, trunk-injections are known to present a great heterogeneity in the quantity delivered (Coslor *et al.*, 2018). Furthermore, it would be of great interest to quantify cinnamaldehyde in the leaves with DHS-GC-MS techniques in order to know more about the translocation of the emulsion to the leaves.

Finally, the product's administration should be of economic interest for the fruit producer and an estimation of the yearly treatment cost should be performed. It is thus crucial to determine the number of applications required for a guaranteed efficiency in the orchard, by considering the aphid biological cycle to deduce the ideal injection timing. The impact on apple quality or yield should be established as well, with a further study of the presence of biopesticide residues in apples and the effect on non-target organisms (such as pollinators).

8. Bibliography

- Achnine, L., Mata, R., Iglesias-Prieto, R., & Lotina-Hennsen, B. (1998). Impairment of Photosystem II Donor Side by the Natural Product Odoranol. *Journal of Agricultural and Food Chemistry*, *46*(12), 5313–5317. <https://doi.org/10.1021/jf980589+>
- Ahuja, N., Singh, H. P., Batish, D. R., & Kohli, R. K. (2015). Eugenol-inhibited root growth in *Avena fatua* involves ROS-mediated oxidative damage. *Pesticide Biochemistry and Physiology*, *118*, 64–70. <https://doi.org/10.1016/j.pestbp.2014.11.012>
- Albert, L., Franck, P., Gilles, Y., & Plantegenest, M. (2017). Impact of agroecological infrastructures on the dynamics of *dysaphis plantaginea* (hemiptera: Aphididae) and its natural enemies in apple Orchards in Northwestern France. *Environmental Entomology*, *46*(3), 528–537. <https://doi.org/10.1093/ee/nvx054>
- Apaaq-W (no date). Fruits produits en Région wallonne. La production de pommes en Wallonie. Available at: <http://www.apaaq.be/productions/les-fruits/fruits-produits-en-wallonie.aspx> (Accessed: 05/03/2021).
- Apel, K., & Hirt, H. (2004). Reactive oxygen species: Metabolism, oxidative stress, and signal transduction. *Annual Review of Plant Biology*, *55*, 373–399. <https://doi.org/10.1146/annurev.arplant.55.031903.141701>
- Baker, N. R. (2008). Chlorophyll fluorescence: A probe of photosynthesis in vivo. *Annual Review of Plant Biology*, *59*, 89–113. <https://doi.org/10.1146/annurev.arplant.59.032607.092759>
- Bakkali, F., Averbeck, S., Averbeck, D., & Idaomar, M. (2008). Biological effects of essential oils - A review. *Food and Chemical Toxicology*, *46*(2), 446–475. <https://doi.org/10.1016/j.fct.2007.09.106>
- Bessin, R. (2006). Rosy Apple Aphid. *Encyclopedia of Entomology*, 1920–1920. https://doi.org/10.1007/0-306-48380-7_3711
- Bird, A. E., Hesketh, H., Cross, J. V., & Copland, M. (2004). The common black ant, *Lasius niger* (Hymenoptera: Formicidae), as a vector of the entomopathogen *Lecanicillium longisporum* to rosy apple aphid, *Dysaphis plantaginea* (Homoptera: Aphididae). *Biocontrol Science and Technology*, *14*(8), 757–767. <https://doi.org/10.1080/09583150410001720716>
- Bisceglia, N., Gravino, M., & Savatin, D. (2015). Luminol-based Assay for Detection of Immunity Elicitor-induced Hydrogen Peroxide Production in *Arabidopsis thaliana* Leaves. *Bio-Protocol*, *5*(24), 16–22. <https://doi.org/10.21769/bioprotoc.1685>
- Blommers, L. H. M., Helsen, H. H. M., & Vaal, F. W. N. M. (2004). Life history data of the rosy apple aphid *Dysaphis plantaginea* (Pass.) (Homopt., Aphididae) on plantain and as migrant to apple. *Journal of Pest Science*, *77*(3), 155–163. <https://doi.org/10.1007/s10340-004-0046-5>
- Bonasera, J. M., Kim, J. F., & Beer, S. V. (2006). PR genes of apple: Identification and expression in response to elicitors and inoculation with *Erwinia amylovora*. *BMC Plant Biology*, *6*, 1–12. <https://doi.org/10.1186/1471-2229-6-23>
- Bourrié, B. (2007). *La Fluorescence Chlorophyllienne Comme Outil De Diagnostic*. 1–11.
- Bresson, J., Bieker, S., Riester, L., Doll, J., & Zentgraf, U. (2018). A guideline for leaf senescence analyses: From quantification to physiological and molecular investigations. In *Journal of Experimental Botany* (Vol. 69, Issue 4, pp. 769–786). <https://doi.org/10.1093/jxb/erx246>
- Bribosia, E., Bylemans, D., Migon, M., & Van Impe, G. (2005). In-field production of parasitoids of *Dysaphis plantaginea* by using the rowan aphid *Dysaphis sorbi* as substitute host. *BioControl*, *50*(4), 601–610. <https://doi.org/10.1007/s10526-004-5526-2>

- Brown, M. W., & Mathews, C. R. (2007). Conservation biological control of rosy apple aphid, *Dysaphis plantaginea* (Passerini), in eastern north America. *Environmental Entomology*, *36*(5), 1131–1139. [https://doi.org/10.1603/0046-225X\(2007\)36\[1131:CBCORA\]2.0.CO;2](https://doi.org/10.1603/0046-225X(2007)36[1131:CBCORA]2.0.CO;2)
- Brumbarova, T., Le, C., & Bauer, P. (2016). Hydrogen Peroxide Measurement in Arabidopsis Root Tissue Using Amplex Red. *Bio-Protocol*, *6*(21), 1–11. <https://doi.org/10.21769/bioprotoc.1999>
- Chen, L., Han, Y., Jiang, H., Korpelainen, H., & Li, C. (2011). Nitrogen nutrient status induces sexual differences in responses to cadmium in *Populus yunnanensis*. *Journal of Experimental Botany*, *62*(14), 5037–5050. <https://doi.org/10.1093/jxb/err203>
- Chowhan, N., Singh, H. P., Batish, D. R., & Kohli, R. K. (2011). Phytotoxic effects of β -pinene on early growth and associated biochemical changes in rice. *Acta Physiologiae Plantarum*, *33*(6), 2369–2376. <https://doi.org/10.1007/s11738-011-0777-x>
- Coats, J. R., Karr, L. L., & Drewes, C. D. (1991). Toxicity and Neurotoxic Effects of Monoterpenoids. In *Naturally Occurring Pest Bioregulators* (Vol. 449, Issue 20, pp. 305–316). <https://doi.org/10.1021/bk-1991-0449.ch020>
- Coslor, C. C., Vandervoort, C., & Wise, J. C. (2019). Insecticide dose and seasonal timing of trunk injection in apples influence efficacy and residues in nectar and plant parts. *Pest Management Science*, *75*(5), 1453–1463. <https://doi.org/10.1002/ps.5268>
- Cross, J. V., Cubison, S., Harris, A., & Harrington, R. (2007). Autumn control of rosy apple aphid, *Dysaphis plantaginea* (Passerini), with aphicides. *Crop Protection*, *26*(8), 1140–1149. <https://doi.org/10.1016/j.cropro.2006.10.007>
- Davey, M. W., Dekempeneer, E., & Keulemans, J. (2003). *Rocket-powered high-performance liquid chromatographic analysis of plant ascorbate and glutathione*. *316*, 74–81. [https://doi.org/10.1016/S0003-2697\(03\)00047-2](https://doi.org/10.1016/S0003-2697(03)00047-2)
- Davey, M. W., Stals, E., Panis, B., Keulemans, J., & Swennen, R. L. (2005). High-throughput determination of malondialdehyde in plant tissues. *Analytical Biochemistry*, *347*(2), 201–207. <https://doi.org/10.1016/j.ab.2005.09.041>
- Dayan, F. E., Cantrell, C. L., & Duke, S. O. (2009). Natural products in crop protection. *Bioorganic and Medicinal Chemistry*, *17*(12), 4022–4034. <https://doi.org/10.1016/j.bmc.2009.01.046>
- Dayan, F. E., & Watson, S. B. (2011). Plant cell membrane as a marker for light-dependent and light-independent herbicide mechanisms of action. *Pesticide Biochemistry and Physiology*, *101*(3), 182–190. <https://doi.org/10.1016/j.pestbp.2011.09.004>
- Dayan, F. E., Romagni, J. G., & Duke, S. O. (2000). Investigating the mode of action of natural phytotoxins. *Journal of Chemical Ecology*, *26*(9), 2079–2094. <https://doi.org/10.1023/A:1005512331061>
- Desikan, R., A.-H.-Mackerness, S., Hancock, J. T., & Neill, S. J. (2001). Regulation of the Arabidopsis transcriptome by oxidative stress. *Plant Physiology*, *127*(1), 159–172. <https://doi.org/10.1104/pp.127.1.159>
- Dias, M. C. (2012). Phytotoxicity: An Overview of the Physiological Responses of Plants Exposed to Fungicides. *Journal of Botany*, *2012*, 1–4. <https://doi.org/10.1155/2012/135479>
- Dib, H., Simon, S., Sauphanor, B., & Capowiez, Y. (2010). The role of natural enemies on the population dynamics of the rosy apple aphid, *Dysaphis plantaginea* Passerini (Hemiptera: Aphididae) in organic apple orchards in south-eastern France. *Biological Control*, *55*(2), 97–109. <https://doi.org/10.1016/j.biocontrol.2010.07.005>

- Douthe, C., Gago, J., Ribas-Carbó, M., Núñez, R., Pedrol, N., & Flexas, J. (2018). Measuring photosynthesis and respiration with infrared gas analysers. In *Advances in Plant Ecophysiology Techniques* (pp. 51–75). https://doi.org/10.1007/978-3-319-93233-0_4
- Dugé de Bernonville, T., Marolleau, B., Staub, J., Gaucher, M., & Brisset, M. N. (2014). Using molecular tools to decipher the complex world of plant resistance inducers: An apple case study. *Journal of Agricultural and Food Chemistry*, 62(47), 11403–11411. <https://doi.org/10.1021/jf504221x>
- Ebrahim, S., Usha, K., & Singh, B. (2011). Pathogenesis Related (PR) Proteins in Plant Defense Mechanism Age-Related Pathogen Resistance. *Curr. Res. Technol. Adv.*, 1043–1054.
- Ekmekci, Y., & Terzioglu, S. (2005). Effects of oxidative stress induced by paraquat on wild and cultivated wheats. *Pesticide Biochemistry and Physiology*, 83(2–3), 69–81. <https://doi.org/10.1016/j.pestbp.2005.03.012>
- Esterbauer, H., & Cheeseman, K. H. (1990). Determination of aldehydic lipid peroxidation products: Malonaldehyde and 4-hydroxynonenal. *Methods in Enzymology*, 186(C), 407–421. [https://doi.org/10.1016/0076-6879\(90\)86134-H](https://doi.org/10.1016/0076-6879(90)86134-H)
- FAO, & WHO. (2017). *Guidelines for the registration of microbial, botanical and semiochemical pest control agents for plant protection and public health uses*. http://www.who.int/whopes/resources/WHO_HTM_NTD_WHOPES_2017.05/en/
- FAOSTAT (2019). Available at: <http://www.fao.org/faostat/en/#data/QC> (Accessed: 05/03/2021).
- Farmer, E. E., & Mueller, M. J. (2013). ROS-mediated lipid peroxidation and RES-activated signaling. *Annual Review of Plant Biology*, 64(February), 429–450. <https://doi.org/10.1146/annurev-arplant-050312-120132>
- Foyer, C. H., Lopez-Delgado, H., Dat, J. F., & Scott, I. M. (1997). Hydrogen peroxide- and glutathione-associated mechanisms of acclimatory stress tolerance and signalling. *Physiologia Plantarum*, 100(2), 241–254. <https://doi.org/10.1034/j.1399-3054.1997.1000205.x>
- Foyer, C. H., & Noctor, G. (2011). Ascorbate and glutathione: The heart of the redox hub. *Plant Physiology*, 155(1), 2–18. <https://doi.org/10.1104/pp.110.167569>
- Gallé, A., & Flexas, J. (2010). Methodologies and results in grapevine research. *Methodologies and Results in Grapevine Research*, 1–448. <https://doi.org/10.1007/978-90-481-9283-0>
- Gamon, J. A., & Pearcy, R. W. (1989). Leaf movement, stress avoidance and photosynthesis in *Vitis californica*. *Oecologia*, 79(4), 475–481. <https://doi.org/10.1007/BF00378664>
- Genty, B., Briantais, J. M., & Baker, N. R. (1989). The relationship between the quantum yield of photosynthetic electron transport and quenching of chlorophyll fluorescence. *Biochimica et Biophysica Acta - General Subjects*, 990(1), 87–92. [https://doi.org/10.1016/S0304-4165\(89\)80016-9](https://doi.org/10.1016/S0304-4165(89)80016-9)
- Gill, S. S., Anjum, N. A., Hasanuzzaman, M., Gill, R., Trivedi, D. K., Ahmad, I., Pereira, E., & Tuteja, N. (2013). Glutathione and glutathione reductase: A boon in disguise for plant abiotic stress defense operations. In *Plant Physiology and Biochemistry* (Vol. 70, pp. 204–212). Elsevier Masson. <https://doi.org/10.1016/j.plaphy.2013.05.032>
- Gitelson, A. A., & Merzlyak, M. N. (2004). Non-destructive assessment of chlorophyll, carotenoid and anthocyanin content in higher plant leaves: Principles and algorithms. *Remote Sensing for Agriculture and the Environment* (S. Stamatiadis, J.M. Lynch, J.S. Schepers Eds.), Greece, Ella, 78–94.
- Giustarini, D., Tsikas, D., Colombo, G., Milzani, A., Dalle-Donne, I., Fanti, P., & Rossi, R. (2016). Pitfalls in the analysis of the physiological antioxidant glutathione (GSH) and its disulfide (GSSG) in biological samples: An elephant in the room. *Journal of Chromatography B: Analytical Technologies in the Biomedical and Life Sciences*, 1019, 21–28. <https://doi.org/10.1016/j.jchromb.2016.02.015>

- Graña, E., Sotelo, T., Díaz-Tielas, C., Araniti, F., Krasuska, U., Bogatek, R., Reigosa, M. J., & Sánchez-Moreiras, A. M. (2013). Citral Induces Auxin and Ethylene-Mediated Malformations and Arrests Cell Division in *Arabidopsis thaliana* Roots. *Journal of Chemical Ecology*, *39*(2), 271–282. <https://doi.org/10.1007/s10886-013-0250-y>
- Grana, E., Diaz-Tielas, C., M. Sanchez-Moreiras, A., & J. Reigosa, M. (2012). Mode of Action of Monoterpenes in Plant-Plant Interactions. *Current Bioactive Compounds*, *4*(1), 80–89. <https://doi.org/10.2174/157340712799828214>
- Gullner, G., & Komives, T. (2006). Defense Reactions of Infected Plants: Roles of Glutathione and Glutathione S-Transferase Enzymes. *Acta Phytopathologica et Entomologica Hungarica*, *41*(1–2), 11–21. <https://doi.org/10.1556/APhyt.41.2006.1-2.2>
- Gupta, K. J., & Igamberdiev, A. U. (2010). Reactive Oxygen and Communication in Signaling and Nitrogen Species Plants. In *Signaling and Communication in Plants*.
- Hajdinák, P., Czobor, Á., Lőrincz, T., & Szarka, A. (2019). The problem of glutathione determination: A comparative study on the measurement of glutathione from plant cells. *Periodica Polytechnica Chemical Engineering*, *63*(1), 1–10. <https://doi.org/10.3311/PPch.11785>
- Hansatech Instruments* (no date) Continuous Excitation Chlorophyll Fluorescence. Available at: <http://www.hansatech-instruments.com/continuous-excitation-chlorophyll-fluorescence/> (Accessed: 20/05/2021).
- Hernández, L. E., Sobrino-Plata, J., Montero-Palmero, M. B., Carrasco-Gil, S., Flores-Cáceres, M. L., Ortega-Villasante, C., & Escobar, C. (2015). Contribution of glutathione to the control of cellular redox homeostasis under toxic metal and metalloid stress. *Journal of Experimental Botany*, *66*(10), 2901–2911. <https://doi.org/10.1093/jxb/erv063>
- Hogarth, L. A., Rabello, C. M. A., & Hall, A. G. (2003). Measurement of Reduced Glutathione Using High-Pressure Liquid Chromatography. *Cytotoxic Drug Resistance Mechanisms*, *28*, 91–94. <https://doi.org/10.1385/1-59259-687-8:91>
- Huang, Y., Ho, S. H. (1998). Toxicity and antifeedant activities of cinnamaldehyde against the grain storage insects, *Tribolium castaneum* (Herbst) and *Sitophilus zeamais* Motsch. *Journal of Stored Products Research*, *34*(1), 11–17. [https://doi.org/10.1016/S0022-474X\(97\)00038-6](https://doi.org/10.1016/S0022-474X(97)00038-6)
- Ibrahim, M. A., Kainulainen, P., Aflatuni, A., Tiilikkala, K., & Holopainen, J. K. (2001). Insecticidal, repellent, antimicrobial activity and phytotoxicity of essential oils: With special reference to limonene and its suitability for control of insect pests. *Agricultural and Food Science in Finland*, *10*(3), 243–259. <https://doi.org/10.23986/afsci.5697>
- Ikbāl, C., & Pavela, R. (2019). Essential oils as active ingredients of botanical insecticides against aphids. *Journal of Pest Science*, *92*(3), 971–986. <https://doi.org/10.1007/s10340-019-01089-6>
- Jambunathan, N. (2010). Plant Stress Tolerance. *NIH Public Access*, *639*, 1–14. <https://doi.org/10.1007/978-1-60761-702-0>
- Jenser, G., Balázs, K., Erdélyi, C., Haltrich, A., Kádár, F., Kozár, F., Markó, V., Rácz, V., & Samu, F. (1999). Changes in arthropod population composition in IPM apple orchards under continental climatic conditions in Hungary. *Agriculture, Ecosystems and Environment*, *73*(2), 141–154. [https://doi.org/10.1016/S0167-8809\(99\)00023-7](https://doi.org/10.1016/S0167-8809(99)00023-7)
- Kellerhals, M., Szalatnay, D., Hunziker, K., Duffy, B., Nybom, H., Ahmadi-Afzadi, M., Höfer, M., Richter, K., & Lateur, M. (2012). European pome fruit genetic resources evaluated for disease resistance. In *Trees - Structure and Function* (Vol. 26, Issue 1, pp. 179–189). <https://doi.org/10.1007/s00468-011-0660-9>

- Khare, P., Srivastava, S., Nigam, N., Singh, A. K., & Singh, S. (2019). Impact of essential oils of *E. citriodora*, *O. basilicum* and *M. arvensis* on three different weeds and soil microbial activities. *Environmental Technology and Innovation*, 14, 100343. <https://doi.org/10.1016/j.eti.2019.100343>
- Kim, S. Il, Roh, J. Y., Kim, D. H., Lee, H. S., & Ahn, Y. J. (2003). Insecticidal activities of aromatic plant extracts and essential oils against *Sitophilus oryzae* and *Callosobruchus chinensis*. *Journal of Stored Products Research*, 39(3), 293–303. [https://doi.org/10.1016/S0022-474X\(02\)00017-6](https://doi.org/10.1016/S0022-474X(02)00017-6)
- Kostyukovsky, M., Rafaeli, A., Gileadi, C., Demchenko, N., & Shaaya, E. (2002). Activation of octopaminergic receptors by essential oil constituents isolated from aromatic plants: Possible mode of action against insect pests. *Pest Management Science*, 58(11), 1101–1106. <https://doi.org/10.1002/ps.548>
- Koul, O., Walia, S., & Dhaliwal, G. S. (2008). Essential Oils as Green Pesticides: Potential and Constraints. *Applied Entomology and Zoology*, 4(1), 63–84. <https://doi.org/10.1303/aez.32.437>
- Kuhns, M. (2011). Getting Chemicals into Trees Without Spraying. *020*.
- Larcher W. (2003). *Physiological plant ecology*. Berlin: Springer Verlag.
- Lee, E. J., Kim, J. R., Choi, D. R., & Ahn, Y. J. (2008). Toxicity of cassia and cinnamon oil compounds and cinnamaldehyde-related compounds to *Sitophilus oryzae* (Coleoptera: Curculionidae). *Journal of Economic Entomology*, 101(6), 1960–1966. <https://doi.org/10.1603/0022-0493-101.6.1960>
- Lins, L., Dal Maso, S., Foncoux, B., Kamili, A., Laurin, Y., Genva, M., Jijakli, M. H., De Clerck, C., Fauconnier, M. L., & Deleu, M. (2019). Insights into the relationships between herbicide activities, molecular structure and membrane interaction of cinnamon and citronella essential oils components. *International Journal of Molecular Sciences*, 20(16). <https://doi.org/10.3390/ijms20164007>
- Long, S. P., Farage, P. K., & Garcia, R. L. (1996). Measurement of leaf and canopy photosynthetic CO₂ exchange in the field. *Journal of Experimental Botany*, 47(304), 1629–1642. <https://doi.org/10.1093/jxb/47.11.1629>
- Lykkesfeldt, J. (2001). Determination of malondialdehyde as dithiobarbituric acid adduct in biological samples by HPLC with fluorescence detection: Comparison with ultraviolet-visible spectrophotometry. *Clinical Chemistry*, 47(9), 1725–1727. <https://doi.org/10.1093/clinchem/47.9.1725>
- Ma, Y. H., Ma, F. W., Wang, Y. H., & Zhang, J. K. (2011). The responses of the enzymes related with ascorbate-glutathione cycle during drought stress in apple leaves. *Acta Physiologiae Plantarum*, 33(1), 173–180. <https://doi.org/10.1007/s11738-010-0535-5>
- Ma, Y. H., Ma, F. W., Zhang, J. K., Li, M. J., Wang, Y. H., & Liang, D. (2008). Effects of high temperature on activities and gene expression of enzymes involved in ascorbate-glutathione cycle in apple leaves. *Plant Science*, 175(6), 761–766. <https://doi.org/10.1016/j.plantsci.2008.07.010>
- Malnoy, M., Borejsza-Wysocka, E. E., Jin, Q. L., He, S. Y., & Aldwinckle, H. S. (2004). Over-expression of the apple gene MpNPR1 causes increased disease resistance in *Malus x domestica*. *Acta Horticulturae*, 663(12), 463–468. <https://doi.org/10.17660/ActaHortic.2004.663.80>
- Maffei, M. (2012). Monoterpenoid Plant-Plant Interactions Upon Herbivory. *Current Bioactive Compounds*, 8(1), 65–70. <https://doi.org/10.2174/157340712799828250>
- Maxwell, K., & Johnson, G. N. (2000). Chlorophyll fluorescence-a practical guide. In *Journal of Experimental Botany* (Vol. 51, Issue 345).
- Miguel, M. G. (2010). Antioxidant and anti-inflammatory activities of essential oils: A short review. *Molecules*, 15(12), 9252–9287. <https://doi.org/10.3390/molecules15129252>

- Miñarro, M., Hemptinne, J. L., & Dapena, E. (2005). Colonization of apple orchards by predators of *Dysaphis plantaginea*: Sequential arrival, response to prey abundance and consequences for biological control. *BioControl*, 50(3), 403–414. <https://doi.org/10.1007/s10526-004-5527-1>
- Minocha, R., Thangavel, P., Dhankher, O. P., & Long, S. (2008). Separation and quantification of monothiools and phytochelatins from a wide variety of cell cultures and tissues of trees and other plants using high performance liquid chromatography. *Journal of Chromatography A*, 1207(1–2), 72–83. <https://doi.org/10.1016/j.chroma.2008.08.023>
- Mittler, R., Vanderauwera, S., Gollery, M., & Van Breusegem, F. (2004). Reactive oxygen gene network of plants. *Trends in Plant Science*, 9(10), 490–498. <https://doi.org/10.1016/j.tplants.2004.08.009>
- Morales, M., & Munné-Bosch, S. (2019). Malondialdehyde: Facts and artifacts. *Plant Physiology*, 180(3), 1246–1250. <https://doi.org/10.1104/pp.19.00405>
- Moretti, M. D. L., Sanna-Passino, G., Demontis, S., & Bazzoni, E. (2002). Essential oil formulations useful as a new tool for insect pest control. *AAPS PharmSciTech*, 3(2), 13. <https://doi.org/10.1208/pt030213>
- Mossa, A. T. H. (2016). Green Pesticides: Essential oils as biopesticides in insect-pest management. *Journal of Environmental Science and Technology*, 9(5), 354–378. <https://doi.org/10.3923/jest.2016.354.378>
- Mulkey, S. S., & Smith, M. (1988). Measurement of photosynthesis by infra-red gas analysis. *Bioinstrumentation. American Biology Teachers Association, Warrenton(VA)*, 79–84.
- Murray, M., & Alston, D. G. (2020). *Fruit Pests : Apple The Backyard Orchardist. January.*
- Mutlu, S., Atici, Ö., Esim, N., & Mete, E. (2011). Essential oils of catmint (*Nepeta meyeri* Benth.) induce oxidative stress in early seedlings of various weed species. *Acta Physiologiae Plantarum*, 33(3), 943–951. <https://doi.org/10.1007/s11738-010-0626-3>
- Neill, S., Desikan, R., & Hancock, J. (2002). Hydrogen peroxide signalling. *Current Opinion in Plant Biology*, 5(5), 388–395. [https://doi.org/10.1016/S1369-5266\(02\)00282-0](https://doi.org/10.1016/S1369-5266(02)00282-0)
- Noctor, G., Mhamdi, A., Chaouch, S., Han, Y., Neukermans, J., Marquez-Garcia, B., Queval, G., & Foyer, C. H. (2012). Glutathione in plants: an integrated overview. *Plant, Cell and Environment*, 35(2), 454–484. <https://doi.org/10.1111/j.1365-3040.2011.02400.x>
- Noctor, G., Queval, G., Mhamdi, A., Chaouch, S., & Foyer, C. H. (2011). *Glutathione*. 1–32. <https://doi.org/10.1199/tab.0142>
- Nowotarska, S., Nowotarski, K., Friedman, M., & Situ, C. (2014). Effect of Structure on the Interactions between Five Natural Antimicrobial Compounds and Phospholipids of Bacterial Cell Membrane on Model Monolayers. *Molecules*, 19(6), 7497–7515. <https://doi.org/10.3390/molecules19067497>
- Oliveira, M. D. M., Varanda, C. M. R., & Félix, M. R. F. (2016). Induced resistance during the interaction pathogen x plant and the use of resistance inducers. *Phytochemistry Letters*, 15, 152–158. <https://doi.org/10.1016/j.phytol.2015.12.011>
- Park, I. K., Lee, H. S., Lee, S. G., Park, J. D., & Ahn, Y. J. (2000). Insecticidal and fumigant activities of Cinnamomum cassia bark-derived materials against *Mechoris ursulus* (Coleoptera: Attelabidae). *Journal of Agricultural and Food Chemistry*, 48(6), 2528–2531. <https://doi.org/10.1021/jf9904160>
- Pavela, R., & Benelli, G. (2016). Essential Oils as Ecofriendly Biopesticides? Challenges and Constraints. In *Trends in Plant Science* (Vol. 21, Issue 12, pp. 1000–1007). Elsevier Ltd. <https://doi.org/10.1016/j.tplants.2016.10.005>

- Perina, F. J., de Andrade, C. C. L., Moreira, S. I., Nery, E. M., Ogoshi, C., & Alves, E. (2019). Cinnamomun zeylanicum oil and trans-cinnamaldehyde against Alternaria brown spot in tangerine: direct effects and induced resistance. *Phytoparasitica*, 47(4), 575–589. <https://doi.org/10.1007/s12600-019-00754-x>
- Poonpaiboonpipat, T., Pangnakorn, U., Suvunnamek, U., Teerarak, M., Charoenying, P., & Laosinwattana, C. (2013). Phytotoxic effects of essential oil from *Cymbopogon citratus* and its physiological mechanisms on barnyardgrass (*Echinochloa crus-galli*). *Industrial Crops and Products*, 41(1), 403–407. <https://doi.org/10.1016/j.indcrop.2012.04.057>
- Potters, G., Horemans, N., & Jansen, M. A. K. (2010). The cellular redox state in plant stress biology - A charging concept. *Plant Physiology and Biochemistry*, 48(5), 292–300. <https://doi.org/10.1016/j.plaphy.2009.12.007>
- Prieto, C., & Calvo, L. (2013). Performance of the Biocompatible Surfactant Tween 80, for the Formation of Microemulsions Suitable for New Pharmaceutical Processing. *Journal of Applied Chemistry*, 2013, 1–10. <https://doi.org/10.1155/2013/930356>
- Queval, G., Jaillard, D., Zechmann, B., & Noctor, G. (2011). Increased intracellular H₂O₂ availability preferentially drives glutathione accumulation in vacuoles and chloroplasts. *Plant, Cell and Environment*, 34(1), 21–32. <https://doi.org/10.1111/j.1365-3040.2010.02222.x>
- Queval, G., & Noctor, G. (2007). A plate reader method for the measurement of NAD, NADP, glutathione, and ascorbate in tissue extracts: Application to redox profiling during Arabidopsis rosette development. *Analytical Biochemistry*, 363(1), 58–69. <https://doi.org/10.1016/j.ab.2007.01.005>
- Radhakrishnan, R., Alqarawi, A. A., & Abd Allah, E. F. (2018). Bioherbicides: Current knowledge on weed control mechanism. In *Ecotoxicology and Environmental Safety* (Vol. 158, pp. 131–138). Academic Press. <https://doi.org/10.1016/j.ecoenv.2018.04.018>
- Riedlmeier, M., Ghirardo, A., Wenig, M., Knappe, C., Koch, K., Georgii, E., Dey, S., Parker, J. E., Schnitzler, J. P., & Vlot, A. C. (2017). Monoterpenes support systemic acquired resistance within and between plants. *Plant Cell*, 29(6), 1440–1459. <https://doi.org/10.1105/tpc.16.00898>
- Rolny, N., Costa, L., Carrión, C., & Guiamet, J. J. (2011). Is the electrolyte leakage assay an unequivocal test of membrane deterioration during leaf senescence? *Plant Physiology and Biochemistry*, 49(10), 1220–1227. <https://doi.org/10.1016/j.plaphy.2011.06.010>
- Rubiolo, P., Sgorbini, B., Liberto, E., Cordero, C., & Bicchi, C. (2010). Essential oils and volatiles: Sample preparation and analysis. A review. *Flavour and Fragrance Journal*, 25(5), 282–290. <https://doi.org/10.1002/ffj.1984>
- Saad, M. M. G., Gouda, N. A. A., & Abdelgaleil, S. A. M. (2019). Bioherbicidal activity of terpenes and phenylpropenes against *Echinochloa crus-galli*. *Journal of Environmental Science and Health - Part B Pesticides, Food Contaminants, and Agricultural Wastes*, 54(12), 954–963. <https://doi.org/10.1080/03601234.2019.1653121>
- Schöttler, M. A., & Tóth, S. Z. (2014). Photosynthetic complex stoichiometry dynamics in higher plants: Environmental acclimation and photosynthetic flux control. In *Frontiers in Plant Science* (Vol. 5, Issue MAY). <https://doi.org/10.3389/fpls.2014.00188>
- Seljeskog, E., Hervig, T., & Mansoor, M. A. (2006). A novel HPLC method for the measurement of thiobarbituric acid reactive substances (TBARS). A comparison with a commercially available kit. *Clinical Biochemistry*, 39(9), 947–954. <https://doi.org/10.1016/j.clinbiochem.2006.03.012>
- Sergent, O., Morel, I., Cogrel, P., Chevanne, M., Padeloup, N., Brissot, P., Lescoat, G., Cillard, P., & Cillard, J. (1993). Simultaneous measurements of conjugated dienes and free malondialdehyde, used as a micromethod for the evaluation of lipid peroxidation in rat hepatocyte cultures. *Chemistry and Physics of Lipids*, 65(2), 133–139. [https://doi.org/10.1016/0009-3084\(93\)90046-6](https://doi.org/10.1016/0009-3084(93)90046-6)

- Shah, K., An, N., Ma, W., Ara, G., Ali, K., Kamanova, S., Zuo, X., Han, M., Ren, X., & Xing, L. (2020). Chronic cement dust load induce novel damages in foliage and buds of *Malus domestica*. *Scientific Reports*, *10*(1), 1–12. <https://doi.org/10.1038/s41598-020-68902-6>
- Shulaev, V., & Oliver, D. J. (2006). Metabolic and proteomic markers for oxidative stress. New tools for reactive oxygen species research. In *Plant Physiology* (Vol. 141, Issue 2, pp. 367–372). <https://doi.org/10.1104/pp.106.077925>
- Sikkema, J., De Bont, J. A. M., & Poolman, B. (1995). Mechanisms of membrane toxicity of hydrocarbons. In *Microbiological Reviews* (Vol. 59, Issue 2, pp. 201–222). <https://doi.org/10.1128/mmbr.59.2.201-222.1995>
- Singh, H. P., Batish, D. R., Kaur, S., Ramezani, H., & Kohli, R. K. (2002). Comparative phytotoxicity of four monoterpenes against *Cassia occidentalis*. *Annals of Applied Biology*, *141*(2), 111–116. <https://doi.org/10.1111/j.1744-7348.2002.tb00202.x>
- Singh, H. P., Batish, D. R., Kaur, S., Arora, K., & Kohli, R. K. (2006). α -Pinene inhibits growth and induces oxidative stress in roots. *Annals of Botany*, *98*(6), 1261–1269. <https://doi.org/10.1093/aob/mcl213>
- Singh, H. P., Batish, D. R., Kaur, G., Arora, K., & Kohli, R. K. (2008). Nitric oxide (as sodium nitroprusside) supplementation ameliorates Cd toxicity in hydroponically grown wheat roots. *Environmental and Experimental Botany*, *63*(1–3), 158–167. <https://doi.org/10.1016/j.envexpbot.2007.12.005>
- Singh, H. P., Kaur, S., Mittal, S., Batish, D. R., & Kohli, R. K. (2009). Essential oil of *Artemisia scoparia* inhibits plant growth by generating reactive oxygen species and causing oxidative damage. *Journal of Chemical Ecology*, *35*(2), 154–162. <https://doi.org/10.1007/s10886-009-9595-7>
- Šircelj, H., Tausz, M., Grill, D., & Batič, F. (2007). Detecting different levels of drought stress in apple trees (*Malus domestica* Borkh.) with selected biochemical and physiological parameters. *Scientia Horticulturae*, *113*(4), 362–369. <https://doi.org/10.1016/j.scienta.2007.04.012>
- Stone, J. R., & Yang, S. (2006). Hydrogen Peroxide: A Signaling Messenger. *Ars*, *8*, 691.
- Suttar, J., Mášová, L., & Dyr, J. E. (2001). Influence of citrate and EDTA anticoagulants on plasma malondialdehyde concentrations estimated by high-performance liquid chromatography. *Journal of Chromatography B: Biomedical Sciences and Applications*, *751*(1), 193–197. [https://doi.org/10.1016/S0378-4347\(00\)00453-9](https://doi.org/10.1016/S0378-4347(00)00453-9)
- Synowiec, A., Możdżeń, K., Krajewska, A., Landi, M., & Araniti, F. (2019). *Carum carvi* L. essential oil: A promising candidate for botanical herbicide against *Echinochloa crus-galli* (L.) P. Beauv. in maize cultivation. *Industrial Crops and Products*, *140*(May), 111652. <https://doi.org/10.1016/j.indcrop.2019.111652>
- Sytykiewicz, H., Czerniewicz, P., Sprawka, I., & Krzyzanowski, R. (2013). Chlorophyll content of aphid-infested seedling leaves of fifteen maize genotypes. *Acta Biologica Cracoviensia Series Botanica*, *55*(2), 51–60. <https://doi.org/10.2478/abcsb-2013-0023>
- Tamburini, E., Ferrari, G., Marchetti, M. G., Pedrini, P., & Ferro, S. (2015). Development of FT-NIR models for the simultaneous estimation of chlorophyll and nitrogen content in fresh apple (*Malus Domestica*) leaves. *Sensors (Switzerland)*, *15*(2), 2662–2679. <https://doi.org/10.3390/s150202662>
- Tausz, M., Šircelj, H., & Grill, D. (2004). The glutathione system as a stress marker in plant ecophysiology: Is a stress-response concept valid? *Journal of Experimental Botany*, *55*(404), 1955–1962. <https://doi.org/10.1093/jxb/erh194>
- Tetyuk, O., Benning, U. F., & Hoffmann-Benning, S. (2013). Collection and analysis of *Arabidopsis* phloem exudates using the EDTA-facilitated method. *Journal of Visualized Experiments*, *80*, 1–11. <https://doi.org/10.3791/51111>

- Tripathi, A. K., & Mishra, S. (2016). Plant Monoterpenoids (Prospective Pesticides). In *Ecofriendly Pest Management for Food Security*. Elsevier Inc. <https://doi.org/10.1016/B978-0-12-803265-7.00016-6>
- Tripathi, A. K., Upadhyay, S., Bhuiyan, M., & Bhattacharya, P. R. (2009). A review on prospects of essential oils as biopesticide in insect-pest management. *Journal of Pharmacognosy and Phytotherapy*, 1(5), 52–63. <http://www.academicjournals.org/jpp>
- Turek, C., & Stintzing, F. C. (2013). Stability of essential oils: A review. In *Comprehensive Reviews in Food Science and Food Safety* (Vol. 12, Issue 1, pp. 40–53). <https://doi.org/10.1111/1541-4337.12006>
- Twozkoski, T. (2002). Herbicide effects of essential oils. *Weed Science*, 50(4), 425–431. [https://doi.org/10.1614/0043-1745\(2002\)050\[0425:heoeo\]2.0.co;2](https://doi.org/10.1614/0043-1745(2002)050[0425:heoeo]2.0.co;2)
- Uchendu, E. E., Leonard, S. W., Traber, M. G., & Reed, B. M. (2010). Vitamins C and E improve regrowth and reduce lipid peroxidation of blackberry shoot tips following cryopreservation. *Plant Cell Reports*, 29(1), 25–35. <https://doi.org/10.1007/s00299-009-0795-y>
- Untiedt, R., & Blanke, M. M. (2004). Effects of fungicide and insecticide mixtures on apple tree canopy photosynthesis, dark respiration and carbon economy. *Crop Protection*, 23(10), 1001–1006. <https://doi.org/10.1016/j.cropro.2004.02.012>
- van Loon, L. C., Pierpoint, W. S., Boller, T., & Conejero, V. (1994). Recommendations for naming plant pathogenesis-related proteins. *Plant Molecular Biology Reporter*, 12(3), 245–264. <https://doi.org/10.1007/BF02668748>
- VanWoerkom, A. H., Aćimović, S. G., Sundin, G. W., Cregg, B. M., Mota-Sanchez, D., Vandervoort, C., & Wise, J. C. (2014). Trunk injection: An alternative technique for pesticide delivery in apples. *Crop Protection*, 65, 173–185. <https://doi.org/10.1016/j.cropro.2014.05.017>
- Velikova, V., Yordanov, I., & Edreva, A. (2000). Oxidative stress and some antioxidant systems in acid rain-treated bean plants protective role of exogenous polyamines. *Plant Science*, 151(1), 59–66. [https://doi.org/10.1016/S0168-9452\(99\)00197-1](https://doi.org/10.1016/S0168-9452(99)00197-1)
- Wang, R., Wang, R., & Yang, B. (2009). Extraction of essential oils from five cinnamon leaves and identification of their volatile compound compositions. *Innovative Food Science and Emerging Technologies*, 10(2), 289–292. <https://doi.org/10.1016/j.ifset.2008.12.002>
- Warneys, R., Gaucher, M., Robert, P., Aligon, S., Anton, S., Aubourg, S., Barthes, N., Braud, F., Cournol, R., Gadenne, C., Heintz, C., Brisset, M. N., & Degrave, A. (2018). Acibenzolar-s-methyl reprograms apple transcriptome toward resistance to rosy apple aphid. *Frontiers in Plant Science*, 871(December), 1–16. <https://doi.org/10.3389/fpls.2018.01795>
- Weber, H., Chételat, A., Reymond, P., & Farmer, E. E. (2004). Selective and powerful stress gene expression in *Arabidopsis* in response to malondialdehyde. *Plant Journal*, 37(6), 877–888. <https://doi.org/10.1111/j.1365-3113.2003.02013.x>
- Weitner, T., Inić, S., Jablan, J., Gabričević, M., & Domijan, A. M. (2016). Spectrophotometric determination of malondialdehyde in urine suitable for epidemiological studies. *Croatica Chemica Acta*, 89(1), 133–139. <https://doi.org/10.5562/cca2902>
- Wheatley, R. A. (2000). Some recent trends in the analytical chemistry of lipid peroxidation. *TrAC - Trends in Analytical Chemistry*, 19(10), 617–628. [https://doi.org/10.1016/S0165-9936\(00\)00010-8](https://doi.org/10.1016/S0165-9936(00)00010-8)
- Wise, J., VanWoerkom, A., Aćimović, S., Sundin, G., Cregg, B., & Vandervoort, C. (2014). Trunk Injection: A Discriminating Delivering System for Horticulture Crop IPM. *Entomology, Ornithology & Herpetology: Current Research*, 03(02), 3–9. <https://doi.org/10.4172/2161-0983.1000126>

- Woo, N. S., Badger, M. R., & Pogson, B. J. (2008). A rapid, non-invasive procedure for quantitative assessment of drought survival using chlorophyll fluorescence. *Plant Methods*, *4*(1), 1–14. <https://doi.org/10.1186/1746-4811-4-27>
- Yamori, W., Evans, J. R., & Von Caemmerer, S. (2010). Effects of growth and measurement light intensities on temperature dependence of CO₂ assimilation rate in tobacco leaves. *Plant, Cell and Environment*, *33*(3), 332–343. <https://doi.org/10.1111/j.1365-3040.2009.02067.x>

9. Appendices

Appendix 1: Cinnamon EO (*Cinnamomum cassia* J.Presl) molecular profile, provided by Pranarôm

Retention time (min)	Compound name	Relative area (%)
7,3	α -PINENE	0,08
7,4	α -THUYENE	0,01
8,7	CAMPHENE	0,05
9,1	HEXANAL	0,01
10,1	β -PINENE	0,03
14,1	LIMONENE	0,04
14,5	1,8-CINEOLE	0,02
17,2	STYRENE	0,17
18	p-CYMENE	0,06
18,7	TERPINOLENE	0,01
21,9	METHYL-5-HEPTENE-2-ONE	0,01
25,5	NONANAL	0,02
26,2	BENZYL COMPOUND	0,02
29,8	SESQUITERPENE	0,01
30,2	SESQUITERPENE	0,02
30,3	δ -ELEMENE	0,01
31	CYCLOSATIVENE + ISOLEDENE	0,12
31,2	YLANGENE	0,06
31,8	α -COPAENE	0,8
32,9	AROMATIC COMPOUND	0,04
33,3	CAMPHRE	0,04
33,6	BENZALDEHYDE	1,14
33,8	β -BOURBONENE	0,02
36,8	LINALOL	0,04
37,6	SESQUITERPENE	0,05
37,9	α -trans-BERGAMOTENE	0,04
38,2	β -CARYOPHYLLENE	0,12
38,5	TERPINENE-4-OL	0,04
38,8	AROMADENDRENE	0,03
40,6	AROMATIC COMPOUND	0,14
41,1	ACETOPHENONE	0,08
41,3	AROMATIC COMPOUND (Mw=132)	0,14
41,8	ALLO-AROMADENDRENE	0,12
42,6	α -HUMULENE + ESTRAGOLE	0,04
43	SALICYLIC ALDEHYDE	0,69
43,8	γ -MUUROLENE	0,14
44,2	BORNEOL	0,3
44,4	α -TERPINEOL + LEDENE	0,08
46	α -MUUROLENE	0,08
46,2	β -BISABOLENE	0,13
47,7	2-METHYL BENZOFURANE	0,4
47,9	δ -CADINENE + γ -CADINENE	0,29
48,3	METHYL SALICYLATE	0,09
49	BENZENEPROPANAL	0,78
49,2	α -CURCUMENE	0,09
49,5	α -trans-BISABOLENE	0,05
50,2	AROMATIC COMPOUND	0,04
50,8	AROMATIC COMPOUND	0,03
51,1	2-PHENYLETHYLE ACETATE	0,03

51,8	Trans-ANETHOL	0,02
52,1	CALAMENENE	0,03
52,9	HEXANOIC ACID	0,03
53,5	PHENOLIC COMPOUND	0,12
54,4	BENZYL ALCOHOL	0,27
55,4	Z-CINNAMALDEHYDE	0,34
56,3	PHENYLETHYLIC ALCOOL	0,98
58,5	AROMATIC COMPOUND	0,05
59,1	2-METHOXY BENZALDEHYDE	0,42
60,2	CARYOPHYLLENE OXIDE	0,05
63,5	E-CINNAMALDEHYDE	79,49
63,8	AROMATIC COMPOUND (Mw=206)	2,46
65,4	2-METHOXYPHENYLACETONE	0,24
67,4	SPATHULENOL	0,1
68,8	CINNAMYL ACETATE	0,46
69,5	EUGENOL	0,04
69,8	TRIMETHYL PENTADECANONE	0,02
70,5	T-CADINOL	0,02
71,3	SANDARACOPIMARADIENE ISOMERE	0,03
72,1	α -BISABOLOL	0,05
72,3	SESQUITERPENOL	0,03
72,6	α -CADINOL	0,02
74,4	2-METHOXY-CINNAMALDEHYDE	0,04
75,1	CINNAMIC ALCOOL	0,13
75,7	CARYOPHYLLA-3,7-DIEN-6-OL	0,02
78,4	SESQUITERPENIC EPOXIDE	0,07
82,2	Trans-o-METHOXY CINNAMALDEHYDE	5,26
82,6	COUMARINE (Mw=146)	2,1
90,3	BENZYL BENZOATE	0,07
93,8	AROMATIC COMPOUND	0,04
99,5	AROMATIC COMPOUND	0,14
	TOTAL	99,99

Appendix 2: EO emulsion formulation

To get a 100 mL EO-emulsion 2% (v/v), 15 mL of distilled water are put under 1 250 rpm agitation with a magnetic stirrer. Then, cinnamon essential oil (Pranarôm, batch number: CCB114) and Tween 80 are added to respect a 1:4 (v/v) EO:Tween 80 ratio. Finally, 20mL of a Na₂EDTA 100mM solution is added to the mix, which is brought to the final volume with distilled water (Table 1). For emulsions applied to leaves, the 20mL of a Na₂EDTA 100mM are replaced by distilled water.

Table 1. Composition of a 100 mL cinnamon essential oil emulsion

EO concentration	EO (mL)	Tween 80 (mL)	Na ₂ EDTA.2H ₂ O 100 mM (mL)	Distilled water (mL)
2 %	2	8	20	70

After 5 minutes of constant agitation at 1 250 rpm, the emulsion is stabilized using the high-speed homogenization (HSH) at 9500 rpm for 6 min (Ultra-Turrax T25) followed by a high-pressure homogenization (HPH) with 8 cycles at 5000 psi (FMC) (inspired by *Jo et al., 2015*). The solution is then stored at 4°C in a container covered with aluminium foil to prevent any degradation of the EO by light or temperature. Indeed, as mentioned by *Turek and Stintzing (2013)*, temperature, light and oxygen availability are recognized to have a crucial impact on essential oil integrity.

Appendix 3: Trunk injection settings

Before injection, the drip pocket are filled up with 20 mL of emulsion. The emulsion flow is allowed through the tube until liquid comes out of the needle in a continuous manner, and until all the bubbles have been removed from the tubing system. This step is performed in order to avoid cavitation in the tree vascular system. As a flow-stopping system, the tubes are pinched with an Hoffmann's clamp. A 1mm-wide hole is drilled at all injection points, at 5 cm above the base of the stem and with an upward orientation along a 60° angle from a vertical basis. Once the injection system well in place, the clamp is opened to allow the emulsion to rise up the xylem, based on the plant's transpiration rate.

Appendix 4: H₂O₂ Amplex Red protocol

Extraction

Fresh leaf samples were ground in liquid nitrogen and 0.1 g were extracted into 1 mL of 0.1 % (w/v) ice-cold TCA and 100 µL of 20 mM KPO₄ buffer (pH 6.5), previously bubbled with N₂. The homogenates were centrifuged in Eppendorf tubes at 13,000 rpm for 90s at 4 °C. 20 µL of supernatant was collected and 100 fold diluted in 1980 µL of 20 mM KPO₄ buffer (pH 6.5).

Assay reaction

Individual components were added to each well of the plate in the following order: 20 mM KPO₄ buffer (pH 6.5) (45 µL), H₂O₂ standard or plant sample (5 µL), and Amplex Red reagent (50 µL, see manufacturer's technical note for preparation), for a total of 100 µL per well. Following addition of all components, the plate was covered using aluminium foil and incubated at room temperature for 30 min. For each plate, a blank (containing 50 µL phosphate buffer (pH 6.5) and 50 µL Amplex Red reagent) was run as a negative control. In addition to the blank, a negative control 'Amplex® Red background' contains only 1µL of Amplex® Red reagent in 99 µL of 20 mM KPO₄ buffer (pH 6.5) is needed in order to monitor the background fluorescence/absorbance of the Amplex® Red reagent itself. Another negative control, termed here 'Sample background' is prepared for each H₂O₂ extract, and contains 50µL of extract in 48 µL of 20 mM KPO₄ buffer (pH 6.5) together with 2µL of HRP enzyme but without Amplex® Red reagent. This control allows to monitor the individual sample background coming from the presence of plant compounds that could potentially serve as substrates for HRP, mimicking resorufin production.

The fluorescence intensity measurements on standards, samples and negative controls were performed on two technical replicates each.

Standard curve

Standard solutions of 0–10 μM H_2O_2 (0; 0,2; 1; 2; 5; 10 μM) were prepared on the day of the analyses from a 880 mM H_2O_2 stock solution (Sigma-Aldrich Co.) diluted in KPO_4 buffer (pH 6.5).

20 mM solution : 22,7 μL of 880 mM in 977 μL KPO_4 buffer

400 μM solution: 20 μL of 20 mM in 980 μL KPO_4 buffer

10 μM	25 μL 400 μM	975 μL KPO_4 buffer
5 μM	500 μL 10 μM	500
2 μM	400 μL 5 μM	600
1 μM	500 μL 2 μM	500
0,2 μM	200 μL 1 μM	800
0 μM	0	1000

Appendix 5: H_2O_2 Luminol protocol

Preparation of plant material

Leaf discs were collected and placed in dark conditions for 2 h in 25 ml of distilled water, with water entirely replaced every 30 min in order to rinse them, and to remove secondary metabolites produced upon wounding. One leaf disc is gently placed per well of a 96-well luminometer plate, each containing 200 μl of distilled water. The plate is then covered with an aluminium foil and incubated overnight.

Assay reaction

For a 30 leaf discs experiment, 3.2 mL of a luminol /peroxidase working solution were prepared by mixing 32 μL of luminol solution (stock solution :15 mg in 1 ml of DMSO), 32 μL of HRP (stock solution :10 mg in 1 ml of water) and 3136 μL of distilled water.

For the elicitor solutions, Fytosave (Syngenta, 12.5 g/L COS-OGA) was diluted in EtOH 0.1% in order to obtain 20 and 200 $\mu\text{g}/\text{mL}$ concentrations. In the same way, 20; 200; 400 $\mu\text{g}/\text{mL}$ solutions of pure cinnamon essential oil were prepared.

The 200 μl of water contained in each well were removed and directly replaced by an equal volume of either Fytosave solutions, or CEO solutions or even EtOH 0.1% for blank samples. The plate is then put under vacuum for 2 minutes, after which 50 μL of luminol /HRP are added. As soon as possible, luminescence intensity measurement is performed every minutes using a microplate spectrofluorometric reader (Tecan Spark®), over at least a 20 minutes period and with a signal integration time of 1 sec. Results are expressed in relative light unites (RLU) and measure are carried out on five technical replicates for each modality (6 in our case).

Appendix 6: Glutathione protocol

Extraction

Fresh leaf samples were ground in liquid nitrogen and 0.1 g were extracted into 1 mL of 1M HCl. The homogenate was centrifuged in Eppendorf tubes at 13,400 rpm for 10 min at 4 °C (centrifuge MiniSpin®).

Sample preparation

400 µL of supernatant was neutralised with 400 µL of 1M NaOH in the presence of 50 µl of 1 M NaH₂PO₄ (pH 5.6). The final pH of the neutralized acid extracts was between 6 and 7.

For each extract, the neutralized supernatant was separated into two aliquots of 200 µL, and these were treated as follows to measure GSH and total GSH respectively.

The first aliquot was added to 200 µL of 0.5 M CHES (2-(Cyclohexylamino)ethanesulfonic acid, pH 9), 20 µL of water and 20µL of 30 mM monobromobimane (MBB) and incubated for 15 min in the dark. The resulting GSH-MBB derivatives were stabilized by the addition of 660 µL of 10% (v/v) acetic acid.

The second aliquot was added to 200 µL of 0.5 M CHES (pH 9) and 20 µL of 10 mM dithiothreitol (DTT). After incubation for 30 min in the dark, thiols were derivatized by the addition of 20 µL of 30 mM MBB. The mixture was incubated for 15 min in the dark, and then the reaction was stopped by the addition of 660 µL of 10% (v/v) acetic acid.

Once the reaction stopped, reaction mixtures were put in vials.

HPLC analysis

All analyses were performed on a Agilent 1260 Infinity HPLC system equipped with an FLD detector (λ_{EX} : 395 nm, λ_{EM} : 477 nm). The autosampler was thermostated at 4°C and 50 µL was injected onto the column. The column used was a Zorbax 300 SB from Agilent (C18; 150x4,6 mm, 3,5 µm) at 40 °C. Bimane derivatives were separated with a linear gradient of 0.25% acetic acid (v/v) (pH 3,5 by adding NaOH) as solvent A and with 100% methanol as solvent B (Table 2), at a flow rate of 0.8 mL/min and a column temperature of 40°C. Under these conditions, each run lasted 32,5 min and based on standards, retention time of GSH–MBB was 4.8– 4.9 min.

Table 2. Linear gradient detail for the quantification of GSH by HPLC-FLD

Time (min)	Solvent A – 0.25% acetic acid (v/v) with NaOH (pH 3,5) (%)	Solvent B – 100% MeOH (%)
0	82	18
17.5	82	18
20	0	100
27.5	0	100
28	82	18
32.5	82	18

Standard curve

Standard solutions of 0–80 μM GSH (0; 5; 10; 20; 40; 60; 80 μM) were prepared on the day of the analyses from a 500 μM GSH stock solution (CAS-No: 70-18-08, 98% purity, Acros Organics). Dilutions were performed in 2 mL balloons with 800 μL of metaphosphoric acid (10% v/v), and 0,2 N HCl was used to complete the final volume. Each calibration point followed the exactly same steps as samples, except the extraction step.

Solution stock 500 μM : 7,84 mg in 50 mL of water

	V solution 500μM	MPA	HCl 0,2 N
80 μM	320 μL	800 μL	0,880 mL
60 μM	240 μl	800	0,960
40 μM	160 μL	800	1,040
20 μM	80 μL	800	1,120
10 μM	40 μL	800	1,160
5 μM	20 μL	800	1,180
0 μM	0	800	1,200

Calculations

After peak integration, the mean area of the small peak obtained with the blank control (0 μM point of the standard curve) was subtracted from the peak areas of standards and samples.

Controls for each sample were prepared by replacing MBB with 0.5 M Ches (pH 9).

GSH and total GSH concentrations were obtained thanks to linear regression equation of the external calibration curve, and the [GSH]/[Tot GSH] ratio, expressed in %, was calculated.

Appendix 7 : MDA protocol

Extraction

Lipid peroxides were extracted by grinding in an ice-cold mortar 0,1 g of leaves with 1 mL of cold 5% (w/v) HCl, vortexed during 30 sec. The extracts were then centrifuged at 13 400 rpm during 10 min at 4°C in Eppendorf tubes.

TBARS assay

To 200 μL aliquot of this HCl extract were added 40 μl of 0,1% butylated hydroxytoluene (BHT) in ethanol and 760 μL of 0,5% TBA in 20% MPA, giving a final pH value of approximately 1.0. The reaction mixture was heated for 30 min at 95°C in screw capped tubes in a temperature-controlled heating block and was then rapidly cooled on ice. Once the reaction stopped, the reaction mixture was centrifuged at 4000 g during 5 min. The supernatant was put in vials.

HPLC analysis

All analyses were performed on a Agilent 1200 Series HPLC system: Pump (LC-10AT), autosampler (SIL-10AD), MWD detector (RF-10AXL), degasser (GT-154), and system controller (SCL-10A) with a PC control program (LC 1200 Data Analysis, version 6.12 SP2).

Samples were analyzed on a 75x4,6 mm, 2,7 μm Halo® C18 column. The column was thermostated at 40 °C and protected with an in-line guard column composed of the same material.. The column was eluted isocratically with 35% methanol in 50mM KPO₄ buffer (pH 6.8) at 1 mL/min. Under these conditions, analyses were complete in 8 min. Chromatograms were monitored at 532 nm, which is the MDA(TBA)₂ maximum absorption wavelength, and injection volume was 20 μL . Based on standards, retention time of MDA(TBA)₂ was 1.9– 2.1 min.

Standard curve

Standard solutions of 0–8 μM MDA (0; 0.5; 1; 2; 4; 8 μM) were prepared on the day of the analyses from a 1 mM MDA stock solution (CAS-No: 100683-54-3, \geq 97.0 % purity, Sigma-Aldrich Co.) diluted in 40% EtOH. Each calibration point followed the exactly same steps as samples, except the extraction step.

Stock solution 1 mM : 6.272 mg in 20 mL of EtOH 40%

50 μM : 100 μL of 1 mM solution in 1.900 mL of EtOH 40%

		EtOH 40%
8 μM	320 μL of 50 μM	1.680 mL
4 μM	1 mL of 8 μM	1
2 μM	1 mL of 4 μM	1
1 μM	1 mL of 2 μM	1
0,5 μM	1 mL of 1 μM	1
0 μM	0	2

Calculations

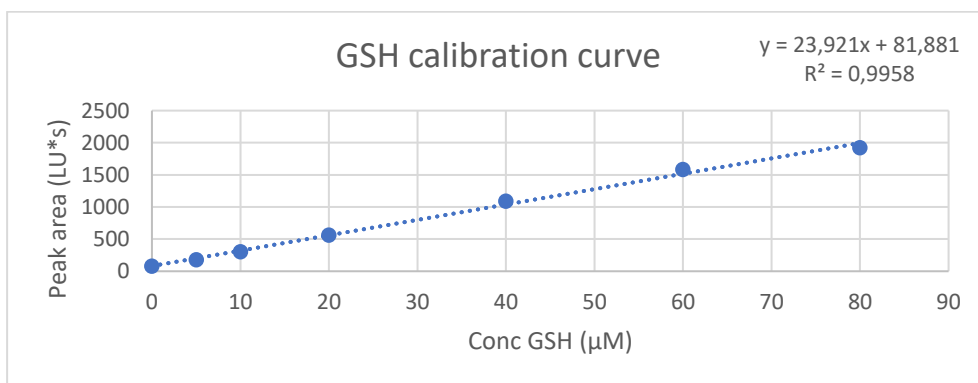
After peak integration, the mean area of the small peak obtained with the blank control (0 μM point of the standard curve) was subtracted from the peak areas of standards and samples. Controls for each sample were prepared by replacing the TBA-MPA solution by 760 μL of MPA 20%. MDA concentrations were obtained thanks to linear regression equation of the external calibration curve.

Appendix 8: Table listing the defence genes studied

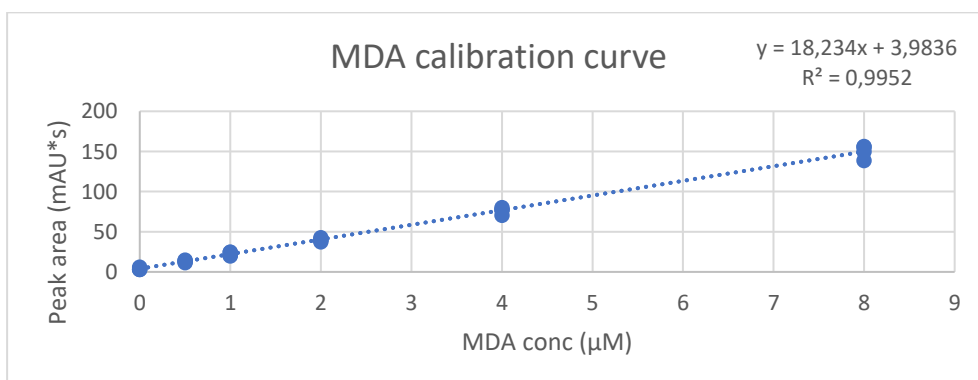
	PR (1,2,4,5,8,14,10)	Pathogenesis-Related protein
Phenylpropanoids pathway	PAL	Phenylalanine Ammonia-Lyase
	CHS	chalcone synthase
	DFR	dihydroflavonol reductase
	BIS2	1,2-bis(2,4-dihydroxyphenyl)propan-1-one
	PPO	polyphenol oxidase
Isoprenoids pathway	HMGR	Hydroxymethyl glutarate-CoA reductase

	FPPS	farnesyl pyrophosphate synthase
	Far	(E,E)- α -farnesene synthase
	CSL	cysteine sulfoxide lyase
Oxidative stress	Apox	ascorbate peroxidase
	GST	glutathione S-transferase
	POX	peroxidase
Cell wall modifications	CalS	callose synthase
	Pect	pectin methyl esterase
	CAD	cinnamyl-alcohol dehydrogenase
Salicylic acid	EDS1	enhanced disease susceptibility 1
	WRKY	WRKY transcription factor 30
Jasmonic acid	Lox2	Lipoxygenase 2
	JAR	jasmonate resistant 1
Ethylene	ACCO	1-aminocyclopropene-1-carboxylate oxidase
	EIN3	EIN3-binding F box protein 1
	AGG	Agglutinin

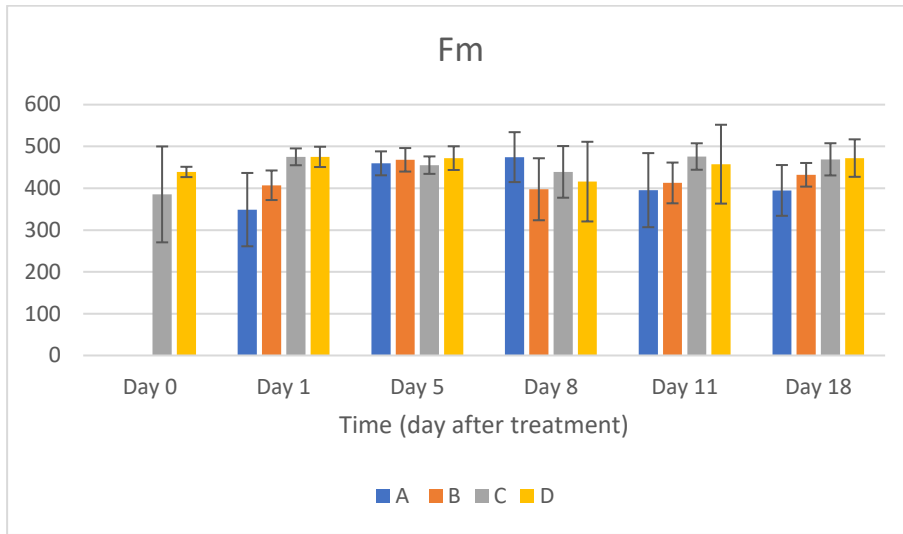
Appendix 9: Glutathione calibration curve



Appendix 10: Malondialdehyde calibration curve



Appendix 11: Maximal fluorescence (Fm) values



Appendix 12: Fisher's tests results of GLM models comparison

```

Analysis of Deviance Table

Model 1: numalive ~ 1
Model 2: numalive ~ Day
  Resid. Df Resid. Dev Df Deviance    F    Pr(>F)
1         97     9663.0
2         96     7238.8  1    2424.2 24.701 2.919e-06 ***
---

Analysis of Deviance Table

Model 1: numalive ~ Day
Model 2: numalive ~ Day + Injection
  Resid. Df Resid. Dev Df Deviance    F    Pr(>F)
1         96       7238.8
2         95     6424.9  1    813.93 10.66 0.001523 **
---

Analysis of Deviance Table

Model 1: numalive ~ Day + Injection
Model 2: numalive ~ Day * Injection
  Resid. Df Resid. Dev Df Deviance    F Pr(>F)
1         95     6424.9
2         94     6285.1  1    139.78 1.8791 0.1737

Signif. codes:  0 '***' 0.001 '**' 0.01 '*' 0.05 '.' 0.1 ' ' 1
    
```